The Pennsylvania State University

The Graduate School

Program in Cellular and Molecular Biology

OGF-OGFR AXIS AND ITS INHIBITORY ACTIONS

ON CELL CYCLE PROGRESSION

A Thesis in

Cellular and Molecular Biology

by

Fan Cheng

Submitted in Partial Fulfillment
of the Requirements
for the Degree of

Doctor of Philosophy

December 2006

The thesis of Fan Cheng was reviewed and approved* by the following:

Patricia J. McLaughlin
Professor of Neural and Behavioral Sciences
Thesis Advisor
Chair of Committee

Ian S. Zagon
Professor of Neural and Behavioral Sciences

Michael F. Verderame
Associate Professor of Medicine

Xuwen Peng
Associate Professor of Comparative Medicine

Henry J. Donahue
Professor of Cellular and Molecular Physiology
Chair of Cell and Molecular Biology Program

*Signatures are on file in the Graduate School.

ABSTRACT

Opioid growth factor (OGF) is an endogenous opioid peptide ([Met^5]-enkephalin) that interacts with the OGF receptor (OGFr), and serves as a tonically active negative growth factor in neoplasia. Previous studies showed that OGF inhibits the growth of human head and neck squamous cell carcinoma (HNSCC) cells and pancreatic cancer cells *in vitro* and *in vivo*, and is targeted to cell proliferation. However, the mechanism by which OGF inhibits cell replication was not clear.

The studies described within this thesis were directed towards defining the molecular mechanisms of OGF inhibitory action. A number of unique findings are presented here.

In SCC1 HNSCC cell cultures synchronized with nocodazole, flow cytometry revealed that OGF treatment (10^{-6} M) resulted in fewer cells exiting the G1 phase of the cell cycle in comparison to controls ($p<0.05$). Subsequent studies showed that OGF decreased the phosphorylation of retinoblastoma protein (Rb) ($p<0.05$) without changing the total Rb expression. Reduced phosphorylated Rb was correlated with reduced cdk4 kinase activity while the total cdk4 expression did not change. Moreover, OGF treatment increased cyclin-dependent kinase inhibitor (CKI) p16 protein expression 2-fold in comparison to controls ($p<0.05$), but had no significant effect on p15, p18, p19, p21 or p27 protein expression. Western blot analysis did not detect p57 protein in the SCC1 cell line. Blockade of OGF-OGFr interactions with the short-acting opioid antagonist, naloxone (NAL), demonstrated that increased expression of p16 protein by OGF was completely abolished by concomitant administration of OGF and NAL. NAL alone had no effect on p16 expression suggesting that this regulation of p16 was an opioid receptor

mediated event. Moreover, OGF treatment increased p16 protein expression in comparison to controls ($p<0.05$) in CAL27 and SCC4 HNSCC cell lines, demonstrating the ubiquitous nature of this observation. Inhibition of p16 (INK4a) activation by p16 specific siRNA blocked OGF inhibitory action on proliferation of SCC1, CAL-27 and SCC4 HNSCC cells. Cultures treated with negative control siRNA, which had no effect on p16 expression, did not block OGF's growth inhibitory action. Collectively, these results indicate that the receptor-mediated, growth inhibitory effects of the OGF-OGFr axis in HNSCC cells are associated with induction of p16/cdk4 resulting in decreased Rb phosphorylation. These data revealed that the target of cell proliferative inhibitory action of OGF in human HNSCC cells is by the way of cyclin dependent kinase inhibitory pathways, specifically, the p16 pathway. Because many human HNSCC tumors retain p16, OGF may be a valuable therapeutic agent in this setting.

Alternatively, pancreatic cancer cells have frequently lost p16 gene expression, and thus other CKI pathways were examined for their role with OGF inhibition of pancreatic cancer growth. BxPC-3 human pancreatic adenocarcinoma cell cultures were synchronized with nocodazole, and flow cytometry revealed that OGF treatment (10^{-6} M) resulted in fewer cells ($p<0.05$) exiting the G1 phase of the cell cycle in comparison to controls. The present studies focused on the role of OGF on regulatory pathways for the G1 to S phase transition. Studies using the BxPC-3 pancreatic adenocarcinoma cell line suggest that OGF decreased the phosphorylation of retinoblastoma protein (Rb) ($p<0.05$). This change was correlated with reduced cdk2 kinase activity. There was no change in total cdk2 expression. Moreover, OGF treatment for 9 hours increased p21 protein expression 2-fold in comparison to control ($p<0.05$), but had no effect on p27 protein

expression. Blockade of the OGF-OGFr axis with the short-acting opioid antagonist naloxone revealed that the increased expression of p21 protein following OGF treatment was completely abolished by concomitant administration of OGF and NAL. NAL alone had no effect on p21 protein expression suggesting that the OGF effects were OGF receptor mediated. Moreover, OGF treatment increased CKI p21 protein expression in comparison to control ($p<0.05$) in Panc1 and Capan2 pancreatic cancer cell lines. Inhibition of p21 activation by p21 specific siRNA blocked the OGF inhibitory action on BxPC3, Panc1 and Capan2 cell proliferation. Scrambled siRNAs (negative controls) had no effect on p21 expression and did not block OGF's growth inhibitory action. Collectively, these results indicate that the receptor-mediated, growth inhibitory effects of the OGF-OGFr axis in human pancreatic cancers are associated with induction of p21 expression and repression of the Rb phosphorylation.

In summary, these studies demonstrate for the first time that the target of cell proliferative inhibitory action of OGF is cyclin dependent kinase inhibitory pathways.

TABLE OF CONTENTS

LIST OF FIGURES

LIST OF ABBREVIATIONS

ATP	adenosine triphosphate
bNLS	bipartite nuclear localization signals
BrdU	bromodeoxyuridine
Ca	calcium
CAM	chick chorioallantoic membrane
CDK(Cdk)	cyclin-dependent kinase
CKI	cyclin-dependent kinase inhibitor
DIM-C-pPhCF_3	1,1-Bis(3'-indolyl)-1-(*p*-trifluoromethylphenyl)methane
DMEM	Dulbecco's Modified Eagle's Medium
DNA	deoxyribonucleic acid
E	embryo
G0	Gap 0
G1	Gap 1
G2	Gap 2
HNSCC	head and neck squamous cell carcinoma
IB	immunoblot
INK4	inhibitors of cyclin-dependent kinase CDK4
IP	immunoprecipitation
K_d	dissociation constant
kDa	kilodalton
L	liter
min	minutes

mL	milliliter
mRNA	messenger RNA
M	molar
mM	millimolar
MAPK	mitogen activated protein kinase
$MgCl_2$	magnesium chloride
NaCl	sodium chloride
NAL	naloxone
ng	nanogram
nmol	nanomole
NP-40	nonidet P-40
NTX	naltrexone
OGF	opioid growth factor
OGFr	opioid growth factor receptor
PAGE	polyacrylamide gel electrophoresis
POMC	proopiomelanocortin
PPE	preproenkephalin
pRb	phosphorylated retinoblastoma
Rb	retinoblastoma
RIPA	radio-immunoprecipitation assay
RNA	ribonucleic acid
S	Serine
SCC	squamous cell carcinoma

SDS	sodium dodecyl sulfate
siRNA	small inhibitory ribonucleic acid
S phase	synthesis phase
T	Threonine
TUNEL	Terminal deoxynucleotidyl Transferase Biotin-dUTP Nick End Labeling
μCi	microcurie
μg	microgram
μL	microliter
μM	micromolar

ACKNOWLEDGMENTS

As with all accomplishments in life, the journey towards this thesis was not made alone. Without the love and support of my family and friends, I could not have come nearly this far. I wish to thank all of those people who have helped me to reach this point, and I can only hope that I have given something back in return.

First and foremost, I owe a great deal to my advisor, Dr. McLaughlin. The things I have learned are beyond measure, but I will always remember her passion for science, her attention to detail, and her pursuit of excellence. Through her example, I have been able to grow and mature as a scientist and a critical thinker.

Secondly, I would like to thank the members of my committee, Drs. Zagon, Verderame and Peng. They have always pushed me to be better and to think about things more critically. Their encouragement has moved me further along than I could have imagined and taught me that there is always something to learn and room for improvement.

I would also like to deeply thank the members of Dr. McLaughlin's laboratory over the past three years, especially Caitlin and Jody. I thank them for all the good times and all the advice and help they have given me both in and out of lab.

Special thanks go to all the friends I have met here in Hershey. They have made my time here much more enjoyable.

Lastly, I want to thank my whole family, especially my husband, Wei Xiao. He has been a constant source of strength and encouragement for me. I also would like to thank my parents, parents-in-law and my daughter. I owe all of my accomplishments to them for their love and support.

CHAPTER I

LITERATURE REVIEW

1.1 Opioids and OGF

Opioids are widely used in medicine as strong analgesics. Opioids are both endogenous and synthetic with four broad classes of opioids being recognized: endogenous opioid peptides, opium alkaloids, semi-synthetic opioids and synthetic opioids. Endogenous opioid peptides include the families of endorphins, enkephalins and dynorphins. Morphine and codeine are opium alkaloids, whereas heroin is a semi-synthetic opioid, and methadone is an example of a synthetic opioid. The term "opiates" refers specifically to the products derived from the juice of the opium poppy, whereas "opioid" refers to any directly acting compound whose effects are stereospecifically antagonized by naloxone [1].

At least three major branches of the superfamily of endogenous opioid peptides have been identified and include: endorphins, enkephalins and dynorphins [2]. Precursor molecules, for each of these classes, respectively, are proopiomelanocortin (POMC), preproenkephalin A and preproenkephalin B, or prodynorphin. The primary active product of POMC is endorphin, a 31-amino acid C-terminal sequence of β-lipotropin (β-LPH); shorter cleavage products, α-endorphin and γ-endorphin have also been purified [2]. The enkephalin family has a core of four amino acids "Tyr-Gly-Gly-Phe" that are the backbone structures of [Met^5]-enkephalin, [Leu^5]-enkephalin and [Met^5]-[Arg^6]-[Phe^7]-enkephalin. These peptides are widely distributed in the mammalian system and are found in endocrine glands, central nervous system, adrenal medulla, and the gastrointestinal tract [2]. Dynorphins derived from the prodynorphin precursor include α/β-neo-endorphin, dynorphin A and dynorphin B. This family of endogenous opioids

has been identified throughout the gastrointestinal system, posterior pituitary, and brain [2].

In the 1980s, studies showed that endogenous opioid peptides function in growth regulation of normal and abnormal cells and tissues [3-5]. Early experiments indicated that [Met^5]-enkephalin acted as an anticancer agent with murine B16 melanoma, L1210 leukemia, and S20Y neuroblastoma [6]. Studies on murine neuroblastoma cells and endogenous opioid peptides showed that [Met^5]-enkephalin was the most potent opioid peptide associated with growth, and that concentrations as low as 10^{-10} M over a 48 hr period of time inhibited the growth of log-phase S20Y neuroblastoma cells [7]. Other opioid peptides and analogs related to prodynorphin and proopiomelanocortin genes had no significant influence on growth of cultured neoplastic or normal cells even at concentrations as high as 10^{-6} M [7]. In a wide variety of normal or abnormal cells and tissues, including colon cancer, heart, squamous cell carcinoma of the head and neck, pancreatic cancer, developing nervous system in humans and animals, both *in vitro* and *in vivo*, [Met^5]-enkephalin has been identified as the primary opioid peptide involved with growth [6]. To distinguish the role of [Met^5]-enkephalin, as a growth factor in neural and non-neural cells and tissues, in prokaryotes and eukaryotes, from its role in neurotransmission, this peptide was termed opioid growth factor (OGF) [6].

Further studies characterized OGF as an autocrine produced and secreted peptide that is not cell, tissue, nor organ specific [7, 8]. OGF exhibits a rapid, direct, and stereospecific biological activity at physiologically relevant concentrations [8]. OGF is very sensitive to the action of peptidases and is rapidly eliminated from plasma; a half-life of less than two minutes has been reported [9]. Disruption of OGF activity

(neutralization with antibodies or application of opioid antagonists) accelerated growth by removing inhibitory signaling [6].

1.2 Opioid Receptors and OGFr

1.2.1 Classical opioid receptors

Three major classes of opioid receptors have been identified in various nervous system sites and in other tissues and include mu (μ), delta (δ) and kappa (κ) opioid receptors [10]. Classic opioid receptors are members of the G protein-coupled family of receptors that affect ion gating, intracellular Ca^{2+} disposition, and protein phosphorylation [10]. The pharmacological activity of these opioid receptors can be blocked by opioid antagonists such as naloxone or naltrexone.

Mu (μ) receptors play an important role in the control of nociception. Nociception is the term commonly used to refer to the perception of pain. Mu receptor agonists block the nociceptive responses to mechanical, thermal or chemical high intensity stimulations [1]. Mu receptors are present in the caudate putamen, neocortex, thalamus, nucleus accumbens, hippocampus and amygdala [1]. They are also widely distributed in the peripheral nervous system, including myenteric neurons in the gut and the vas deferens [1]. The gene encoding the mu receptor is on the distal arm of human chromosome 6 [1].

Delta (δ) receptors have a role in analgesia, motor integration, gastro-intestinal motility, olfaction, respiration, cognitive function, mood driven behavior [1]. [Met]- and [Leu]-enkephalin have high affinities for δ-receptors, ten-fold lower affinities for μ-receptors and negligible affinity for κ-receptors [2]. Delta receptors present in olfactory

bulb, neocortex, caudate putamen and nucleus accumbens [1]. In the human genome, the gene encoding the δ receptor is located on chromosome 1 [1].

Kappa (κ) receptors have been implicated in the regulation of nociception, diuresis, feeding and neuroendocrine secretions [1]. In addition, evidence of the expression of κ receptors by lymphoma cells suggests that these receptors also participate in the control of immune function [1]. The most probable endogenous ligands of κ receptors are dynorphins [1]. The gene encoding the κ receptor is on the proximal long arm of human chromosome 8 [1].

1.2.2 Other opioid receptors and OGFr

1.2.2.1 Other types of opioid receptors

Extending the screening of genomic and cDNA libraries, resulted in the identification of a novel receptor that bore as high a degree of homology (>60%) towards the classical opioid receptors, as they shared among each other [11]. This receptor was originally referred to as opioid receptor-like (ORL_1), and now is accepted as a member of the 'family' of opioid receptors on the basis of its structural homology towards the classical types [12].

In addition to the μ-, δ-, κ- and ORL_1-receptors, other types of novel but poorly characterized opioid receptors were proposed: these include ε-, ι-, λ-, and σ-receptors [12].

1.2.2.2 OGFr

OGF inhibits growth in S20Y murine blastoma cells and based on pharmacological characteristics, the receptor was originally termed the zeta (ζ)-opioid

receptor [8]. Later, the receptor for OGF in rat and human was cloned, sequenced, expressed, and functionally analyzed [8, 13]. This receptor has no substantial homology to the classical opioid receptors in terms of nucleotides or amino acids [6]. In addition, gene location, gene expression pattern and the functions of this receptor differ from classical opioid receptors. Given the differences in function, pharmacology, physiology, biochemistry, and anatomy, as well as the molecular biology, between the receptor of OGF and classical opioid receptors, the receptor for OGF was termed OGF receptor (OGFr) [8].

To initially identify the receptor related to growth, and specifically to determine whether classical opioid receptors, most notably μ and δ receptors, were associated with the growth related effects of methionine enkephalin or another receptor, binding studies with radiolabeled [Met^5]-enkephalin were performed in normal rat brain as well as neuroblastoma cells. The murine neuroblastoma cell line---S20Y, which has been extensively characterized to respond to OGF by inhibiting proliferation, was used for pharmacological binding assays with radiolabeled OGF. Specific and saturable binding activity in whole homogenates of S20Y was consistent with a single binding site [14]. Likewise, binding affinity (K_d) for radiolabeled [Met^5]-enkephalin in enriched nuclear fractions of whole brain homogenates revealed a significantly higher binding affinity (K_d) for OGFr than for any of the classical μ, δ, or κ receptors. These data supported the identification of a distinct receptor that mediated OGF activity. Moreover, binding of radiolabeled OGF displayed stereospecificity, with (-)-naloxone being 18-fold more potent than (+)-naloxone at displacing OGF [6]. Using whole homogenates of the 6-day-old rat cerebellum, a tissue where OGF was found to modulate DNA synthesis,

radiolabeled OGF binding was maximal in the P1 (nuclear) fraction, and no binding was detected in the P2 (cytoplasmic) fraction [15]. Immunoblotting of two-dimensional NEPHGE gels with polyclonal antibodies revealed staining of 32-, 30-, 17- and 16-kDa polypeptides isolated in the nuclear enriched fraction but no detection in the cytoplasmic fractions [6].

Thus, OGFr was determined to be different from classical opioid receptors. Gene location, gene expression pattern and the functions further distinguished it from classical opioid receptors.

1.3 OGF-OGFr Axis

1.3.1 OGFr Gene Location

Pharmacological studies showed that OGFr shares characteristics of classical opioid receptors---specifically, naltrexone or naloxone-reversibility and stereospecificity. However, the molecular and genomic nature of this receptor is distinctly different from classical opioid receptors [8]. Using fluorescence in situ hybridization, the chromosomal location of the human OGF receptor was determined to be 20q13.3 [6].

1.3.2 OGFr Gene Expression

The gene for the human OGFr has been filed in GenBank (AF112980) [6] and is at least 9 kb in length, consisting of seven exons and six introns [6]. The presence and interaction of OGF-OGFr have been documented in a wide variety of human cells and tissues. Northern blot analysis of human fetal and adult tissues, as well as cancer tissues and cell lines identified OGFr mRNA in fetal human brain, lung, liver and kidney;

transcript sizes of 1.7 and 2.4 kb were observed. In adult tissues, including heart, brain, liver, skeletal muscle, kidney, pancreas, and cancer cell lines, including BxPC-3, MiaPaCa-2, CAL27, SK-N-SH, and tumor tissues, including human tongue cancer and human renal tumor, only the 2.4 kb mRNA was detected [6].

1.3.3 OGFr Protein and Distribution

OGFr has no substantial homology to the classical opioid receptors in terms of nucleotides or amino acids [6]. Multiple alignment of human, mouse and rat OGFr sequences revealed that the OGFr sequences contain bipartite nuclear localization signals (bNLS) without any other recognizable protein domains [6]. Studies also identified the binding subunit(s) of the OGFr [16]. Protein of rat cerebellum from 6-day-old animals was separated and electrophoretically transferred onto nitrocellulose. Ligand blotting of these blots with 1.5 nM [^{125}I]-[Met^{5}]-enkephalin revealed four binding polypeptides of 32, 30, 17, and 16 kDa. Binding was blocked by cold ligand and opioid antagonists, and exhibited a stereospecific response. Subcellular fractionation studies using ligand blotting and receptor-binding analysis indicated that these binding subunits were associated with the nuclear enriched fraction and were similar subunits to those identified with antibodies [16]. Using a double-face immunogold staining procedure, immunoelectron microscopic studies showed that colocalization of OGF and OGFr can be observed on the outer nuclear envelope, in the perinuclear cytoplasm, traversing the nuclear pore, in association with the inner nuclear lamina, and at the periphery of heterochromatin aggregations [6].

1.3.4 Function

1.3.4.1 Normal growth/re-epithelialization

The OGF-OGFr system has a tonic, reversible, and species/tissue non-specific action on growth [6]. OGF-OGFr action has been found to be associated with cell proliferation and DNA synthesis in a variety of normal animal tissues [17-20]. Adult mice given systemic injections of OGF and examined 2 h later revealed depressed levels of DNA synthesis in the epithelial cells in the tip, and dorsal and ventral surfaces of the tongue (42-44% of control levels) [17]. OGF also depressed DNA synthesis in the dorsum and plantar surface of basal epithelial cells of normal skin of mice by 42% and 19%, respectively, within 2 h [20].

The OGF-OGFr axis has been found to be important for tissue and organ development [21-25]. Northern blot analysis of the whole brain and cerebellum showed that preproenkephalin (PPE) message is present in the fetal nervous system on prenatal day 15 (the earliest time point examined), is expressed at relatively similar levels within each tissue during the first 2 postnatal weeks, and reaches adult levels by the beginning of the 3rd postnatal week [22]. Studies also showed that fetal human cells displayed OGF and OGFr [24]. Acute exposure of the pregnant female to OGF resulted in a decrease in DNA synthesis in cells of organs representing all three germ layers, and did so in a receptor-mediated fashion [24]. Continuous OGFr blockade from birth to postnatal day 6 increased body weight and increased the number of layers of germinal cells in the cerebellum [21]. These results support that the OGF-OGFr axis plays an important role in embryonic, and particularly, brain development.

The OGF-OGFr axis was found to be important for cellular renewal [26-28] and wound healing [29-32]. Early studies showed that both OGF and OGFr were present in

epithelial cells [26]. Rabbit cornea epithelial outgrowths exposed to OGF for 7 days were subnormal in outgrowth and labeling index (DNA synthesis) and displayed alterations in architectural pattern. The effects of OGF on epithelial outgrowth were blocked by concomitant exposure to the opioid antagonist naloxone; naloxone alone had no effect on growth at the concentration utilized [33]. Investigation was done to examine the role of OGF-OGFr on corneal epithelial wound closure in the rabbit [30] and rat [29] under *in vitro* and *in vivo* conditions. The action of excessive agonist (OGF) application revealed that exposure of wounded epithelium to OGF delayed wound closure under *in vitro* conditions, and did so in a receptor-mediated fashion [30]. The modulatory capability of OGF on wound healing *in vivo* was explored by examining the effects of opioid peptide-receptor disruption using topical application of NTX; enhanced healing of the abraded cornea was noted.

The OGF-OGFr system has been found to be important for angiogenesis [33]. The chick chorioallantoic membrane (CAM) assay was used for the *in vivo* quantitation of angiogenesis [33]. OGF notably decreased the total number and length of blood vessels in the CAM preparations. However, OGF had a disproportionately greater inhibitory effect on arterial angiogenesis as reflected in decreased artery/vein ratios for vessel number and length. These results support that OGF-OGFr system had a greater inhibitory effect on arterial angiogenesis as compared with venous angiogenesis.

1.3.4.2 Abnormal growth: neoplasia in general

The OGF-OGFr system plays an important role in modulating the growth of neoplasia [34-38]. Early studies showed that OGF influences the growth of transplanted neuroblastoma [39]. Using a tissue culture system, OGF depressed the growth of S20Y

murine neuroblastoma, N115 murine neuroblastoma, SK-N-MC human neuroblastoma, and HT-1080 human fibrosarcoma [7]. Further studies showed that OGF treatment decreased the growth of a variety of human cancer cells both *in vivo* and *in vitro* including head and neck squamous cell carcinoma cell lines [37], pancreatic tumor cells [35, 36], colon adenocarcinoma cell lines [40], and renal cancer [38]. OGF functions under anchorage-dependent and anchorage-independent conditions [41].

1.3.4.2.1 Abnormal growth: Anchorage-independent growth

Anchorage-independent growth is characteristic of neoplastic cells. To inquire whether OGF modulates anchorage-independent growth, HT-29 human colon cancer cells were grown in soft agar and subjected to this peptide. In contrast to controls, HT-29 cells exposed to OGF had 57% fewer colonies, and these colonies were reduced in area by 75% [41]. Effects on anchorage-independent growth by OGF observed for the HT-29 cells were observed for pancreatic adenocarcinoma cells (MiaPaca-2, Panc1) and squamous cell carcinoma of the head and neck (CAL-27). These results using anchorage-independent conditions suggest that OGF-OGFr exerts its inhibitory actions on both anchorage-independent and anchorage-dependent models of neoplasia.

1.3.4.2.2 Abnormal growth: Tonic Activity

The OGF-OGFr system has a tonic inhibitory action on growth of head and neck squamous cell carcinoma (HNSCC) cells. Log-phase cultures of HNSCC cells UM-SCC-1, SCC-4, SCC-9, SCC-25 and UM-SCC-38 were treated with OGF or NTX [37]. Two days later, OGF had significantly reduced the number of cells in all cell lines by approximately 19-36% with respect to control values, while NTX elevated the number of cells from control levels by 14-30% [37]. Since OGF is a constitutively expressed native

opioid, blockade of OGFr by NTX and this blockade of OGF actually increased cell numbers. These results support that OGF has tonic activity on cell growth.

1.3.4.2.3 Abnormal growth: Reversibility

The OGF-OGFr system has a tonic, reversible inhibitory action on growth of pancreatic cancer cells. After 48 hours exposure to OGF, half of the plates of MiaPaca-2 cells had their media removed and fresh media added without OGF; another half of the cultures continued to receive new media and OGF. At 96 hours, the OGF and OGF-reversal groups differed from controls. The OGF-reversal group had 16% more cells than in the OGF group continuing with OGF exposure [42]. These results support that the inhibitory effects of OGF are reversible and that OGF does not lead to cytotoxicity or cell death.

1.3.5 Pathways of cellular maintenance

1.3.5.1 Proliferation

The growth function of the OGF-OGFr system was associated with both inhibition of cell proliferation and DNA synthesis. The role of OGF-OGFr axis on cell proliferation was measured by BrdU, which was used to determine whether the OGF-OGFr was effective in regulating DNA synthesis. The number of BrdU-positive basal cells in the peripheral epithelium of the OGFr-transfected cornea of rat was one-third of that in the naive cornea [28]. This result indicated that overexpression of OGFr shifts the balance of the OGF-OGFr axis resulting in down-regulation in terms of cell proliferation events [28] and supported at a molecular level the target of OGF-OGFr axis being DNA synthesis.

1.3.5.2 Apoptosis

Three human cancer cell lines: MiaPaCa-2 pancreatic adenocarcinoma, HT-29 colon adenocarcinoma, and CAL-27 squamous cell carcinoma of the head and neck, were treated with OGF. The effects on apoptosis were evaluated by TUNEL assay and Annexin V analysis; necrosis was evaluated by trypan blue. The results indicated that the inhibitory action of OGF on cell growth in tissue culture was not due to alterations in apoptotic or necrotic pathways [43].

1.3.5.3 Differentiation

The role of OGF-OGFr axis on differentiation was examined in three human cancer cell lines: SK-N-SH neuroblastoma, SCC-1 and CAL-27 squamous cell carcinoma of the head and neck. Cells were treated with OGF for up to 6 days and effects on differentiation were evaluated by neurite formation, process lengths, as well as the presence of betaIII-tubulin and involucrin. The results indicated that the inhibitory actions of OGF on cell growth in tissue culture are not due to alterations in differentiation pathways [44].

1.3.5.4 Migration

On going studies suggest that OGF has no effect on migration [personal communication].

1.3.5.5 Summary

The OGF-OGFr axis does not induce necrosis and apoptosis [43] or alter differentiation [44]. Thus, the present study was designed to assess the mechanism of the OGF-OGFr axis on the cell cycle progression.

1.4 Pathways of Cellular Maintenance Involved In the OGF-OGFr Axis

Our understanding of the mechanisms of action of the OGF-OGFr system on inhibition of cell growth are unclear. Here, we focused on the OGF-OGFr axis and cell cycle progression.

1.4.1 Cell Cycle

The mammalian cell division cycle is divided into G_1, S, G_2 and M phases: S phase for DNA synthesis, M phase for mitosis, and two gap phases G_1 (before DNA synthesis) and G_2 (before mitosis). In addition, there is a resting phase termed G_0. Progression through each phase of the cell cycle is controlled by the activity of different cyclin-dependent kinases (CDKs) and their regulatory subunits (cyclins). The decision to proliferate in normal mammalian cells is made during the G_1 phase of the cell cycle [45]. Cancer cells often abandon these controls and tend to remain in cycle [46] thus resulting in immortalized growth. Previous studies in our lab reported that OGF exposure of cancer cells resulted in an increased proportion of cells in the G_0/G_1 phase with a compensatory reduction in the proportion of cells in S and G_2/M phases [47]. These results suggested that one mechanism of action of the OGF-OGFr axis may be directed at the G_0/G_1 phase of the cell cycle [47].

1.4.2 Regulation of G1 phase

Cell passage through the G1 restriction point and entry into the S phase is controlled by cyclin-dependent kinases (CDKs), including CDK4 and the homologous CDK6 as well as CDK2 [48]. CDK activity is regulated by its association with cyclins, and the phosphorylation status and interaction with specific CDK inhibitory proteins.

CDK4 and CDK6 are activated by D-type cyclins at early to mid-G1 phase, whereas CDK2 is activated by E- and A-type cyclins during late G1 and S phase [48]. Upon mitogen stimulation, cyclin D protein is expressed. It binds and activates CDK4/6, which then initiates the phosphorylation of its target protein, the retinoblastoma protein, Rb. After mid-G1 phase, cyclin E-CDK2 becomes active and completes this process by phosphorylating Rb on additional sites [48]. In resting cells, Rb is present in a hypophosphorylated form that binds and inactivates the transcription factor E2F. Hyperphosphorylated Rb releases E2F, which stimulates the transcription of a number of gene products necessary for DNA synthesis [49]. One of these products is cyclin E, which then binds to CDK2. This complex also phosphorylates Rb, leading to a proliferative cascade that results in the cells entering S phase [49]. Therefore, Rb is a key regulator for cell cycle G1 phase.

Cyclin dependent kinase inhibitors (CKIs) are responsible for much of the negative regulation of the cell cycle. There are two families of CKIs, CIP/KIP family and INK4 family. CIP/KIP family includes p21, p27 and p57, which inhibit Cdk4/6-cyclin D and cdk2-cyclin E complexes. INK4 family includes p16, p15, p18 and p19, which selectively inhibit cdk4/6-cyclin D complex [50]. Unique among the CKI inhibitors, p16 is a tumor suppressor associated with many cancers [51].

1.4.2.1 Retinoblastoma protein

Retinoblastoma (Rb) is a key regulator of cell cycle progression. Human genetic studies of retinoblastoma syndrome led to the cloning of the gene for the retinoblastoma protein Rb in 1986, which encodes a protein of 928 amino acid [52]. The Rb protein shares regions of homology with two other proteins, p107 and p130. These three proteins

are all targeted by viral onco-proteins for cell transformation [52]. These three proteins are collectively called the “pocket proteins” [53] because the shared sequences for onco-protein binding are called the “pocket”. Studies showed that all three pocket proteins associate with members of the E2F transcription factor family, and this common activity may provide the molecular basis for many of their overlapping functional properties [53].

E2F repression has been widely accepted as the mechanism by which Rb suppresses cell proliferation at G1-S transition [52]. In early G1 phase, Rb is hypo-phosphorylated and interacts with E2F. When CDKs are activated during G1-S transition, Rb becomes hyper-phosphorylated and loses its ability to interact with E2F. E2F family of transcription factors consists of E2F and DP sub-groups [52]. E2F1, 2 and 3 are traditionally believed to be governed by Rb while E2F4 and 5 governed by p107/130 [52]. Releasing of E2F transcription factors leads to the transcription of genes such as thymidine kinase, DNA polymerase, cyclin A and E, cdk2, c-myc and E2F1, which are necessary for G1-S transition [54].

The function of the Rb protein is regulated mainly by Rb phosphorylation status [55-57]. Rb can be phosphorylated by several different cyclin-Cdk combinations, including cyclin D in combination with Cdk4 or Cdk6, cyclin E or cyclin A associated with Cdk2 [58]. There are 16 consensus CDK phosphorylation sites (Ser/Thr-Pro motifs) on Rb [59]. Using a microinjection-based cell cycle arrest assay, Connell-Crowley and her colleagues [57] found that S^{795} residue phosphorylation played a critical role in Rb inactivation . Mutation of S^{795} to alanine prevented Rb inactivation by CDK4 phosphorylation in the microinjection assay [57]. Using polyclonal antibodies that recognize unique phosphorylation sites within Rb protein, Pan and his colleagues found

that S^{780}, S^{795} and $S^{807/811}$ were functioning at the G1-S transition boundary [60]. Studies showed that CDK4/cyclin D was a very efficient kinase for S^{795} [57], as well as CDK2/cyclin [61]. Studies also showed that $S^{807/811}$ was specifically phosphorylated by CDK4/cyclin D, not by CDK2/cyclin [59]. Using two-dimensional tryptic phosphopeptide maps of Rb, Zarkowska and his colleagues [59] found that T^{821} were specifically phosphorylated by CDK2/cyclin, not by CDK4/cyclin D. This evidence suggests that phosphorylation at particular residues of Rb may be affected by the binding of its interacting partners.

Evidence showed that CDK4/cyclin D, CDK2/cyclin E or CDK2/cyclin A cooperate to neutralize the ability of Rb to suppress cell growth [62]. Phosphorylation of the C-terminal region of Rb by Cdk4/cyclin D triggers an initial intramolecular interaction with the central pocket domain, and this facilitates further phosphorylation by Cdk2/cyclin E or cyclin A [63].

1.4.2.2 $p16^{INK4a}$

The p16 protein was originally identified as a CDK4 interacting protein that inhibits CDK4 kinase activity [64]. In 1994, a tumor suppressor gene, designated *MTS1* (multiple tumor suppressor 1), was located on human chromosome 9p21 [65]. Today, this gene is known as p16INK4a and serves as prototype for the INK4 (inhibitors of CDK4) family of cell cycle inhibitors [66].

Regulation of CDK4/6 activity by cyclin D and p16 was extensively studied. CDKs have an N-terminal lobe, a C-terminal domain lobe and a deep cleft at the junction of the two lobes. This cleft harbors the ATP binding site and the catalytic domain. A PSTAIRE sequence and a regulatory loop (the T loop) that contains an activating

phosphorylation site are important regulatory elements. Monomeric CDKs are inactive. Binding to cyclins activates the CDKs by inducing conformational changes. These changes include rotation of the T-loop to open the catalytic cleft to allow binding of ATP and to expose its phosphorylation site. Binding of p16 to CDK4/6 prevents their interaction with their cognate cyclins. However, there is no overlap between the p16 and cyclin D binding sites. Instead, p16 binding induces allosteric changes by rotating the two CDK lobes, thus mislocating the cyclin-interacting sequences, and distorting the ATP binding site [66]. Decreased CDK4/6 activity leads to less Rb phosphorylation, which in turn induces G1 phase arrest.

p16 plays a role in loss of cell adhesion, in cell spreading, and in angiogenesis [67]. Elevated levels of p16 are observed in senescent cells, suggesting that p16 is responsible for this state of permanent growth arrest [67]. p16 plays an important role in tumorigenesis. Silencing of the p16 gene are frequently found in a variety of human malignancies and transformed cells [67]. Studies showed a high frequency of homozygous deletions in the p16 gene in cell lines derived from a variety of human tumors, including melanomas, lung, brain, breast, kidney, and ovarian cancers, osteosarcomas, and leukemia [68]. In addition to homozygous deletion and inactivating mutations, recent studies have identified inappropriate methylation of the p16 promoter as a major mechanism of gene silencing [67].

p16 has been considered as a target for potential anticancer drugs. Indole-3-carbinol (I3C), a naturally occurring component of Brassica vegetables, strongly stimulated the production of the p16 CDK inhibitor and induces a block in G1 cell cycle in LNCaP prostate carcinoma cells [69]. Recently, studies showed that transfection of

exogenous wild p16 gene induced the bladder cancer cells arrested in G0/G1 phase [70]. Here in our *in vitro* study, we will show that the growth inhibitory effects of the OGF-OGFr axis in HNSCC cells are associated with induction of p16/CDK4 inhibitor resulting in decreased Rb phosphorylation.

1.4.2.3 $p21^{WAF1/CIP1}$

$p21^{WAF1/CIP1}$ is a well-characterized cyclin-dependent kinase inhibitor that belongs to the Cip/Kip family of CDK inhibitors [71]. In 1993, Xiong and his group [72] found that p21 inhibits the activity of each member of the cyclin/CDK family. Furthermore, overexpression of p21 inhibits the proliferation of mammalian cells [72]. More results indicate that p21 is a potent, tight-binding inhibitor of CDKs and can inhibit the phosphorylation of Rb by cyclin A-Cdk2, cyclin E-Cdk2, cyclin D1-Cdk4, and cyclin D2-Cdk4 complexes [73]. However, p21 also stabilizes interactions between CDK4/6 and cyclin D thereby promoting the formation of active complexes in a concentration-dependent manner [74].

p21 has been shown to inhibit the growth of malignant cells *in vitro* and *in vivo* [75, 76]. Using recombinant adenoviral system (rAd-p21), Joshi et al. [75] found the growth of two pancreatic tumor cell lines can be inhibited by rAd-p21 *in vitro*, with significant numbers of tumor cells reverting from S to G0/G1. Studies also showed that TGF-beta induced $p21^{waf1}$ expression in Panc1 cells and subsequent growth inhibition [76].

p21 is a transcriptional target of p53 and plays an important role in mediating growth arrest in response to DNA damage agents [77, 78]. p21-deficient cells fail to undergo cell cycle arrest in response to p53 activation after DNA damage [79]. In

addition, p21 also response to p53-independent pathway [80]. Studies showed that serum or individual growth factors such as platelet-derived growth factor, fibroblast growth factor, and epidermal growth factor but not insulin were able to induce $p21^{WAF1/CIP1}$ in quiescent p53-deficient cells as well as in normal cells [80]. These results suggested the existence of two separate pathways for the induction of $p21^{WAF1/CIP1}$, a p53-dependent one activated by DNA damage and a p53-independent one activated by mitogens at the entry into the cell cycle [80]. Furthermore, p21 also plays an important role at the G2/M phase transition [81, 82].

Despite being a central player in cell cycle regulation, p21's role in tumorigenesis is not clear. Mutations in p21 are extremely rare in human malignancies [83]. Various mechanisms exist to regulate the levels of p21 in a cell, including transcriptional regulation, epigenetic silencing, mRNA stability, and ubiquitin-dependent and – independent degradations of the protein [71]. Here in our *in vitro* study, we will show that the growth inhibitory effects of the OGF-OGFr axis on human pancreatic cancer are associated with induction of p21 expression that, in turn, repressed the Rb phosphorylation.

1.5 Head And Neck Squamous Cell Carcinoma (HNSCC)

Head and neck cancer is the sixth most common malignancy in the world and 90% of these are of squamous cell derivation [84]. It is an epithelial malignant disease arising from the mucosa of the upper aerodigestive tract (oral cavity, larynx, oropharynx and hypopharynx). The overall 5-year survival rate for patients with this type of cancer is

among the lowest of the major cancer types and has not improved dramatically during the last decade.

Patient survival in head and neck squamous cell cancer (HNSCC) has not changed significantly in many years, despite progress in surgical, radiotherapy and chemotherapy techniques [84]. The low rate of survival of patients has highlighted the need for new approaches for diagnosis and treatment. A current focus of research is trying to find some markers to serve as selective targets for the therapy of HNSCC, such as the use of adenoviral vectors to restore p53 expression, anti-EGFR immunotherapy and small molecule kinase inhibitors [85]. Other research efforts are trying to use immunotherapy to combat the disease [84]. These are in various stages of testing and clinical trials.

At present, the role of p16 in HNSCC carcinogenesis and progression has not been clearly established [86]. Studies showed a high frequency of homozygous deletions in the p16 gene in HNSCC cell lines [87]. However, studies also showed that genetic alterations leading to p16 inactivation have been detected in 10% to 20% of primary HNSCC [68, 88, 89]. Studies also revealed that transfection of p16 resulted in marked growth inhibition in three HNSCC cell lines and a marked increase in cells in G0/G1 phase [90]. These results support that p16 plays a growth inhibitory role in HNSCC.

1.6 Pancreatic Adenocarcinoma

Cancer of the pancreas is the fourth leading cause of cancer death in the United States. Histologically, the pancreas is divided into the exocrine pancreas and the endocrine pancreas. Most pancreatic cancer arises from the exocrine pancreas, consisting of ducts and acini. Tumors originating from the epithelial lining of the pancreatic duct

represent 85% of pancreatic cancers [91]. The overall 5-year survival of pancreatic cancer is 0.4% [92]. Despite the medical advances made over the last 20 years, pancreatic cancer would appear to have benefited the least in terms of survival. For these and other reasons, cancer of the pancreas has been called “the challenge of the twenty-first century” [92].

Currently, potentially curative surgical resection is possible in only about 10%-15% of patients [92]. Radiotherapy and chemotherapy regimens have not shown improved survival in advanced disease [92]. The low rate of survival of patients has highlighted the need for new approaches for diagnosis and treatment. Certain biological markers of pancreatic cancer are under evaluation, such as growth factors and their receptors, tumor suppressor genes, angiogenic factors and apoptotic genes [91]. For example, loss of expression of p16 is observed in most pancreatic tumors [91] and it appears to be a relatively early event in the progression of pancreatic cancer [93]. Loss of p21 activity has been observed in approximately 20%-40% of pancreatic tumor specimens [94-96].

Many studies found that novel anticancer agents are targeting p21 to inhibit pancreatic cancer cell growth. Studies showed that vitamin D3 analog, maxacalcitol and calcitriol, up-regulate p21, which in turn could block the G1/S transition and induce growth inhibition in pancreatic cancer cells [97]. Studies also showed that DIM-C-pPhCF3 significantly inhibited G0/G1 to S phase progression, and this was associated with decreased retinoblastoma protein phosphorylation and increased p21 protein and mRNA expression [98]. These results support that p21 has growth inhibitory activity in pancreatic tumor.

1.7 Summary

The OGF-OGFr axis plays an important role in cellular renewal during homeostasis, wound healing, development, and angiogenesis, and in the growth and progression of cancer [6]. Knowledge about the biology of the OGF receptor and its interaction with the cell cycle, as well as understanding the mechanism of OGF as an inhibitory growth factor will provide significant insight into understanding the etiology and pathogenesis of some neoplasias.

1.8 Hypothesis and Specific Aims

1.8.1 Hypothesis

Our *long-range goal* is to understand the OGF-OGFr biological activities in cancer, and to utilize OGF with chemotherapy agents as an appropriate anti-cancer treatment. As our next objective in pursuit of this goal, we propose in these studies to investigate the effect of OGF-OGFr signal transductions on cell growth inhibition. The *central hypothesis* of this study is that OGF-OGFr inhibits cell proliferation through cell cycle regulatory proteins. In particular, on the basis of work that will be presented in this thesis, we demonstrate that the OGF-OGFr axis inhibits cell proliferation by interacting with the Rb regulatory pathway.

1.8.2 Specific Aims

To determine which phases of cell cycle are related to the effect of OGF-OGFr induced growth inhibition.

To determine what major pathways are related to the effect of OGF-OGFr induced growth inhibition.

To determine what specific components in that pathway are related to the effect of OGF-OGFr induced growth inhibition.

At the conclusion of this study, we expect to have knowledge on precisely how the OGF-OGFr axis induced signal pathways in the cell cycle.

1.8.3 Significance

OGF-OGFr's inhibitory function on cell proliferation makes it an attractive therapeutic target for the treatment of a number of human cancers. The amount of work devoted to the study of OGF-OGFr in the last decade has yielded a wealth of information that may ultimately prove beneficial for clinical purposes. However, some questions remain to be answered, which will improve our ability to therapeutically use OGF in cancer patients. These include understanding the downstream targets of OGF-OGFr and the arising signal transduction pathways involved in OGF-OGFr inhibition of cell growth. The data generated from this *in vitro* model for OGF-OGFr induced inhibitory effects will provide insight into the effect of OGF-OGFr on cell cycle regulatory mechanisms.

CHAPTER II

OGF-OGFR AXIS UTILIZES THE p16 PATHWAY TO INHIBIT PROGRESSION OF HUMAN SQUAMOUS CELL CARCINOMA OF THE HEAD AND NECK

Abstract

Opioid growth factor (OGF) is an endogenous opioid peptide ([Met^5]-enkephalin) that interacts with the OGF receptor (OGFr), and serves as a tonically active negative growth factor in neoplasia. Previous studies showed that OGF inhibits the growth of human head and neck squamous cell carcinoma (HNSCC) *in vitro* and *in vivo*, and is targeted to cell proliferation. To clarify the mechanism by which OGF inhibits cell replication, we investigated the effect of OGF on cell cycle activity in the HNSCC cell line SCC1. In cultures synchronized with nocodazole, flow cytometry revealed that OGF treatment resulted in fewer cells exiting the G1 phase of the cell cycle in comparison to controls ($p<0.05$). The present studies focused on the signaling pathways used by OGF in the regulation of the G1 to S transition. Studies using SCC1 cells suggest that OGF decreased the phosphorylation of retinoblastoma protein (Rb) ($p<0.05$) without changing the total Rb expression. This change was correlated with reduced cdk4 kinase activity while the total cdk4 expression did not change. Moreover, OGF treatment increased cyclin-dependent kinase inhibitor (CKI) p16 protein expression 2-fold in comparison to controls ($p<0.05$), but had no significant effect on p15, p18, p19, p21 or p27 protein expression. Western blot analysis did not detect p57 protein in SCC1 SCCHN cells. Blockade of OGF-OGFr interactions with the short-acting opioid antagonist, naloxone (NAL), revealed that increased expression of p16 protein by OGF was completely abolished by NAL. NAL alone had no effect on p16 expression suggesting that this regulation of p16 was an opioid receptor mediated event. Inhibition of p16 (INK4a) activation by p16 specific siRNA blocked OGF inhibitory action on proliferation of SCC1, CAL-27 and SCC4 HNSCC cells. Cultures treated with negative control siRNA,

which had no effect on p16 expression, did not block OGF's growth inhibitory action. Collectively, these results indicate that the receptor-mediated, growth inhibitory effects of the OGF-OGFr axis in HNSCC cells are associated with induction of p16/cdk-4 inhibitor resulting in decreased Rb phosphorylation. These data revealed that the target of cell proliferative inhibitory action of OGF in human HNSCC is by the way of a cyclin dependent kinase inhibitory pathway. Because most human HNSCC tumors retain p16, OGF may be a valuable therapeutic agent in this setting.

Introduction

Endogenous opioid peptides are known to be potent regulators of growth, as well as neuromodulators and neurotransmitters [6]. To distinguish the role of [Met^5]-enkephalin, as a growth factor in neural and non-neural cells and tissues, and in prokaryotes and eukaryotes, this peptide was termed opioid growth factor (OGF) [6]. The biological activities of OGF involve OGF receptor (OGFr) and can be blocked by naloxone (NAL) [17] or naltrexone (NTX) [26]. OGFr is an integral membrane protein that is associated with the nucleus. Binding assays have exhibited ligand selectivity, saturability, stereospecificity, competitive displacement, and the presence of an endogenous agonist [6]. After binding to OGFr, OGF functions to set off a signaling cascade related to growth [6].

The mammalian cell division cycle is divided into G1, S, G2 and M phases. Cell passage through G1 restriction point and entry into S phase is controlled by cyclin-dependent kinases (CDKs), including CDK4 and the homologous CDK6 as well as CDK2 [48]. CDK activity is regulated by its association with cyclins, phosphorylation

status and interaction with specific inhibitory proteins (CKIs). CDK4 and CDK6 are activated by D-type cyclins at early to mid-G1 phase, whereas CDK2 is activated by E- and A-type cyclins during late G1 and S phase [48]. CKIs are responsible for much of the negative regulation of the cell cycle. There are two families of CKIs, CIP/KIP family and INK4 family. CIP/KIP family includes p21, p27 and p57, which inhibit Cdk4/6-cyclin D and cdk2-cyclin E complexes. INK4 family includes p16, p15, p18 and p19, which selectively inhibit cdk4/6-cyclin D complex [50]. Unique among the CKI inhibitors, p16 is a tumor suppressor associated with many cancers [51].

Head and neck squamous cell carcinoma (HNSCC) represents 6% of all cancers [85]. It is an epithelial malignant disease arising from the mucosa of the upper aerodigestive tract (oral cavity, larynx, oropharynx and hypopharynx) [99]. The overall 5-year survival rate for patients with this type of cancer is among the lowest of the major cancer types and has not improved dramatically during the last decade [85].

OGF inhibits cell growth, including normal cells, such as epidermal cells [20], and cancer cells, such as neural tumor cells [7], colon cancer [100], pancreatic cancer cell [36], renal cell [38] and HNSCC cells [101]. Previous studies indicate that the inhibitory (OGF) action on cell growth in tissue culture is not due to alterations in apoptotic pathways [43] or differentiation [44]. OGF has been reported to inhibit cell cycle progression of a variety of neoplastic cell lines including HNSCC [47]. However, the cell cycle progression and OGF-OGFr signaling pathways are unknown. To examine which pathways are involved, OGF on cell cycle activity in the HNSCC cell lines are investigated. Here, we identify that decreased Rb phosphorylation occurs in OGF treatment of HNSCC, occurring as a result of decreased Cdk4 kinase activity due to

increased expression of p16. Increasing p16 effect could be blocked by naloxone. Furthermore, targeted decrease of p16 using siRNA blocked OGF inhibiting action. Thus, these studies identify p16 as a selective target in OGF-OGFr inhibitory action and provide a mechanistic basis for OGF treatment for head and neck cancer patients.

Materials and Methods

Cell Culture. Human head and neck squamous cell carcinoma (HNSCC) cells, SCC1 and CAL27 were maintained in logarithmic phase growth in Dulbecco's modified medium (DMEM; Penn State University). The culture medium for SCC4 consisted of 1:1 Ham's F-12 medium (Mediatech, Herndon, VA) and DMEM (HFDM) supplemented with 0.1 μg/ml hydrocortisone (Sigma, St. Louis, MO). SCC1 cells were obtained from University of Michigan; the other two cell lines were purchased from American Type Culture Collection, Manassas, VA. All media contained 10% fetal bovine serum (FBS; HyClone, Logan, Utah), 1.2% sodium bicarbonate (Penn State University) and 0.25% antibiotics (5000 units/ml penicillin, 5 μg/ml streptomycin and 10 μg/ml neomycin; Mediatech, Herndon, VA). Cell cultures were grown in a humidified atmosphere of 5% CO_2 at 37^{o}C.

OGF Treatment. [Met^5]-enkephalin (OGF) (Sigma, St. Louis, MO) was dissolved in sterile water at the concentration of 10^{-3} M as a stock solution. In all experiments, 1 μl of the stock OGF or 1 μl sterile water (vehicle control) was added per milliliter of medium and the final OGF concentration was 10^{-6} M.

Synchronization of Cells. SCC1, CAL27 and SCC4 cells were synchronized with 0.5 μg/ml nocodazole (Sigma, St. Louis, MO) for 24 hours; Cells were washed with complete media (plus serum) three times. Cells were released from growth arrest by addition of complete medium and some cultures were treated with OGF-supplemented media as described above.

Flow Cytometric Analysis of Cell Cycle. Synchronized SCC1 cells were treated with 10^{-6} M OGF for 14 hours. Cells were harvested with 0.25% trypsin-EDTA (Mediatech, Herndon, VA) and fixed with 70% ethanol at -20^{o}C for up to 7 days before DNA analysis. After the removal of ethanol by centrifugation, cells were washed with PBS (Penn State University). After centrifugation, cells were stained with a solution containing 1 mg/ml sodium citrate (Sigma, St. Louis, MO), 0.3% Triton-X (Sigma, St. Louis, MO), 0.1 mg/ml propidium iodide (PI) (Sigma, St. Louis, MO), 0.02 mg/ml ribonuclease A (Sigma, St. Louis, MO) at room temperature for 15 minutes. Stained nuclei were analyzed for DNA-PI fluorescence using a Becton Dickinson FACScan flow cytometer. Resulting DNA distributions were analyzed by Modfit Software for the proportion of cells in G0/G1, S and G2/M phases of the cell cycle.

Preparation of whole-cell extracts. Frozen cell pellets consisting of 2×10^6 cells per sample were thawed on ice and resuspended in 200 μl RIPA buffer (1X PBS, 10 μM IGEPAL, 1 mg/ml sodium dodecyl sulfate [SDS], 5 mg/ml deoxycholic acid), containing protease and phosphatase inhibitors (2 μg/ml aprotinin, 3 mg/ml phenylmethyl sulfonyl fluoride [PMSF], 1 mM sodium orthovanidate, 1 μM okadaic acid). All chemicals were

purchased from Sigma, St. Louis, MO. Samples were passed through a 25-gauge needle three times and then centrifuged at 14000 ×g for 20 min at 4°C and the supernatants were collected. Total protein concentrations were measured using the DC protein assay kit (Bio-Rad, Hercules, CA). For each sample, a 180 μl aliquot of the supernatant was removed and added to 36 μl 6× sample loading buffer (25 mg/ml DTT, 0.5 g/ml sucrose, 1.5 mg/ml EDTA, 50mg/ml SDS, 10 mg/ml bromophenol blue).

Western Blot Analysis and Chemiluminescence. Protein extracts (40 μg) were resolved by SDS-polyacrylamide gel (acrylamide/bis-acrylamide ratio, 30:0.8). Gel compositions for resolving various proteins were as follows: 7.5% gel to detect Rb, 12% gel for cdk4, cyclin D1, p27 or p21, and 15% gel for p15, p16, p18 or p19. Proteins were transferred to a nitrocellulose membrane (Whatman, Sanford, ME) for 1 hour at 100V in transfer buffer. Membranes were blocked for 1 hour at room temperature or overnight at 4°C in 5% BSA in TBS with 0.1% Tween. Membranes were incubated for 1 hour at room temperature or overnight at 4°C with primary antibodies. The following antibodies were purchased from commercial sources: phospho-Rb (Ser795), phospho-Rb (Ser807/811) (Cell Signaling Technology, Beverly, MA); phospho-Rb (Thr821) (Biosource, Camarillo, CA); cdk4, cyclin D1, p16 (Santa Cruz Biotechnology, Santa Cruz, CA); total Rb, p21, p27 (BD PharMingen, San Diego, CA); β-actin (Clone AC-15, Sigma, St. Louis, MO). The following dilutions of primary antibodies were used to detect respective proteins. 1:200 phospho-Rb (Ser795), 1:200 phospho-Rb (Ser807/811); 1:200 phospho-Rb (Thr821); 1:200 cdk4, 1:200 cyclin D1, 1:100 p16; 1:200 total Rb, 1:200 p21, 1:100 p27. Following the incubation with the primary antibody, blots were washed and exposed to

secondary antibody and visualized by chemiluminescence Western blotting detection system (Amersham, Piscataway, NJ). In order to determine equal loading of total protein samples, blots were reprobed with monoclonal antibody against β-actin at a dilution of 1:2000. If necessary, membranes were stripped in stripping buffer (62.5 mM Tris-HCL and 100 mM β-mercaptoethanol/2% SDS, pH6.7) at 50^{o}C before being reprobed.

Immunoprecipitation. For immunoprecipitating protein complexes, cell extracts were prepared as follows: 2×10^6 cells per sample were rinsed in cold PBS once followed by lysis in 100 μl NP40 immunoprecipitation buffer (1% NP-40, 50 mM Tris-HCl [pH7.4], 150 mM NaCl, 1 mM EDTA, 10 mM NaF, 2 μg/ml antipain, 1 mM sodium orthovanidate, 2 μg/ml aprotinin, 2 μg/ml leupeptin, 1 μg/ml pepstatin A, 1 μM okadaic acid, 1 mM PMSF, 1 mM dithiothreitol [DTT]). All chemicals were purchased from Sigma. Samples were collected and transferred into a 1.5-ml microcentrifuge tube. Supernatants were collected by centrifugation at 10000 ×g for 15 min at 4^{o}C. Protein concentrations were measured using the Bio-Rad Protein Assay (Bio-Rad, Hercules, CA).

For each immunoprecipitation reaction mixture, a total of 500 μg of protein extract was used. The volume was made up to 1 ml with NP40 immunoprecipitation buffer. The lysates were then subjected to immunoprecipitation using 10 μl polyclonal antibody against CDK4 prebound with agarose conjugate (sc-601 AC, Santa Cruz) for 60 min at 4^{o}C. Agarose beads were pelleted by centrifugation at 4500 rpm for 15 seconds and then washed three times with 500 μl ice-cold immunoprecipitation wash buffer (1% NP40, 50 mM HEPES, 150 mM NaCl, 1 mM EDTA, 1 mM DTT). After the final wash the agarose beads were resuspended in 20 μl of 2× sample loading buffer (0.5M Tris-HCl

(pH 6.8), 4.4% (w/v) SDS, 20% (v/v) glycerol, 2% (v/v) 2-mercaptoethanol, and bromophenol blue in distilled/deionized water) and the supernatants were loaded onto gels, transferred and blotted with candidate antibodies.

Rb kinase assay for CDK4 activity. An immune complex kinase assay was performed to measure immunoprecipitated CDK4 activity. Immunoprecipitation of samples was performed using polyclonal antibodies against CDK4 as described above. Immunoprecipitates were washed three times with immunoprecipitation wash buffer (described above) and then twice with 500 μl ice-cold RB kinase wash buffer (50 mM HEPES, 10 mM $MgCl_2$, 1 mM DTT), followed by incubation of the immunoprecipitates in a mixture of kinase buffer (25mM HEPES [pH7.4], 10mM $MgCl_2$), 5 μCi γ^{32}P-ATP, and Rb(769-921) (sc-4112, Santa Cruz) as the substrate for Cdk4. After incubation for 30 min at 30^0C, with occasional mixing, the reaction was stopped by the addition of 2× sample loading buffer (0.5M Tris-HCl (pH 6.8), 4.4% (w/v) SDS, 20% (v/v) glycerol, 2% (v/v) 2-mercaptoethanol, and bromophenol blue in distilled/deionized water). Samples were boiled for 5 min and then pelleted by centrifugation. Proteins in the reaction mixture were separated by a 10% SDS-PAGE gel. The cdk4 kinase activity pattern was visualized by autoradiography of phosphorylated Rb.

siRNA knockdown of $p16^{INK4a}$. The p16-targeted siRNAs (antisense:5'-acaccgcttctgccttttctt-3'; sense: 5'-gaaaaggcagaagcggtgttt-3') [102] were obtained as ready-annealed, purified duplex probes (Invitrogen, Carlbad, CA). The negative control siRNAs were from Ambion (Ambion, INC., Austin, TX). For transfection, 2 x 10^5 cells

per well were seeded in 6-well plates containing 1 ml media without antibiotics. For each well, 1 μl of siRNA stock (20 μM) was mixed with 175 μl DMEM (for SCC1 and CAL27) or HFDM (for SCC4) containing 1.2% sodium bicarbonate (serum free media). Next, 2 μl of Oligofectamine reagent (Invitrogen) was diluted in 15 μl serum free media by gentle mixing. The two solutions were gently combined and added to serum free media prewashed cells in each well. The final concentration for siRNA in each well was approximately 20 nM. Cells were incubated for 4h at 37^{o}C prior to the addition of OGF. Cultures were then left overnight before washing and adding 1ml fresh complete media either lacking or containing OGF. At the indicated time points, cells were collected for growth curves or Western blotting.

Cell counts. Cells were trypsinized on the indicated days and counted with a hemocytometer. Cell viability was assessed by trypan blue exclusion.

Densitometry Analysis. For Western blots, the optical density of each band was determined by densitometer and analyzed by the software QuickOne (Biorad). Each protein expression was normalized to β-actin from the same blot and protein expressions induced by OGF were compared to control.

$$\text{Fold of control} = \frac{\text{Protein from OGF treatment} / \beta\text{-actin from OGF treatment}}{\text{Protein from control} / \beta\text{-actin from control}}$$

For CDK4 kinase activity, the cdk4 kinase activity pattern was visualized by autoradiography of phosphorylated Rb. The optical density of each band was quantified

using a PhosphoImager. To quantify OGF induced cdk4 kinase activity, phosphorylated Rb was normalized to cdk4 protein and cdk4 kinase activities induced by OGF were compared to control.

$$\text{Fold of control} = \frac{\text{pRb from OGF treatment /Cdk4 from OGF treatment}}{\text{pRb from control/Cdk4 from control}}$$

Statistical analysis. The data are reported as mean ± SEM. Values were assessed by one-way analysis of variance (ANOVA) and Newman Kaul's post multiple comparison tests, at a significance level of $p<0.05$.

Results

OGF and cell cycle distribution of SCC1 cells

Continuous exposure to exogenous OGF inhibited the growth of SCC1 human HNSCC cells. Analysis of growth curves indicated that cell number was significantly depressed beginning at 72 h after addition of OGF; cell number in the OGF-treated wells was 87.5% compared to controls at 72 h, and 59.0% of controls at 96 h (Fig. 2.1A). Linear analysis of the data revealed mean doubling times for the control and OGF groups of approximately 21.6 h and 41.3 h, respectively.

Because OGF inhibits cell growth, we analyzed the effect of OGF on cell cycle distribution by flow cytometry (Fig. 2.1B and 2.1C). The percentage difference between OGF-treated and control cells in the G0/G1 phase increased from 22.0% to 34.0%, while the number of cells in the S phase decreased from 51.4% to 43.7%, the number of cells in

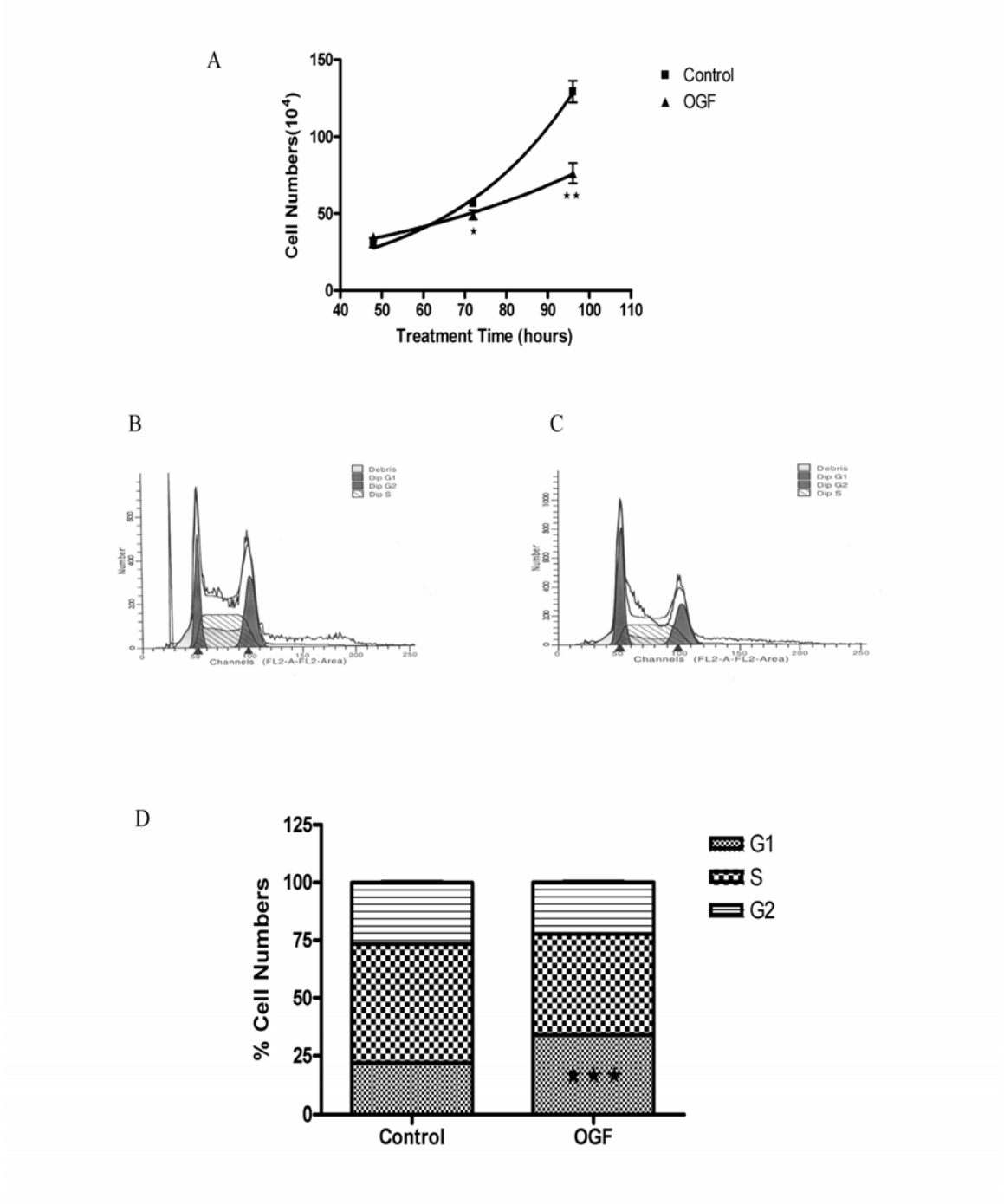

Figure 2.1 (A) Growth curves for SCC1 cells treated with OGF, or equivalent volume of sterile water (control) for a 96h period of time. Data represent means ± S.E.M for 3 samples per treatment group for each time point. Cell cycle distribution of SCC1 cells grown in either the absence (control) (B) or presence (C) of OGF, as determined by FACS analysis. (D) Data (percentage of cells in the indicated phases) are the means of three experiments. Significantly different from the control group at $p<0.05$ (*), $p<0.01$ (**) or $p<0.001$ (***).

the G2/M phase decreased from 26.6% to 22.4% (Fig. 2.1D). Thus, after 14 hours OGF treatment, the percentage of cells in G0/G1 increased by 11.9%, the number of cells in the S phase was decreased by 7.7%, and the percentage of cells in the G2/M phase was decreased by 4.2% relative to controls.

OGF and Rb phosphorylation

The phosphorylation of Rb protein is necessary for cells to progress from G1 into S phase. To elucidate the role of Rb in the OGF-induced SCC1 cell growth inhibition, Rb expression and the phosphorylated state of Rb was assessed in synchronized SCC1 cells. The results showed that the expression of total Rb protein was not decreased significantly after OGF treatment (Fig. 2.2). However, the level of phospho-Rb (Ser801/811), which was specifically phosphorylated by cdk4 in G1 phase [59], was significantly decreased by treatment with 10^{-6}M OGF after 6 hours (Fig. 2.3). Although phospho-Rb (pT821) was specifically phosphorylated by cdk2 in G1 phase [59], after OGF treatment, Western blot analysis showed that phospho-Rb (pT821) level did not change significantly between OGF treatment and controls (Fig. 2.3). These results suggest that cdk4/6, not cdk2, was involved in the OGF-induced cell cycle block at G1 phase in SCC1 cells.

OGF and cdk4 kinase activity

To verify whether OGF-induced downregulation of pRb was associated with changes of CDK4, CDK4 expression was measured by an *in vitro* kinase assay. The expression of CDK4 protein did not change significantly following OGF treatment (Fig.

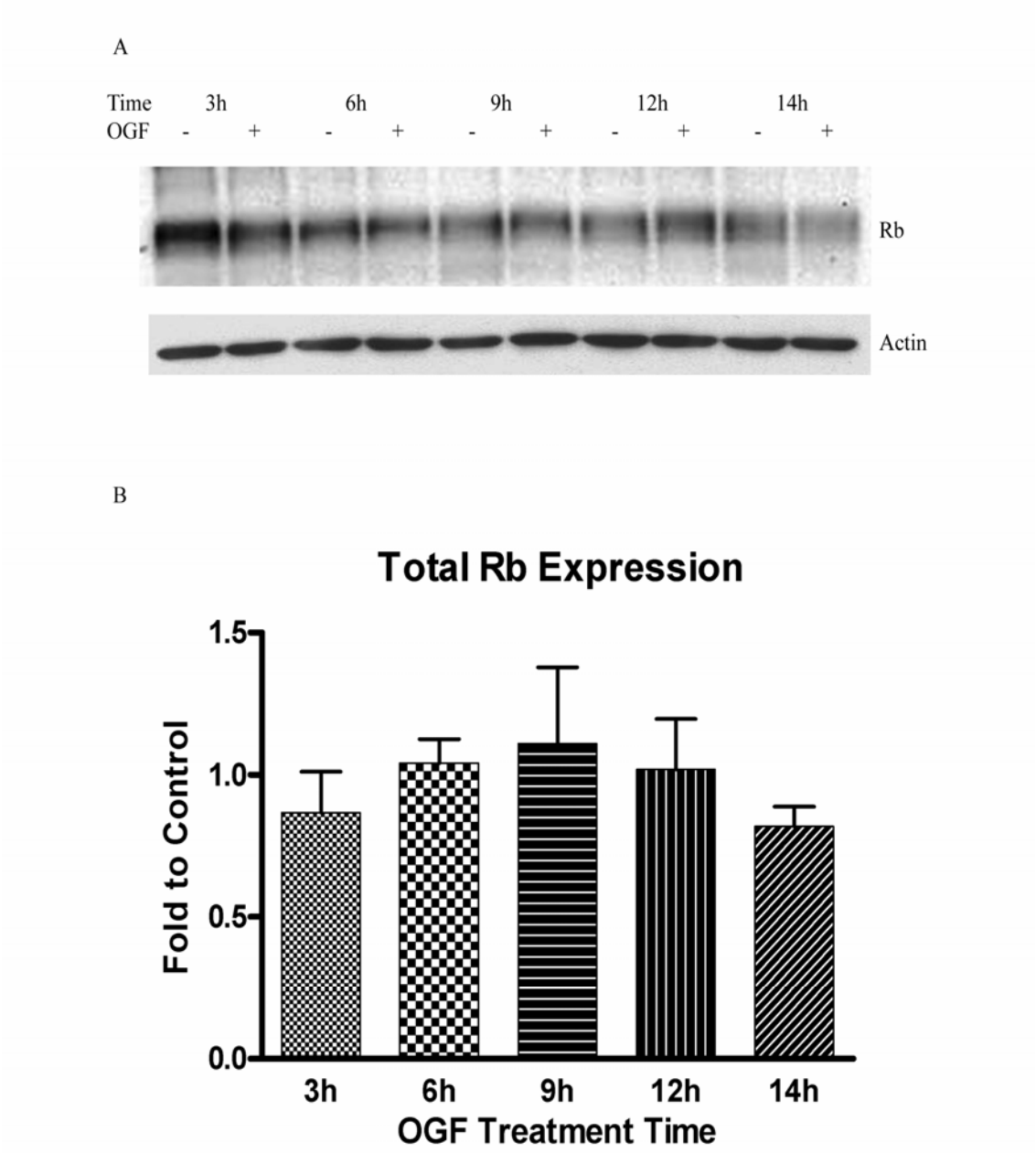

Figure 2.2 OGF and total Rb expression. (A) SCC1 cells were synchronized by nocodazole (0.5μg/ml) for 24 hours. Nocodazole were washed out and the cells were treated with or without OGF (10^{-6} M) for indicated times. Total proteins were resolved by SDS-PAGE and subjected to Western blotting of total Rb. (B) Densitometric analysis of the western blots was performed. OGF and total Rb expression was expressed relative to controls. Values represent means ± S.E.M for 3 independent experiments.

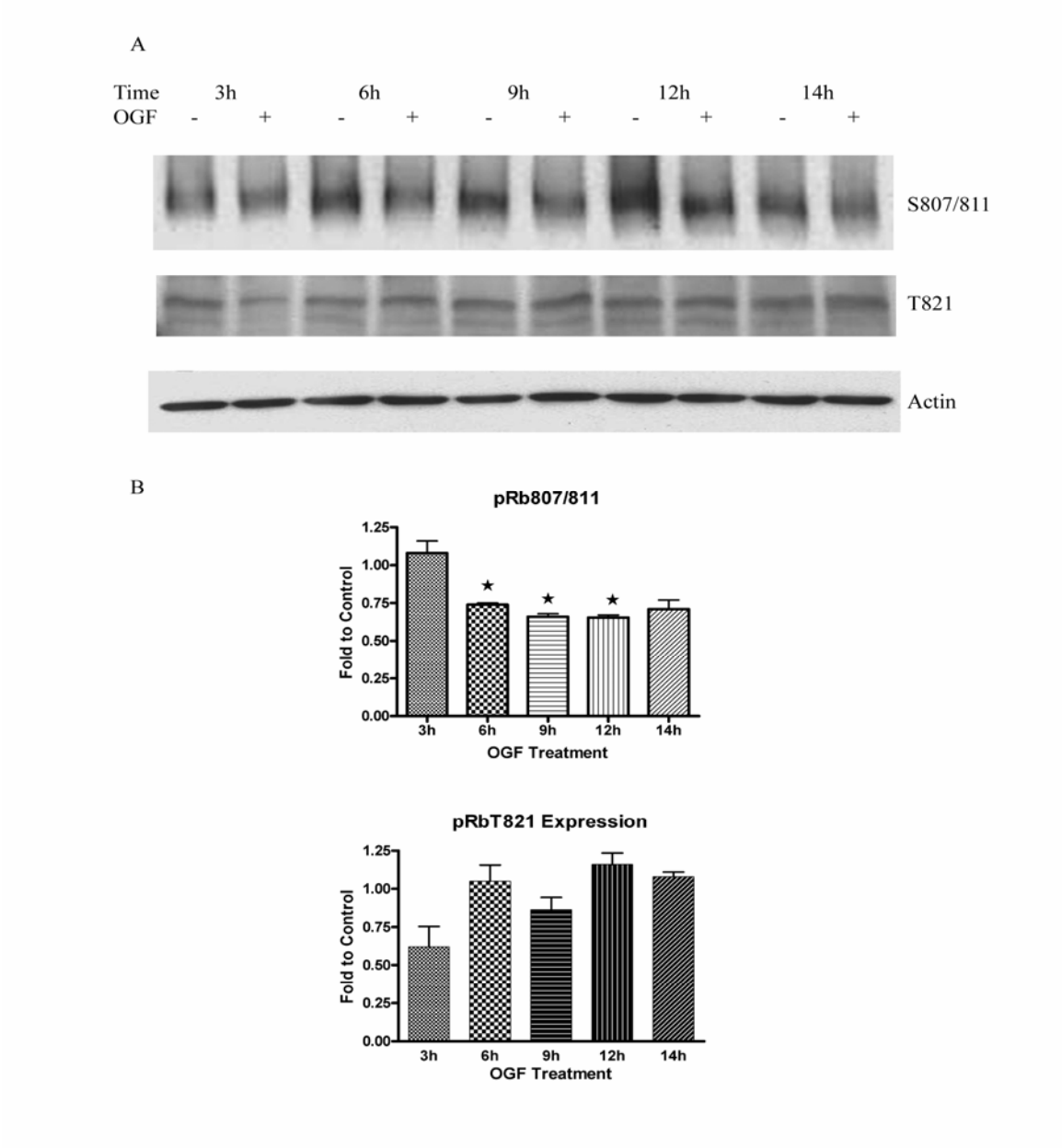

Figure 2.3 OGF decreased Rb phosphorylation (Ser807/811). (A) SCC1 cells were synchronized by nocodazole (0.5μg/ml) for 24 hours. Nocodazole were washed out and the cells were treated with or without OGF (10^{-6} M) for indicated times. Total proteins were resolved by SDS-PAGE and subjected to Western blotting of phosphorylated Rb (T821) or phosphorylated Rb (Ser807/811). (B) Densitometric analysis of the western blots was performed, and the OGF induced Rb phosphorylation was expressed relative to controls. Values represent means ± S.E.M for 3 independent experiments. Significantly different from the control group at $p<0.05$ (*).

2.4). When Rb was used as substrate in immunoprecipitation experiments performed with antibodies against CDK4, lysates from cells treated with OGF for 3 h showed a transient increase of CDK4 kinase activity, 6 h, 9 h and 12 h showed a marked decrease in CDK4 kinase activities (Fig. 2.5). Our previous data showed that OGF induced decreasing of Rb phosphorylation. These results suggested that OGF-mediated decrease of pRb was correlated with the reduction in CDK4 kinase activities.

OGF and G1 cell cycle regulatory proteins in SCC1 cells

Cyclins are positive regulators of cell cycle progression. To verify whether OGF-induced downregulation of CDK4 kinase activity was based on cyclin D1 expression, CDK4 immunoprecipitation and cyclin D1 Western blots were performed. The level of CDK4/cyclin D1 complex after OGF treatment revealed that OGF treatment did not change the formation of CDK4/cyclin D1 complex significantly (Fig. 2.6).

OGF and CDK inhibitor p16 expression in SCC1 cells

Cell cycle progression depends on both positive and negative regulators. Analysis of the expression of cell cycle inhibitors p15, p16, p18, p19, p21 and p27 revealed that OGF treatment resulted in an induction of p16 expression at 3 hours (Fig.2.7). Treatment with naloxone and OGF together, OGF-induced p16 expression was blocked (Fig. 2.8A, lane 2 and lane 4). This result showed that OGF-induced p16 upregulation was OGFr mediated. p16 is known as a tumor suppressor gene, functioning as a cell cycle inhibitor by forming heterotrimeric complexes with CDKs and cyclins. Therefore, the data suggested that under the effect of OGF, p16 protein level was upregulated, and activated

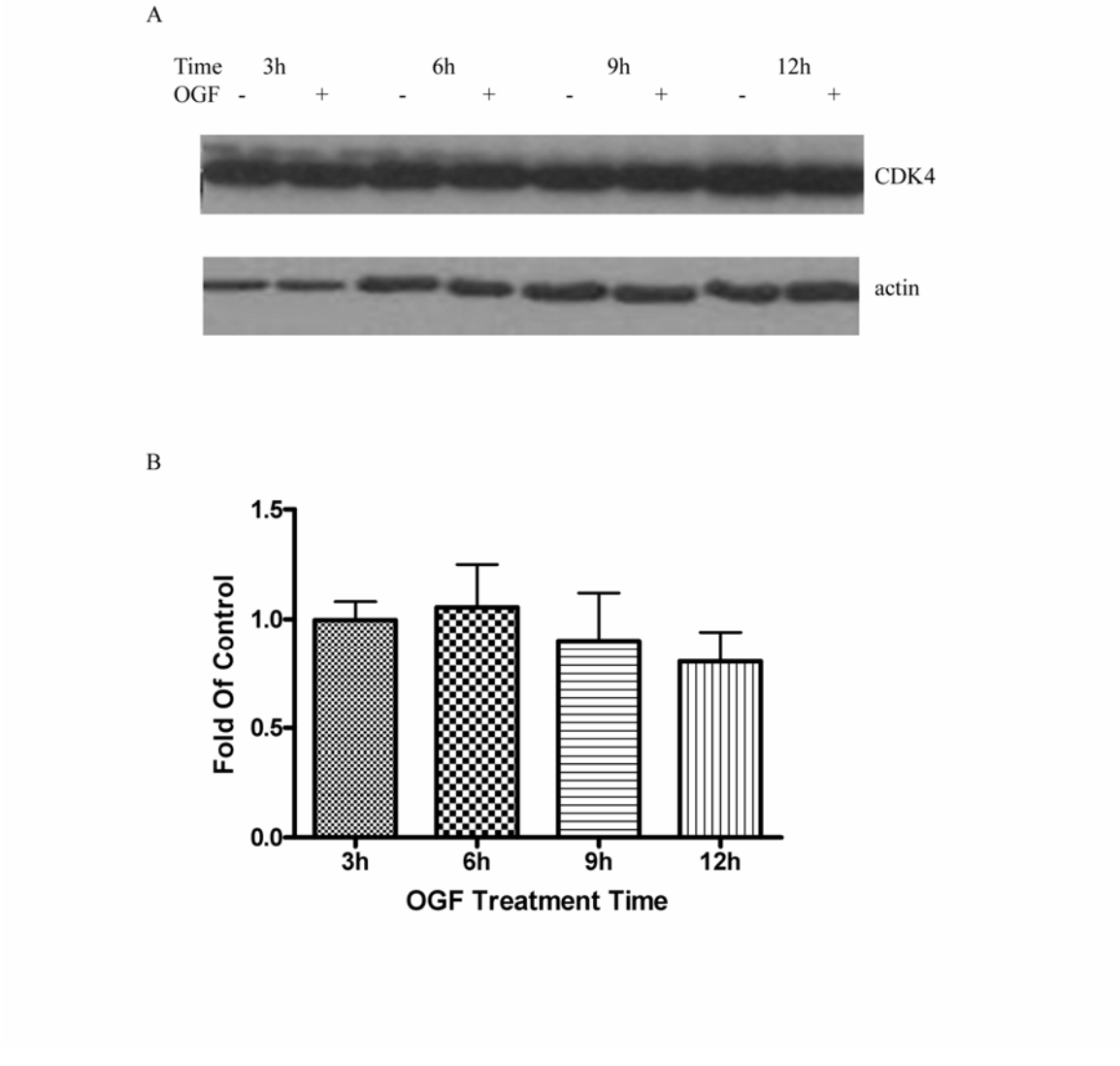

Figure 2.4 OGF and CDK4 expression. (A) SCC1 cells were synchronized by nocodazole (0.5μg/ml) for 24 hours. Nocodazole were washed out and the cells were treated with or without OGF (10^{-6} M) for indicated times. Total proteins were resolved by SDS-PAGE and subjected to western blotting of CDK4. (B) Densitometric analysis of the Western blots was performed. OGF and CDK4 expression was expressed relative to controls. Values represent means ± S.E.M for 3 independent experiments.

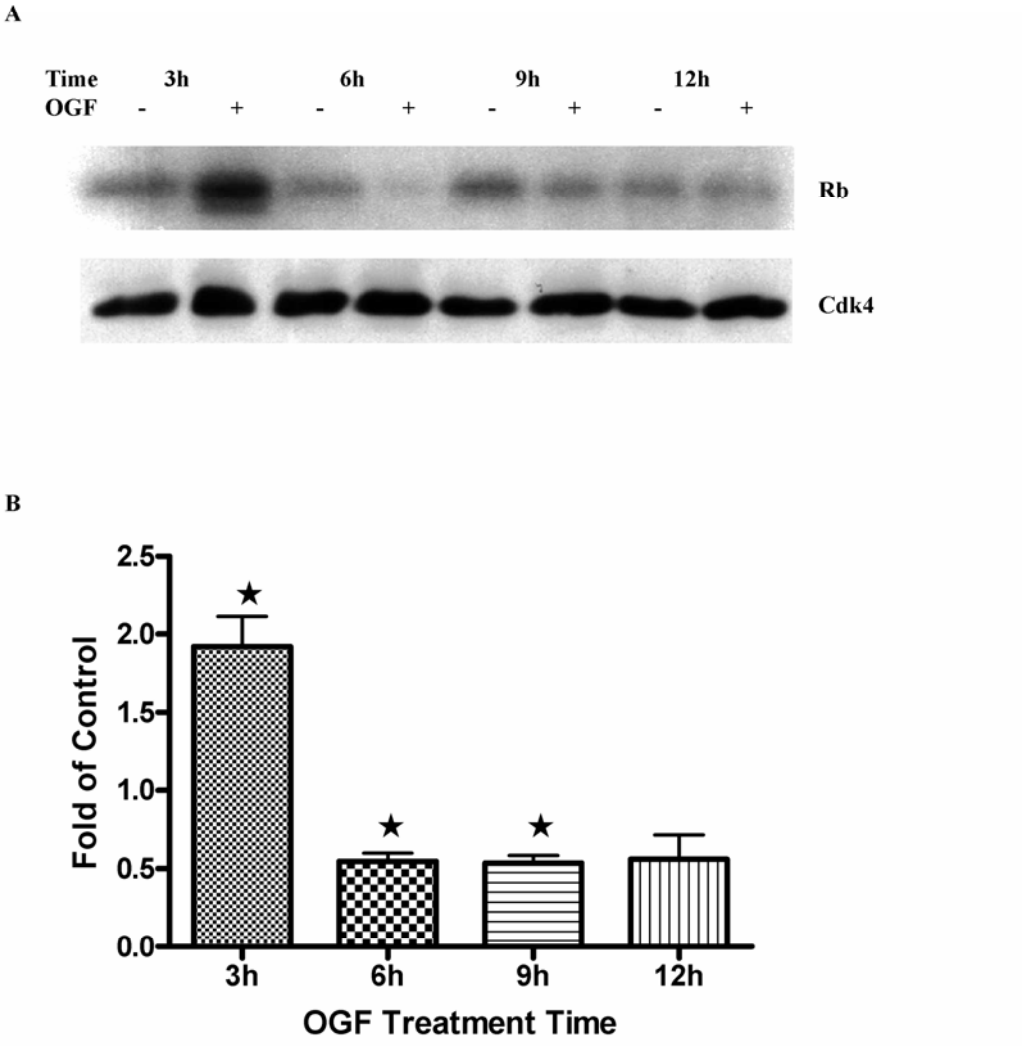

Figure 2.5 OGF and CDK4 kinase activity. (A) The CDK4 kinase activity was evaluated by measuring the capacity of phosphorylation of Rb protein in the presence of radioactive ATP. (B) Densitometric analysis was performed and the CDK4 activity was measured relative to controls. The quantitative data represent means ± S.E.M of 3 experiments. Significantly different from the control group at $p<0.05$ (*).

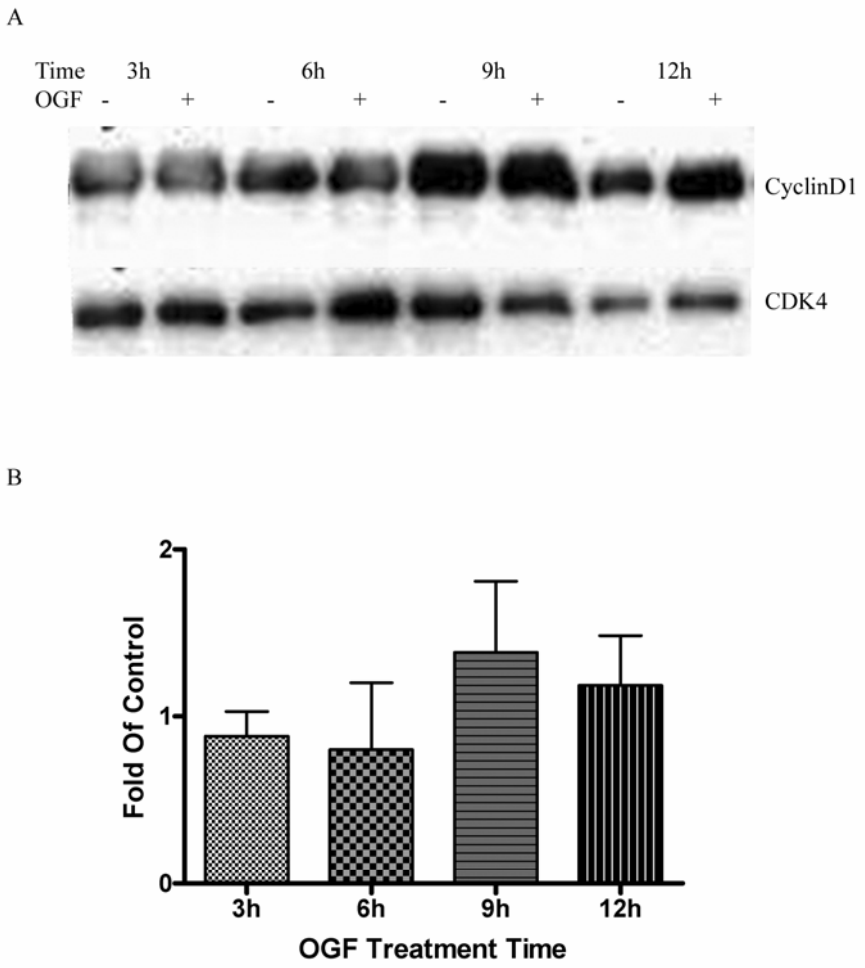

Figure 2.6 OGF does not affect Cyclin D1/CDK4 complex formation. (A) SCC1 cells were synchronized by nocodazole (0.5μg/ml) for 24 hours. Nocodazole were washed out and the cells were treated with or without OGF (10^{-6} M) for indicated times. Cell lysates were incubated with cdk4-agorose to immunoprecipitate total CDK4 and then immunoblotted with cyclin D1 antibody. (B) Densitometric analysis was performed, and the ratio of Cyclin D1/CDK4 complex was expressed relative to controls. Values represent means ± S.E.M of 3 independent experiments.

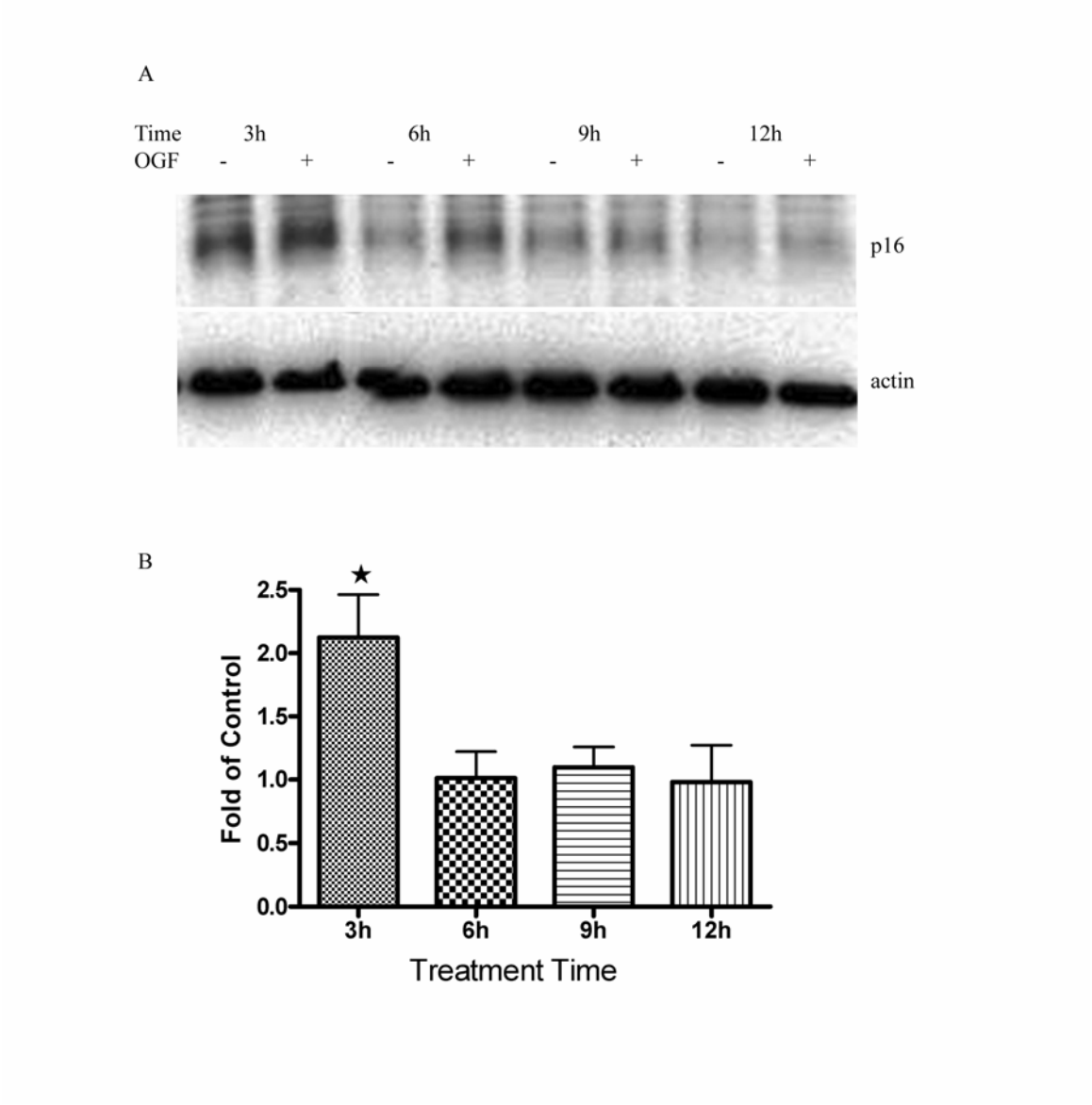

Figure 2.7 OGF induced p16 expression. (A) SCC1 cells were synchronized by nocodazole (0.5μg/ml) for 24 hours. Nocodazole were washed out and the cells were treated with or without OGF (10^{-6} M) for indicated times. Total proteins were resolved by SDS-PAGE and subjected to Western blotting of p16. (B) Densitometric analysis of the Western blots was performed. OGF and p16 expression was expressed relative to controls. Values represent means ± S.E.M for 3 independent experiments. Significantly different from the control group at $p<0.05$ (*).

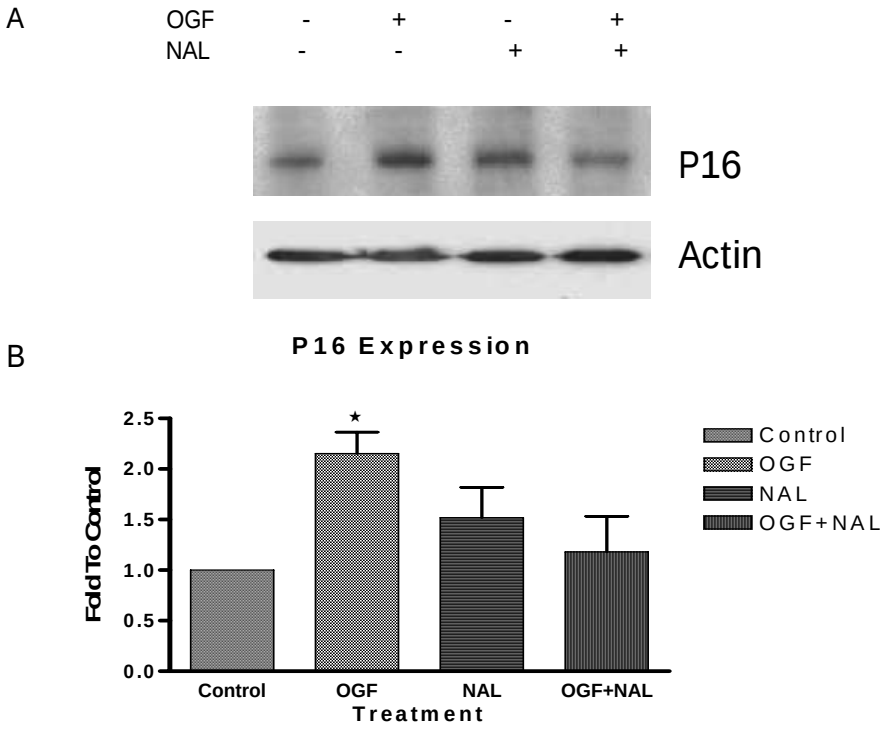

Figure 2.8 NAL blocked OGF inducing p16 expression. (A) SCC1 cells were synchronized by nocodazole (0.5μg/ml) for 24 hours. Nocodazole were washed out and the cells were treated with OGF (10-6 M) alone, NAL (10-5 M) alone or both OGF (10-6 M) and NAL (10-5 M) for 3 hours. Total lysates were resolved by SDS-PAGE and subjected to Western blotting for p16 expression. (B) Densitometric analysis was performed, and P16 expression was expressed relative to control. Values represent means ± S.E.M of 3 independent experiments. Significantly different from the control group at $p<0.05$ (*).

the p16-Rb pathway that, in turn, mediated the cell cycle block. Western blot analysis of p15, p18, p19, p21 and p27 expression after OGF treatment revealed that OGF had no significant effect on these CKIs (Fig. 2.9).

siRNA directed against p16 blocked OGF inhibiting action

To test the role of p16 in OGF-induced inhibitory action on SCC1 cell growth, siRNA knockdown experiments were used. SCC1 cells were treated with p16 siRNA or, as controls, with negative control siRNA. As revealed by Western blot analysis, the p16 siRNA efficiently reduced the level of p16 protein compared to control cells at 72h (Fig. 2.10A). Strikingly, in cells that lack sufficient p16, OGF no longer leads to inhibition of cell growth (Fig. 2.10B). This p16 siRNA knockdown assay showed that p16 induction is sufficient for the OGF-induced inhibitory actions on SCC1 cell growth. Other HNSCC cells were also treated with OGF, including CAL27 and SCC4. In CAL27 cells, OGF treatment increased p16 expression at 9h compare to control cells (Fig. 2.11A). CAL27 cells were treated with p16 siRNA or, as controls, with negative control siRNA. As revealed by Western blot analysis (see Appendix Fig.1), the p16 siRNA efficiently reduced the level of p16 protein compared to control cells at 96h. Strikingly, in cells that lack sufficient p16, OGF no longer leads to inhibition of cell growth in CAL27 (Fig. 2.11B). In SCC4 cells, OGF treatment increased p16 expression at 3h compared to control cells (Fig. 2.12A). SCC4 cells were treated with p16 siRNA or, as controls, with negative control siRNA. As revealed by Western blot analysis (see Appendix Fig.2), the p16 siRNA efficiently reduced the level of p16 protein compared to control cells at 72h.

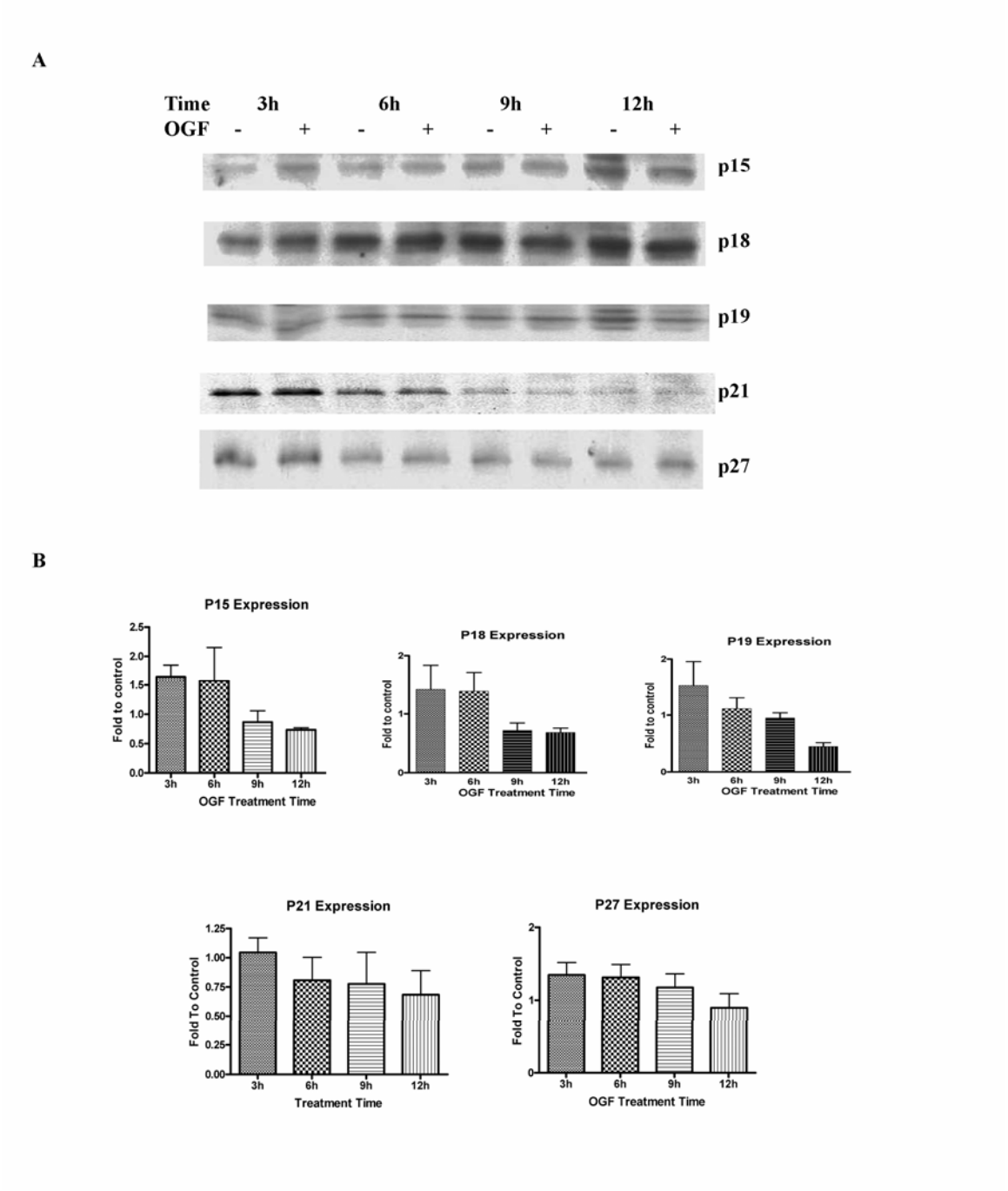

Figure 2.9 OGF and p15, p18, p19, p21 and p27 expression. (A) SCC1 cells were synchronized by nocodazole (0.5μg/ml) for 24 hours. Nocodazole were washed out and the cells were treated with OGF (10-6 M) for 3, 6, 9 or 12h. Total lysates were resolved by SDS-PAGE and subjected to Western blotting for p15, p18, p19, p21 or p27 expression. (B) Densitometric analysis was performed, and p15, p18, p19, p21 or p27 expression was expressed relative to control. Values represent means ± S.E.M of 3 independent experiments.

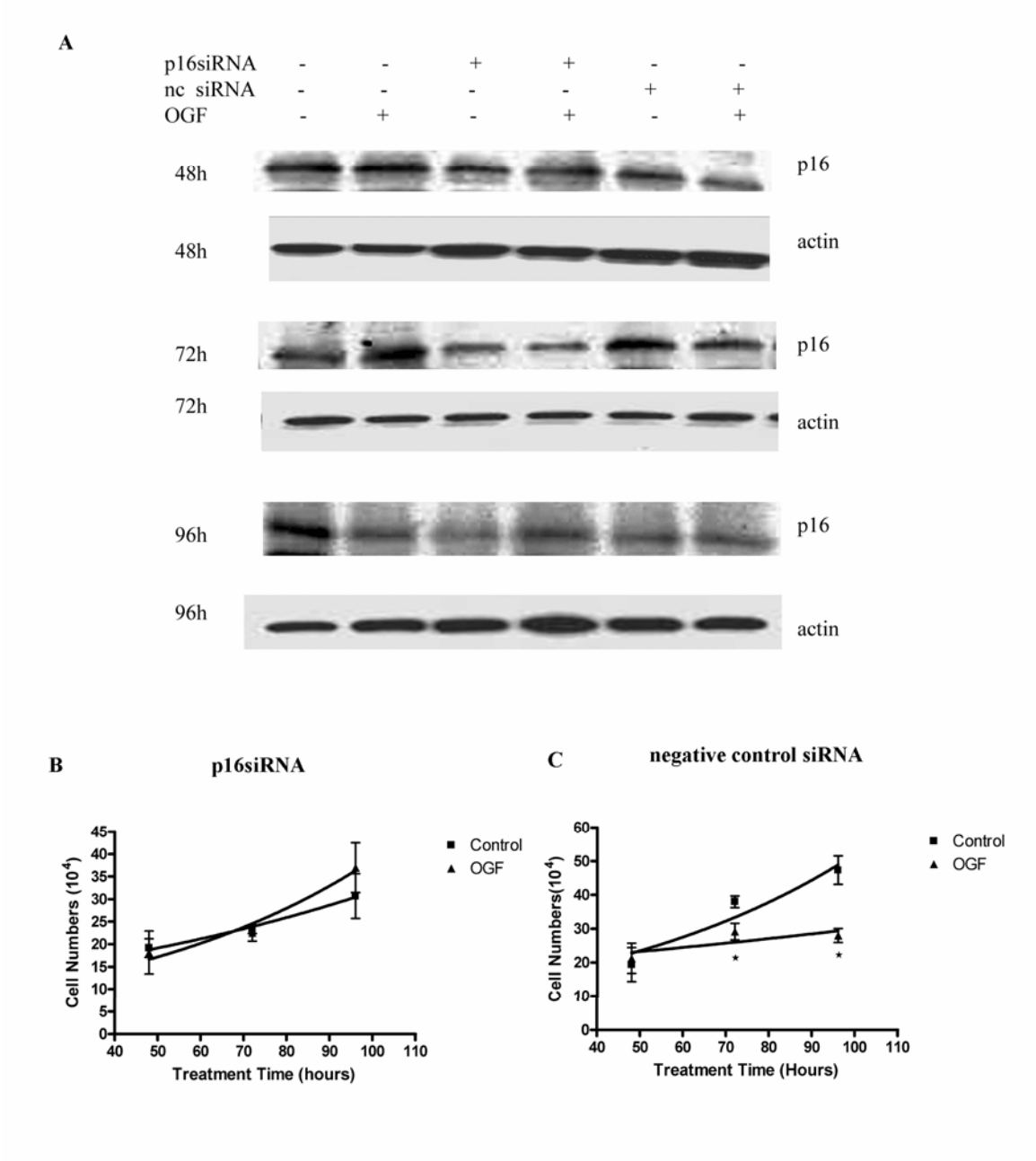

Figure 2.10 p16 is required for OGF induced growth inhibition. (A) Total proteins from SCC1 cells transfected with either p16 siRNA or negative control siRNA for 48h, 72h or 96h were separated by SDS-PAGE and immunoblotted with monoclonal antibody to p16. Growth curves for SCC1 cells transfected with either p16 siRNA (B) or negative control siRNA (C) and grown in the presence or absence (control) of OGF. siRNAs were transfected in SCC1 cells 24h after cells were seeded at 200,000 cells/well; OGF was added 4h later after transfection. Media and OGF were replaced daily. Data represent means ± S.E.M for 3 samples per treatment group for each time point. Significantly different from the control group at $p<0.05$ (*).

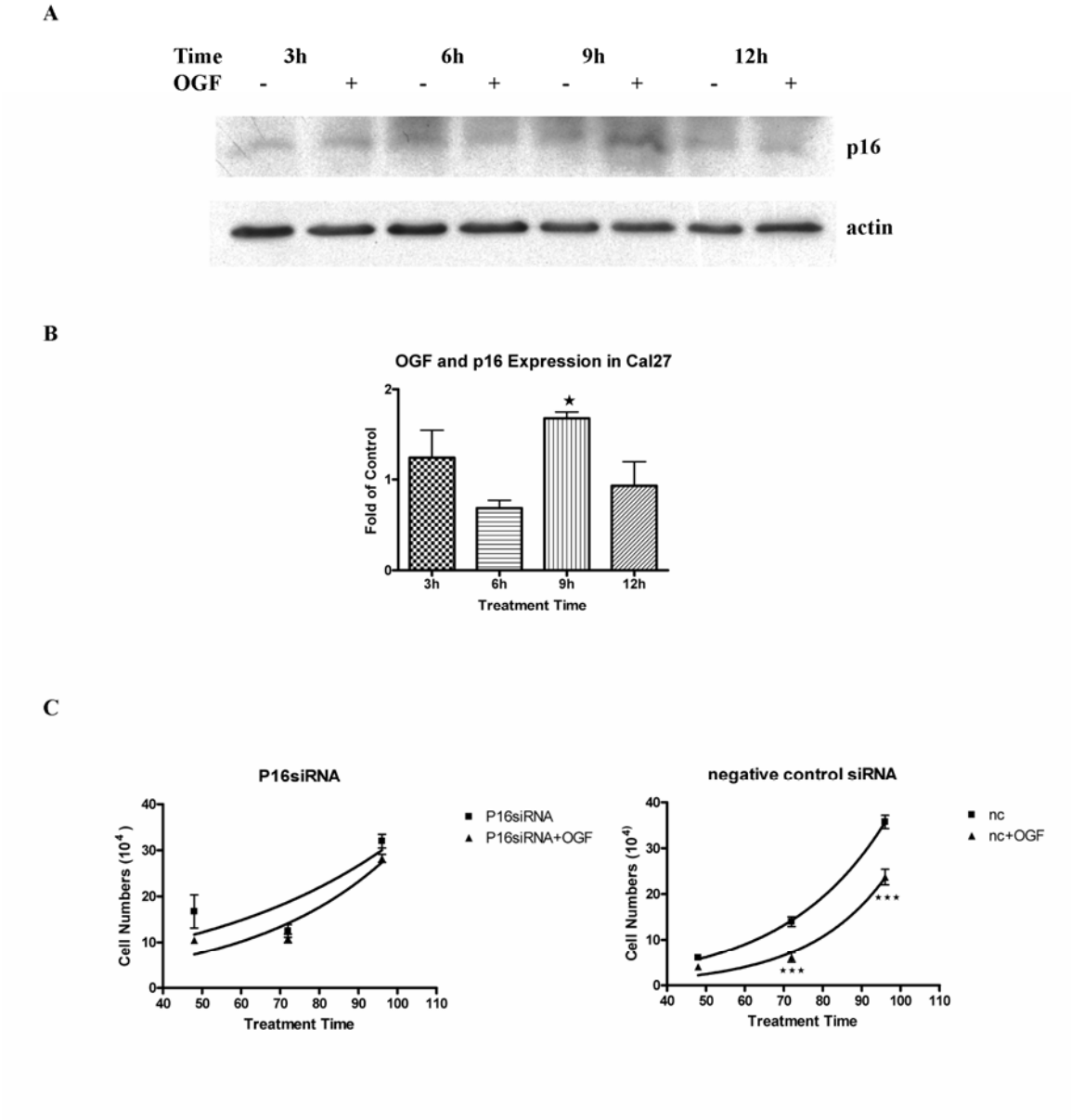

Figure 2.11 OGF induced p16 expression in CAL27. (A) Total proteins were resolved by SDS-PAGE and subjected to Western blotting of p16. (B) Densitometric analysis of the Western blots was performed. OGF and p16 expression was expressed relative to controls. Values represent means ± S.E.M for 3 independent experiments. Significantly different from the control group at $p<0.05$ (*). (C) Growth curves for CAL27 cells transfected with either p16 siRNA or negative control siRNA and grown in the presence or absence (control) of OGF. Data represent means ± S.E.M for 3 samples per treatment group for each time point. Significantly different from the control group at $p<0.05$ (*).

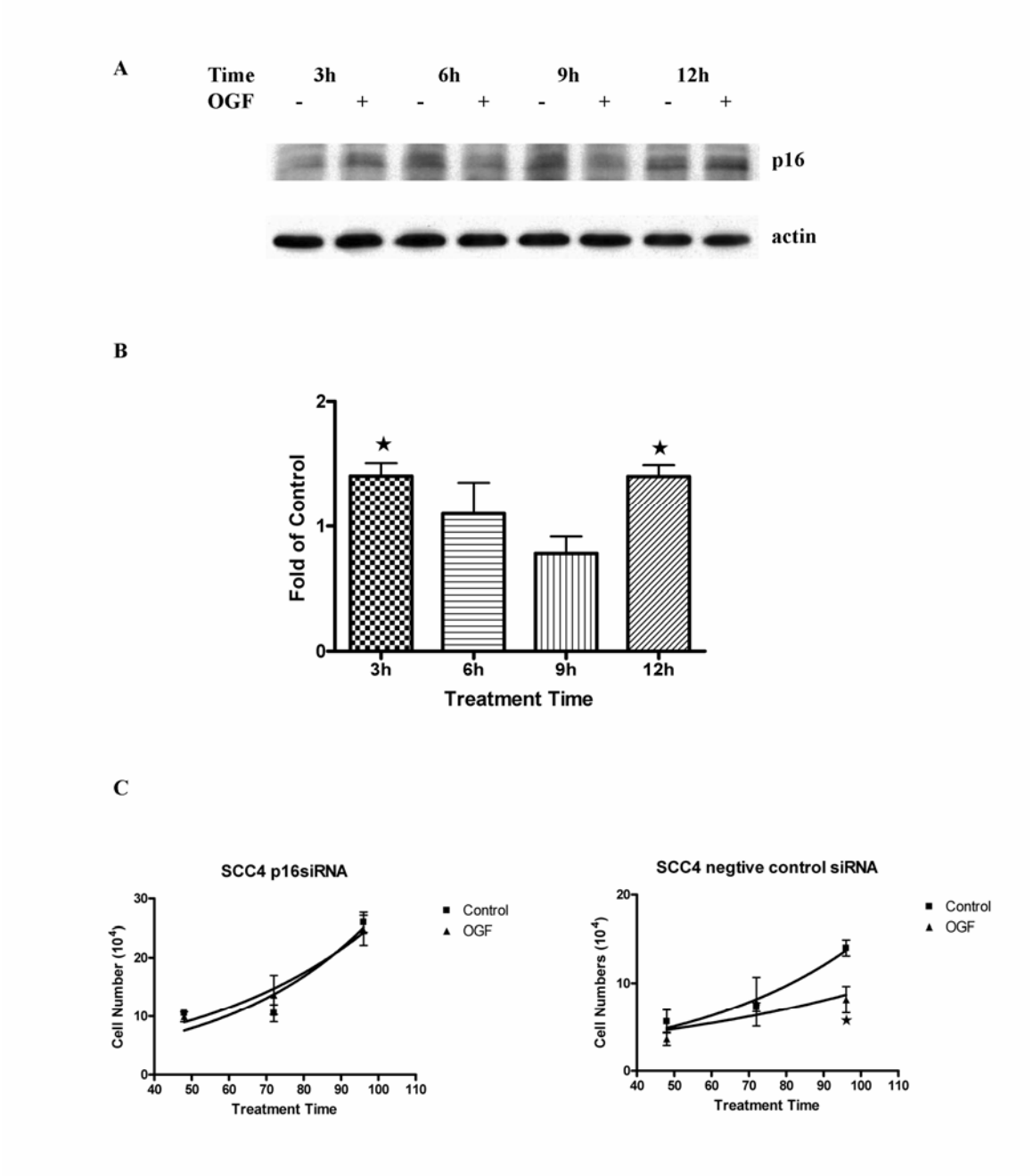

Figure 2.12 OGF induced p16 expression in SCC4. (A) Total proteins were resolved by SDS-PAGE and subjected to western blotting of p16. (B) Densitometric analysis of the western blots was performed. OGF and p16 expression was expressed relative to controls. Values represent means ± S.E.M for 3 independent experiments. Significantly different from the control group at $p<0.05$ (*). (C) Growth curves for SCC4 cells transfected with either p16 siRNA or negative control siRNA and grown in the presence or absence (control) of OGF. Data represent means ± S.E.M for 3 samples per treatment group for each time point. Significantly different from the control group at $p<0.05$ (*).

Strikingly, in cells that lack sufficient p16, OGF no longer leads to growth inhibition of SCC4 (Fig. 2.11B).

Discussion

A Model for the OGF-OGFr Inhibitory Pathway

OGF, an endogenous autocrine peptide, was proposed to be a valuable anti-cancer agent because of its inhibitory effect on the growth of cancer cells. However, the mechanism of the OGF-OGFr axis inhibitory action was poorly understood. Using the HNSCC cell line SCC1, the present study suggests, for the first time, that OGF inhibits HNSCC growth by down-regulation of Rb phosphorylation, down-regulation of Cdk4 activity and up-regulation of the CDK inhibitor p16. In addition, the OGF antagonist, NAL, blocked OGF induced p16 upregulation. Targeted decrease of p16 using siRNA blocked OGF inhibiting action. Thus, these findings suggest that the receptor-mediated, growth inhibitory effects of the OGF-OGFr axis in HNSCC cells are associated with induction of p16/cdk4 inhibitor resulting in decreased Rb phosphorylation. The decreased level of Rb in its hyperphosphorylated state is antiproliferative, resulting in fewer cells exiting G0/G1 phase, thus, inhibiting cell growth.

Potential OGF-OGFr Targets

Initial studies in our lab demonstrated that OGF did not induce necrosis, apoptosis [43] or differentiation in *in vitro* models [44]. Previous studies in our lab also demonstrated that OGF induced less cells exiting G0/G1 phase [47]. These findings demonstrated that the inhibitory effect of OGF on cell replication is not related to a broad-based action on the cell cycle, but rather is directed to a singular phase of the cell

cycle: G0/G1. These helped us to narrow down OGF targets. A key regulator of the G1 to S phase transition in the cell cycle is retinoblastoma (Rb) protein, a tumor suppressor. During the cell cycle progression, Rb is sequentially phosphorylated by different cyclin/CDK complexes [63]. Different phosphorylation sites in Rb have been demonstrated, with the preferred site being $S^{807/811}$ by CDK4/cyclin D and T^{821} by CDK2 [59]. This coincided with our observation that OGF down-regulated the phosphorylation of Rb on $S^{807/811}$, presumably because of a decreased CDK4 kinase activity. However, *in vitro* assay of CDK4 kinase activity showed transient increase at 3 hours of OGF treatment. This indicates that there may be some other signaling pathways affecting CDK4 activity. However, Rb inhibitory functions needs sequentially phosphorylation by both Cdk4 and Cdk2 [63]. We also observed that OGF had no effect on Rb T^{821} phosphorylation, which means OGF did not affect CDK2 activity. These suggest that transient increasing of CDK4 activity has no relationship with growth inhibitory function of OGF.

p16 has been considered as a target for potential anticancer drugs. Indole-3-carbinol (I3C), a naturally occurring component of Brassica vegetables, strongly stimulated the production of the p16 CDK inhibitor and induced a block in G1 cell cycle in LNCaP prostate carcinoma cells [69]. Recently, studies showed that transfection of exogenous wild p16 gene induced the bladder cancer cells arrested in G0/G1 phase [70]. Our results also support that OGF inhibited cell growth by upregulating p16 expression. However, these changes are transient and not permanent. It suggests that OGF has cytostatic effect but not cytotoxic effect. It may explain that OGF has no effect on apoptosis [43].

Studies showed that a combination of OGF and paclitaxol has a potent inhibitory effect on the growth of SCC1 both *in vivo* and *in vitro* [103]. Since OGF has its effect on G1 phase, it can be synergic to paclitaxol, which acts by stabilizing microtubules in G2/M phase, to inhibit HNSCC cell growth [103, 104].

Clinical Correlation

The endogenous CDK inhibitor p16 is a known tumor suppressor. In this report, we suggest that OGF can promote the accumulation of p16. In HNSCC, overexpression of cyclin D1, LOH (loss of heterozygosity) of 9p21 (p16) and MTS2 (p15) have been demonstrated [88, 105, 106]. However, studies also showed that in primary HNSCC tumors, p16 mutation and deletion were not as frequently as in HNSCC cell lines [68, 88, 107, 108]. Zhang *et al* [68] have reported 10% of mutations and deletions of p16 in primary tumors and 44% in cell lines. Lydiatt *et al* [88] have reported 19% of genetic alterations of p16 in HNSCC tumors and 75% in cell lines. Since most of HNSCC patients' tumors contain p16 and OGF targets p16 in HNSCC cells, this information suggests OGF may be a useful drug for HNSCC patients.

Taken together, our findings indicate that the upregulation of p16 after OGF treatment occurs with decreasing Cdk4 kinase activity and Rb phosphorylation. We anticipate that a more complete understanding of OGF regulating p16 expression will explain crucial links underlying the regulation of genes that control tumor suppression.

CHAPTER III

INHIBITION OF PANCREATIC CANCER THROUGH THE OGF-OGFR AXIS IS MEDIATED BY THE CYCLIN-DEPENDENT KINASE INHIBITOR p21

Abstract

Opioid growth factor (OGF) is an endogenous opioid peptide ([Met^5]-enkephalin) that interacts with the OGF receptor (OGFr), and serves as a tonically active negative growth factor in neoplasia. Previous studies showed that OGF targets cell proliferative pathways as a mechanism to inhibit the growth of human pancreatic cancer *in vitro* and *in vivo*. OGF is also known to block proliferation of HNSCC cell lines by inducing the cyclin-dependent kinase inhibitor (CKI) p16. However, pancreatic cancer cells have frequently lost p16 gene expression, and thus other CKIs were examined further in regulating growth of pancreatic cancer. BxPC-3 human pancreatic adenocarcinoma cell cultures were synchronized with nocodazole, and flow cytometry revealed that OGF treatment resulted in 14% fewer cells ($p<0.05$) exiting the G1 phase of the cell cycle in comparison to controls. The present studies focused on the role of OGF on regulatory pathways for the G1 to S phase transition. Studies using BxPC-3 cells suggest that OGF decreased the phosphorylation of retinoblastoma (Rb) protein by approximately 40% ($p<0.05$). This change was correlated with reduced cdk2 kinase activity but no change in total cdk2 expression. Moreover, OGF treatment for 9 hours increased cyclin-dependent kinase inhibitor (CKI) p21 protein expression 2-fold in comparison to control ($p<0.05$), but had no effect on p27 protein expression. Blockade of the OGF-OGFr axis with the short-acting opioid antagonist, naloxone (NAL), revealed that the increased expression of p21 protein following OGF treatment was completely abolished by NAL. NAL alone had no effect on p21 protein expression suggesting that the OGF effects were opioid receptor (OGFr) mediated. Inhibition of p21 activation by p21 specific siRNA blocked the OGF inhibitory action on BxPC3 cell proliferation. Scrambled siRNAs (negative controls) had

no effect on p21 expression and did not block OGF's growth inhibitory action. Collectively, these results indicate that the receptor-mediated, growth inhibitory effects of the OGF-OGFr axis are associated with induction of p21 expression that in turn, repressed the Rb phosphorylation. The data reveal that the target of cell proliferative inhibition action of OGF in human pancreatic cancer is by the way of a cyclin dependent kinase inhibitory pathway.

Introduction

Endogenous opioid peptides are known to be potent regulators of growth, as well as neuromodulators and neurotransmitters [6]. There are three families of endogenous opioid peptides, enkephalins, endorphins and dynorphins. In these opioid peptides, [Met^5]-enkephalin gets more attention because it has been reported to be a negative regulator of growth [35, 37, 40]. To distinguish the role of [Met^5]-enkephalin, as a growth factor in neural and non-neural cells and tissues, and in prokaryotes and eukaryotes, this peptide was termed opioid growth factor (OGF) [6]. The biological activities of OGF involve OGF receptor (OGFr) and can be blocked by naloxone (NAL) [17] or naltrexone (NTX) [26]. OGFr is an integral membrane protein that is associated with the nucleus. Binding assays have exhibited ligand selectivity, saturability, stereospecificity, competitive displacement, and the presence of an endogenous agonist [6]. After binding to OGFr, OGF functions to set off a signaling cascade related to growth [6].

Cancer of the pancreas is the fourth leading cause of cancer death in the United States. The overall 5-year survival of pancreatic cancer is 0.4% [92]. Despite the medical advances made over the last 20 years, pancreatic cancer patients would appear to have benefited the least in terms of survival. Currently, potentially curative surgical resection is possible in only about 10%-15% of patients [92]. Radiotherapy and chemotherapy regimens have not shown improved survival in advanced disease [92]. The low rate of survival of patients has highlighted the need for new approaches for diagnosis and treatment. Certain biological markers of pancreatic cancer are under evaluation, such as growth factors and their receptors, tumor suppressor genes, angiogenic factors and apoptotic genes [91]. For example, loss of expression of p16 is observed in most

pancreatic tumors [91] and it appears to be a relatively early event in the progression of pancreatic cancer [93]. Loss of p21 activity has been observed in approximately 20%-40% of pancreatic tumor specimens [94-96]. Previous studies in our lab showed that OGF can inhibit pancreatic cancer cell growth both *in vivo* [36] and *in vitro* [35].

Recent studies indicate that the OGF-OGFr inhibitory action on cell growth in tissue culture is not due to alterations in apoptotic pathways [43] or differentiation [44]. Our latest study have reported that OGF was able to inhibit cell cycle progression [47]. Therefore, it is logical to investigate the cell cycle progression and OGF-OGFr signaling pathways. Here, we identify that decreased Rb phosphorylation occurs in OGF treatment of pancreatic cancer, occurring as a result of decreased Cdk2 kinase activity due to increased expression of p21. Increasing p21 effect could be blocked by naloxone. Furthermore, targeted decrease of p21 using siRNA blocked OGF inhibiting action. Thus, these studies identify p21 as a selective target in OGF-OGFr inhibitory action and provide a mechanistic basis for OGF treatment for pancreatic cancer patients.

Materials and Methods

Cell Culture. Human pancreatic cancer cell line Panc1 cells were maintained in logarithmic phase growth in Dulbecco's modified medium (DMEM; Penn State University). BxPC3 pancreatic cancer cells were cultured in RPMI medium (Penn State University). Capan2 pancreatic cancer cells were cultured in McCoy’s 5A medium (Mediatech, Herndon, VA). All cells were purchased from American Type Culture Collection, Manassas, VA. All media contained 10% fetal bovine serum (FBS; HyClone, Logan, Utah), 1.2% sodium bicarbonate (Penn State University) and 0.25% antibiotics

(5000 units/ml penicillin, 5 μg/ml streptomycin and 10 μg/ml neomycin; Mediatech, Herndon, VA). Cell cultures were grown in a humidified atmosphere of 5% CO_2 at 37^{o}C.

OGF Treatment. [Met^{5}]-enkephalin (Sigma, St. Louis, MO) was dissolved in sterile water at the concentration of 10^{-3} M as a stock solution. In all experiments, 1 μl of the stock OGF or 1 μl sterile water (vehicle control) was added per milliliter of medium and the final OGF concentration was 10^{-6} M.

Synchronization of Cells. BxPC3, Capan2 and Panc1 cells were synchronized with nocodazole (67 ng/ml) for 24 hours; Nocodazole was washed out with complete media (contain serum) three times. Cells were released from growth arrest by feeding them with complete medium, and some cells were treated with OGF-supplemented media as described above.

Flow Cytometric Analysis of Cell Cycle. Synchronized BxPC3 cells were treated with 10^{-6} M OGF for 21 hours. Cells were harvested with 0.25% trypsin-EDTA (Mediatech, Herndon, VA) and fixed with 70% ethanol at -20^{o}C for up to 7 days before DNA analysis. After the removal of ethanol by centrifugation, cells were washed with PBS once. After centrifugation, cells were stained with a solution containing 1 mg/ml sodium citrate (Sigma, St. Louis, MO), 0.3% Triton-X (Sigma, St. Louis, MO), 0.1 mg/ml propidium iodide (Sigma, St. Louis, MO), 0.02 mg/ml ribonuclease A (Sigma, St. Louis, MO) at room temperature for 15 minutes. Stained nuclei were analyzed for DNA-PI fluorescence using a Becton Dickinson FACScan flow cytometer. Resulting DNA

distributions were analyzed by Modfit Software for the proportion of cells in G0/G1, S and G2/M phases of the cell cycle.

Preparation of whole-cell extracts. To prepare total protein extracts, frozen cell pellets consisting of 2×10^6 cells per sample were thawed on ice and resuspended in 200 µl RIPA buffer (1X PBS, 10 µM IGEPAL, 1 mg/ml sodium dodecyl sulfate [SDS], 5 mg/ml deoxycholic acid), containing protease and phosphatase inhibitors (2 µg/ml aprotinin, 3 mg/ml phenylmethyl sulfonyl fluoride [PMSF], 1 mM sodium orthovanidate). All chemicals were purchased from Sigma, St. Louis, MO. Samples were passed through a 25-gauge needle three times and then transferred into 1.5- ml microcentrifuge tubes. The supernatants were collected by centrifugation 14000 ×g for 20 min at 4°C. Total protein concentrations were measured using the DC protein assay kit (Bio-Rad, Hercules, CA). For each sample, a 180 µl aliquot of the supernatant was removed and added to 36 µl 6× sample loading buffer (25 mg/ml DTT, 0.5 g/ml sucrose, 1.5 mg/ml EDTA, 50mg/ml SDS, 10 mg/ml bromophenol blue).

Western Blot Analysis and Chemiluminescence. Protein extracts (40 µg) were resolved by SDS-polyacrylamide gel (acrylamide/bis-acrylamide ratio, 30:0.8). Gel compositions for resolving various proteins were as follows: 7.5% gel to detect Rb, 12% gel for cdk2, cyclin A, cyclin E, p27 or p21. Proteins were transferred to a nitrocellulose membrane for 1 hour at 100V in transfer buffer. Membranes were blocked for 1 hour at room temperature or overnight at 4°C in 5% BSA in TBS with 0.1% Tween. Membranes were incubated for 1 hour at room temperature or overnight at 4°C with primary

antibodies. The following dilutions of primary antibodies were used to detect respective proteins. 1:200 phospho-Rb (Ser795), 1:200 phospho-Rb (Ser807/811); 1:200 phospho-Rb (Thr821); 1:200 cdk2, 1:200 cyclin A, 1:200 cyclin E, 1:200 total Rb, 1:200 p21, 1:100 p27, 1:200 p57. Following the incubation with the primary antibody, blots were washed and exposed to secondary antibody and visualized by chemiluminescence Western blotting detection system (Amersham, Piscataway, NJ). In order to determine equal loading of total protein samples, monoclonal antibody against β-actin at a dilution of 1:2000 were used in the identical blots. When required, membranes were stripped in stripping buffer (62.5 mM Tris-HCL and 100 mM β-mercaptoethanol/2% SDS, pH6.7) at 50^{o}C and reprobed with antibody against β-actin. The following antibodies were purchased from commercial sources: phospho-Rb (Ser795), phospho-Rb (Ser807/811) (Cell Signaling Technology, Beverly, MA); phospho-Rb (Thr821) (Biosource, Camarillo, CA); cdk2, cyclin A, cyclin E, p57 (Santa Cruz Biotechnology, Santa Cruz, CA); total Rb, p21, p27 (BD PharMingen, San Diego, CA); β-actin (Clone AC-15, Sigma, St. Louis, MO).

Immunoprecipitation. For immunoprecipitating protein complexes, cell extracts were prepared as follows. 2×10^6 cells per sample were rinsed in cold PBS once followed by lysis in 200 μl immunoprecipitation buffer (1% NP-40, 10 mM HEPES [pH7.5], 200 mM NaCl, 5 mM EDTA, 50 mM NaF, 0.2 mM sodium orthovanidate, 1 mM PMSF, 2 mM dithiothreitol [DTT], 1X Halt^{TM} protease inhibitor cocktail [Pierce, Rockford, IL]). Samples were collected by scraping and transferred into a 1.5-ml microcentrifuge tube. Supernatants were collected by centrifugation at 10000 ×g for 15

min at 4°C. Protein concentrations were measured using the Bio-Rad Protein Assay (Bio-Rad, Hercules, CA).

For each immunoprecipitation reaction mixture, a total of 500 μg of protein extract was used. The volume was made up to 1 ml with immunoprecipitation buffer. To each sample, 50 μl of protein A beads (Santa Cruz Biotechnology, Santa Cruz, CA) were added and incubated at 4°C for 30 min with rotation. Beads were removed by centrifugation at 14000 rpm for 15s. The supernatant was removed and added to a fresh tube. The lysates were then subjected to immunoprecipitation using 10 μl polyclonal antibody against CDK2 (sc-163, Santa Cruz Biotechnology, Santa Cruz, CA) and incubated at 4°C for 1.5h with rotation, followed by addition of 20 μl of protein A beads as the immune complex binding agent. Samples were further incubated at 4°C for 1h with rotation. Beads were pelleted by centrifugation at 14000 rpm for 15s and then washed three times with 500 μl ice-cold immunoprecipitation wash buffer (1% NP40, 50 mM HEPES, 150 mM NaCl, 1 mM EDTA, 1 mM DTT). After the final wash the agarose beads were resuspended in 20 μl of 2× sample loading buffer (Santa Cruz Biotechnology, Santa Cruz, CA) and boiled for 3 min in a water bath. A total of 20 μl of each sample was used for detecting respective proteins in the immunoprecipitated complexes utilizing Western blot analysis.

Histone H1 kinase assay for CDK2 activity. An immune complex kinase assay was performed to measure immunoprecipitated CDK2 activity. Immunoprecipitation of samples was performed using polyclonal antibodies against CDK2 as described above. Immunoprecipitates were washed three times with immunoprecipitation wash buffer

(described above) and then twice with 500 μl ice-cold H1 kinase buffer (50 mM HEPES [pH 7.5], 10 mM $MgCl_2$, 10 mM $MnCl_2$, 1 mM DTT). The kinase assay involves incubation of the immunoprecipitates in a mixture of kinase buffer (described above), 10 μCi γ^{32}P-ATP, and 1 μg of histone H1 (Roche) as the substrate for Cdk2. After incubation for 30 min at 30^0C, with occasional mixing, the reaction was stopped by the addition of 2× sample loading buffer (Santa Cruz Biotechnology, Santa Cruz, CA). Samples were boiled for 5 min and then pelleted by centrifugation. Proteins in the reaction mixture were separated by a 12% SDS-PAGE gel. The cdk2 kinase activity pattern was visualized by autoradiography of phosphorylated H1.

SiRNA knockdown of $p21^{WAF1/CIP1}$. The p21-targeted siRNAs were obtained from Santa Cruz (Santa Cruz Biotechnology, Santa Cruz, CA). The negative control siRNA were from Ambion (Ambion, INC., Austin, TX). For transfection, 2×10^5 cells per well were seeded in 6-well plates containing 1ml media without antibiotics. For each well, 1 μl of siRNA stock (20 μM) was mixed with 175 μl DMEM (for Panc1), McCoy's (for Capan 2) or RPMI (for BxPC3) containing 1.2% sodium bicarbonate (SFM). Next, 2 μl of Oligofectamine reagent (Invitrogen) were diluted in 15 μl SFM by gentle mixing. The two solutions were then gently combined and 193 μl of the solution was added to SFM- prewashed cells in each well. The final concentration for siRNA in each well is about 20 nM. Cells were incubated for 4h at 37^oC prior to the addition of OGF. Cultures were then left overnight before washing and adding 1ml fresh complete media either lacking or containing OGF. At the indicated time points, cells were collected for different assays performed as described.

Cell counts. Cells were trypsinized on the indicated days and counted with a hemocytometer. Cells viability was assessed by trypan blue exclusion staining (Sigma).

Densitometry analysis. For Western blots, the optical density of each band was determined by densitometer and analyzed by the software QuickOne (Biorad). Each protein expression was normalized to β-actin from the same blot and protein expressions induced by OGF were compared to control.

$$\text{Fold of control} = \frac{\text{Protein from OGF treatment } / \beta\text{-actin from OGF treatment}}{\text{Protein from control} / \beta\text{-actin from control}}$$

For CDK2 kinase activity, the cdk2 kinase activity pattern was visualized by autoradiography of phosphorylated H1. The optical density of each band was quantified using a PhosphoImager. To quantify OGF induced cdk2 kinase activity, phosphorylated H1 was normalized to cdk2 protein and cdk4 kinase activities induced by OGF were compared to control.

$$\text{Fold of control} = \frac{\text{H1 from OGF treatment } / \text{Cdk2 from OGF treatment}}{\text{H1 from control} / \text{Cdk2 from control}}$$

Statistical analysis. Data were analyzed by one-way analysis of variance (ANOVA) with Newman kaul's post multiple comparison tests; significance levels of $p<0.05$ were reported.

Results

Effect of OGF on cell cycle distribution of BxPC3 cells. Growth curves for BxPC3 cell cultures treated with 10^{-6} M OGF or sterile water (controls) revealed that continuous exposure to exogenous OGF inhibited the growth of BxPC3 pancreatic cancer cells (Fig. 3.1A). OGF inhibited growth at 48h and 72h relative to controls, with percentage in cell number of controls as 66% and 55%, respectively. Linear analysis of the data revealed mean doubling times for the control and OGF groups of 28.6h and 51.0h.

Because OGF inhibited BxPC3 cell growth, the effects of OGF on BxPC3 cell cycle distribution by flow cytometry were examined (Fig. 3.1B). As shown in Fig. 3.1C, the percentage difference between OGF-treated and control cells in the G0/G1 phase increased from 54.54% to 68.62%, while the number of cells in the S phase decreased from 45.37% to 27.58%, the number of cells in the G2/M phase increased from 0.08% to 3.80%. Thus, after 21 hours OGF treatment, the percentage of cells in G0/G1 increased by 14.08%, the number of cells in the S phase was decreased by 17.79%, and the percentage of cells in the G2/M phase was increased by 3.80% relative to controls.

OGF induced less pRb phosphorylation. The phosphorylation of Rb protein is necessary for cells to progress from G1 into S phase. To elucidate the role of Rb in OGF-induced cell growth inhibition of BxPC3, we assessed the total Rb expression and the phosphorylated state of Rb in BxPC3 cells. The results showed that the expression of total Rb protein was not decreased significantly after OGF treatment (Fig. 3.2). The level

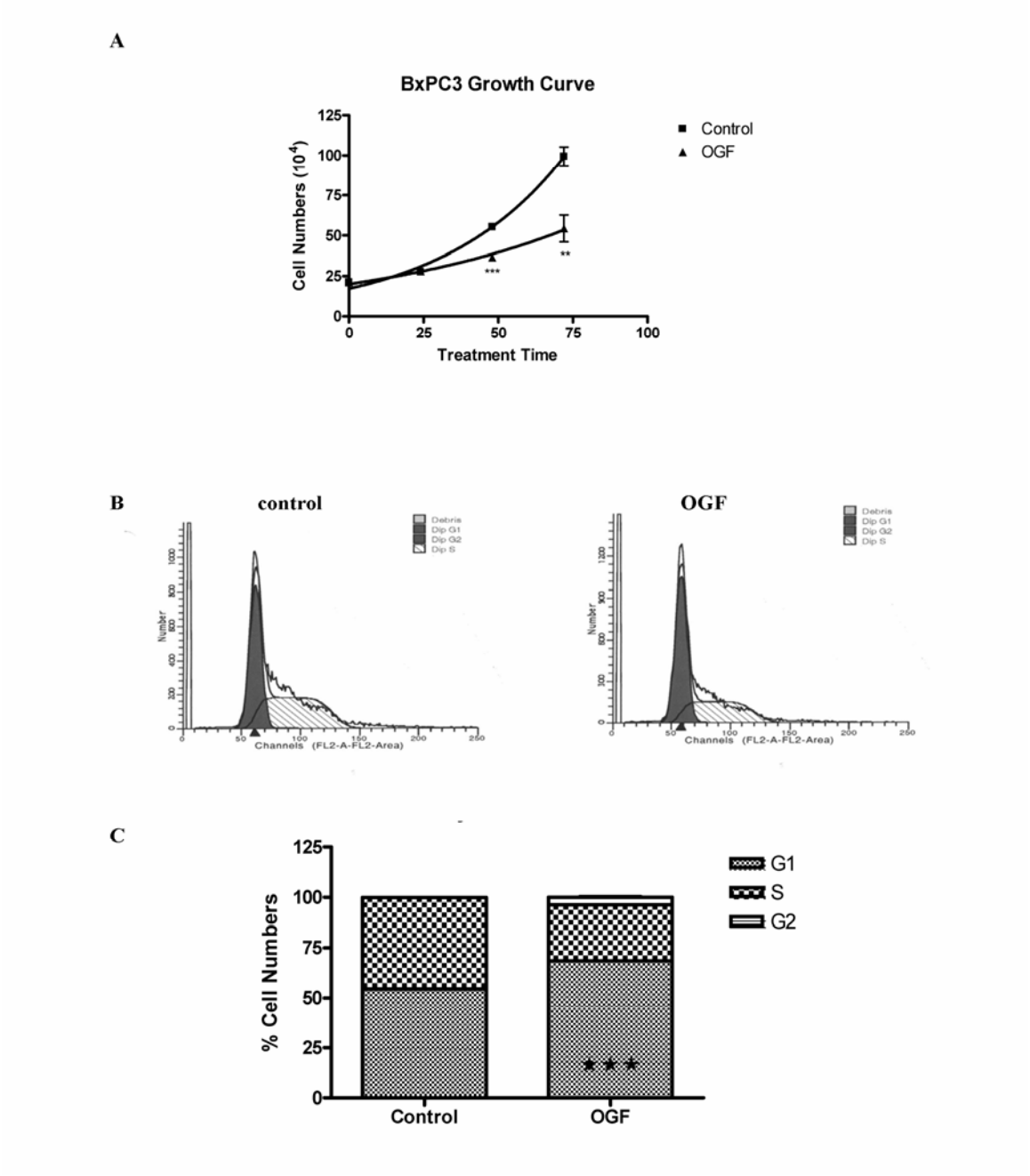

Figure 3.1 (A) Growth curve for BxPC3 cells treated with 10^{-6} M OGF or equivalent volume of sterile water (control) over a 72-h period of time. Data represent means ± S.E.M for 3 samples per treatment group for each time point. (B) Cell cycle distribution of BxPC3 cells grown in either the absence (control) or presence of OGF, as determined by FACS analysis. (C) OGF induced fewer cells to exit the G0/G1 phase. Data (percentage of cells in the indicated phases) are the means of three experiments. Significantly different from the control group at $p<0.01$ (**) or $p<0.001$ (***).

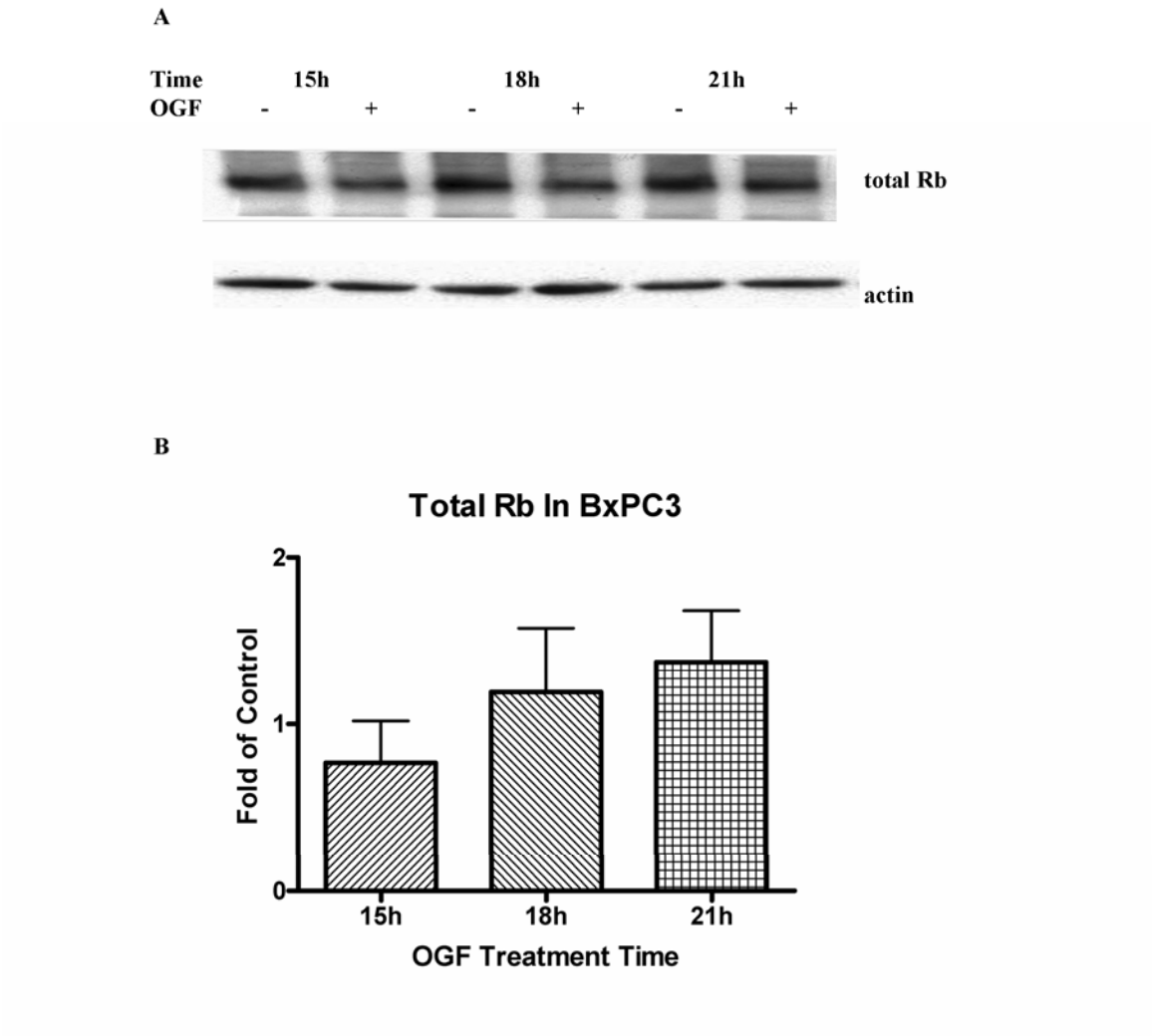

Figure 3.2 OGF and total Rb expression. (A) BxPC3 cells were synchronized by nocodazole (67ng/ml) for 24 hours. Nocodazole were washed out and the cells were treated with or without OGF (10^{-6} M) for indicated times. Total proteins were resolved by SDS-PAGE and subjected to western blotting of total Rb. (B) Densitometric analysis of the Western blots was performed. OGF and total Rb expression was expressed relative to controls. Values represent means ± S.E.M for 3 independent experiments.

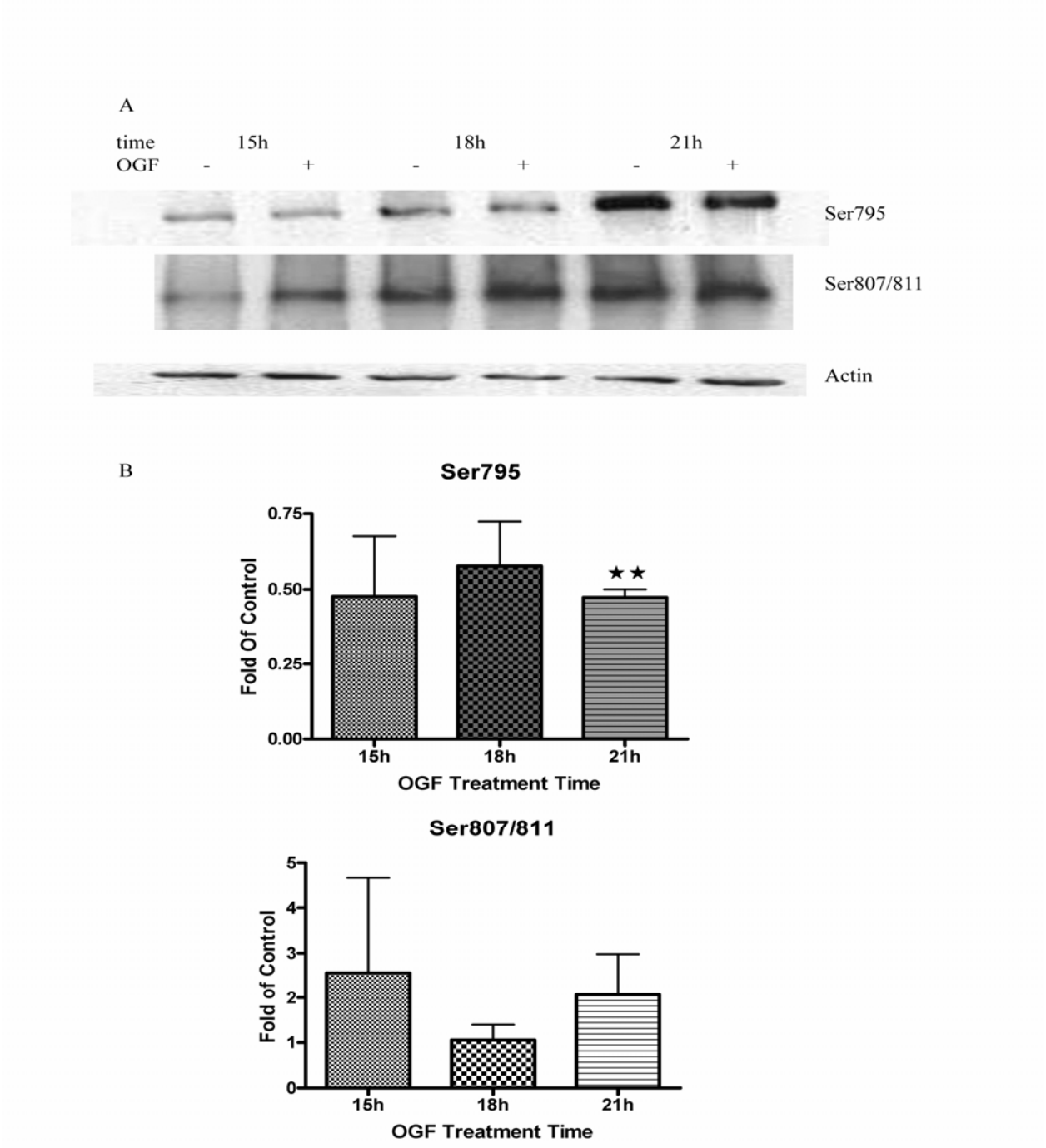

Figure 3.3 OGF decreased Rb phosphorylation (Ser795). (A)Total proteins were resolved by SDS-PAGE and subjected to western blotting of phosphorylated Rb (Ser795) or phosphorylated Rb (Ser807/811). (B) Densitometric analysis of the Western blots was performed, and the OGF induced Rb phosphorylation was expressed relative to controls. Values represent means ± S.E.M for 3 independent experiments. Significantly different from the control group at $p<0.01$ (**).

of phospho-Rb (Ser795) was decreased by the treatment of 10^{-6}M OGF significantly (Fig. 3.3). We also checked the level of phospho-Rb (pS807/811), which was specifically phosphorylated by cdk4 in G1 phase. The result showed that pS807/811 level did not change significantly after OGF treatment (Fig. 3.3). These results indicated that cdk2, not cdk4, was involved in the OGF-induced cell cycle block at G1 phase.

OGF induced less cdk2 kinase activity. To verify whether OGF-induced downregulation of pRb was associated with changes of CDK2, CDK2 expression and *in vitro* kinase assay were performed. Results indicated that the expression of CDK2 protein did not change significantly following OGF exposure (Fig. 3.4). When histone H1 was used as substrate in immunoprecipitation experiments performed with antibodies against CDK2, lysates from cells treated with OGF for 15h, 18h and 21h showed a marked decrease in kinase activities, 78%, 46% and 82% compared to control, respectively (Fig. 3.5). These results demonstrated that OGF-mediated decrease of pRb was consistent with the reduction in CDK2 kinase activities.

Effect of OGF on G1 cell cycle regulatory proteins in BxPC3 cells. Cyclins are positive regulators of cell cycle progression. To verify whether OGF-induced downregulation of CDK2 kinase activity was dependent on cyclin A or cyclin E expression, the level of cyclin A/CDK2 complex and cyclin E/CDK2 complex was analyzed by immunoprecipitation. Levels of CDK2/cyclin A complex after OGF treatment revealed that OGF treatment decreased cyclin A/CDK2 complex significantly

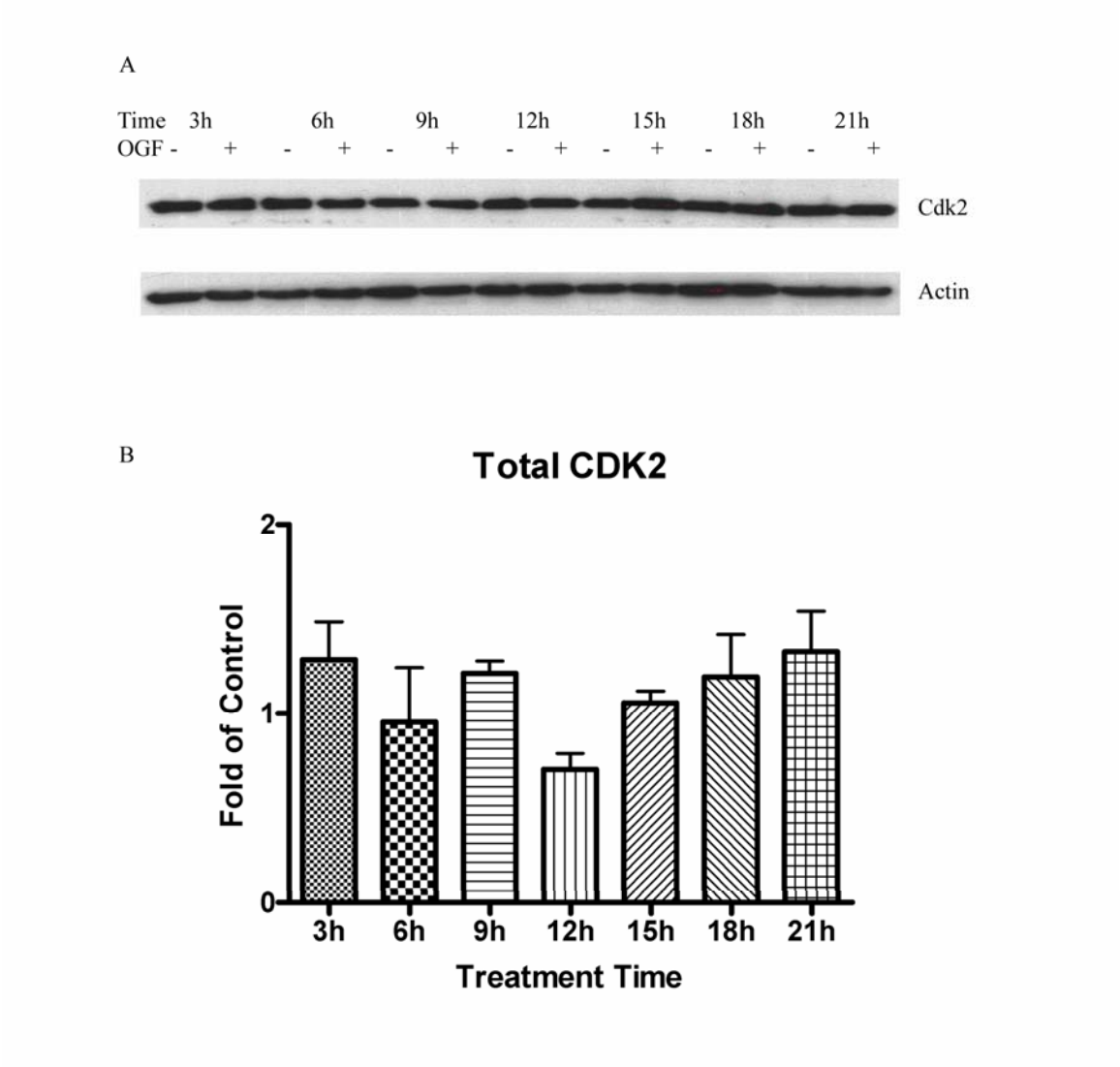

Figure 3.4 OGF and total CDK2 expression. (A) BxPC3 cells were synchronized by nocodazole (67ng/ml) for 24 hours. Nocodazole was washed out and the cells were treated with OGF (10^{-6} M) for 3, 6, 9, 12, 15, 18 or 21 hours. Total lysates were resolved by SDS-PAGE and subjected to Western blotting for CDK2 expression. (B) Densitometric analysis was performed, and CDK2 expression was expressed relative to control. Values represent means ± S.E.M of 3 independent experiments.

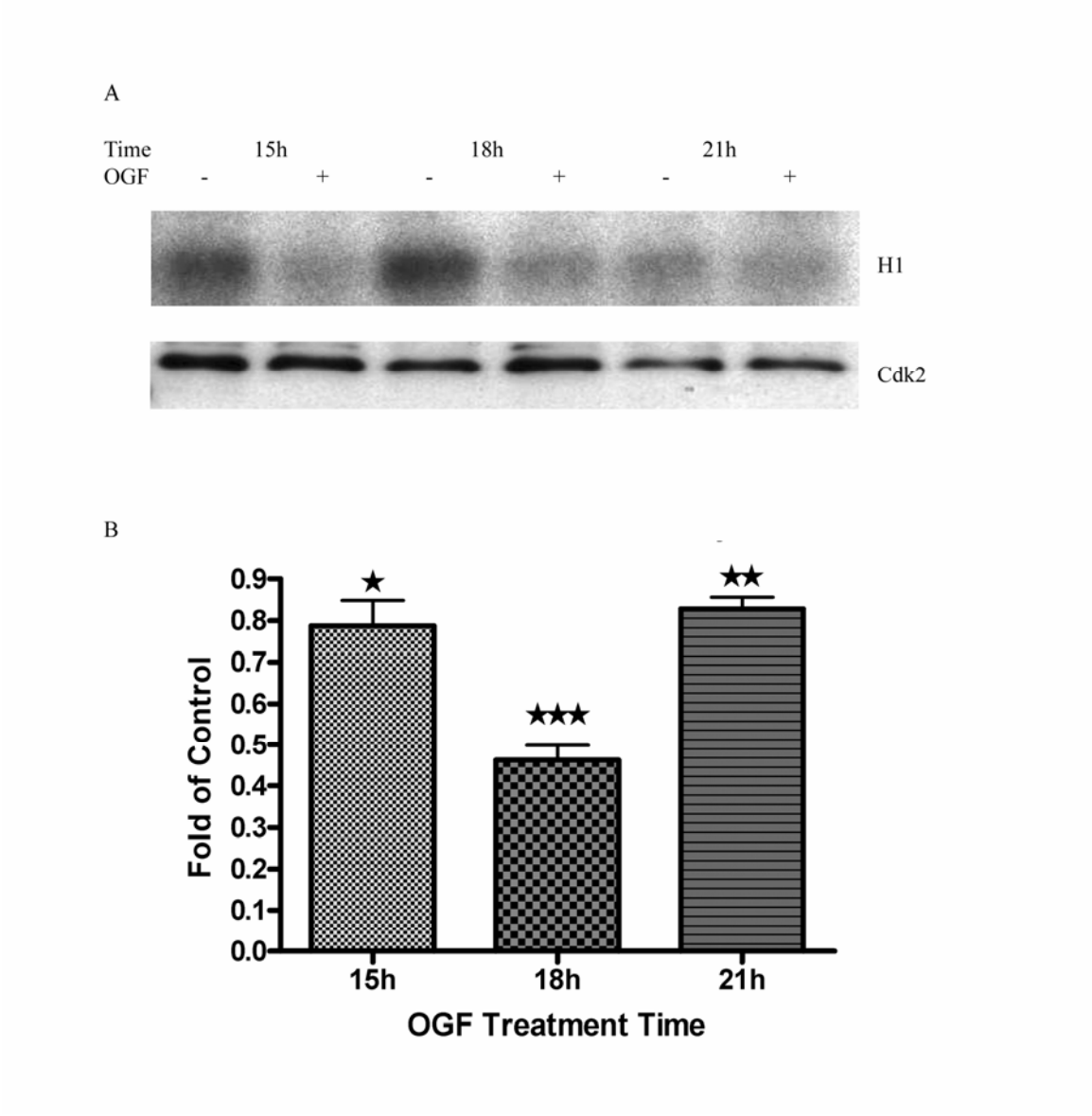

Figure 3.5 OGF decreased CDK2 kinase activity. (A) BxPC3 cells were synchronized by nocodazole (67 ng/ml) for 24 hours. Nocodazole was washed out and the cells were treated with or without OGF (10^{-6} M) for indicated times. Cell lysates were incubated with cdk2-protein A beads to immunoprecipitate total CDK2. The CDK2 kinase activity was evaluated by measuring the capacity of phosphorylation of H1 histone protein in the presence of radioactive ATP. (B) Densitometric analysis was performed and the CDK2 activity was measured relative to controls. The quantitative data represent means ± S.E.M of 4 experiments. Significantly different from the control group at $p<0.05$ (*), $p<0.01$ (**) or $p<0.001$(***).

at 9h and 18h (Fig. 3.6). Levels of cyclin E/CDK2 complex after OGF treatment revealed that OGF treatment did not change the formation of CDK2/cyclin E complex significantly (Fig.3.6). Levels of total cyclin A expression after OGF treatment revealed that OGF treatment did not change total cyclin A expression significantly (Fig. 3.7). Taken together, the results suggest that OGF-induced less cells exiting G0/G1 phases is associated with the cyclin A/CDK2 complexes level. OGF may affect CKI level, which affect CDK2/cyclin A complex formation.

Effect of OGF on protein expression of cdk inhibitor in BxPC3 cells. Because cell cycle progression depends on both positive and negative regulators, the expression of cell cycle inhibitors p21 and p27 were examined. Western blot analysis revealed that OGF treatment resulted in a 1.6 fold induction of p21 expression at 9 hours, comparing to control cells (Fig.3.8). When treated with naloxone, which is the antagonist of OGF, OGF-induced p21 expression was blocked (Fig.3.9). This result showed that OGF-induced p21 upregulation was OGFr mediated. The result of p27 expression after OGF treatment showed that OGF had no significant effect on p27 in BxPC3 cells (Fig. 3.10).

Effect of OGF on protein expression of cdk inhibitor p21 in Capan2 and Panc1 cells. Since OGF increases p21 expression in BxPC3 cells, it is interesting to know if OGF increasing p21 expression is a common way in pancreatic cancer cells. In

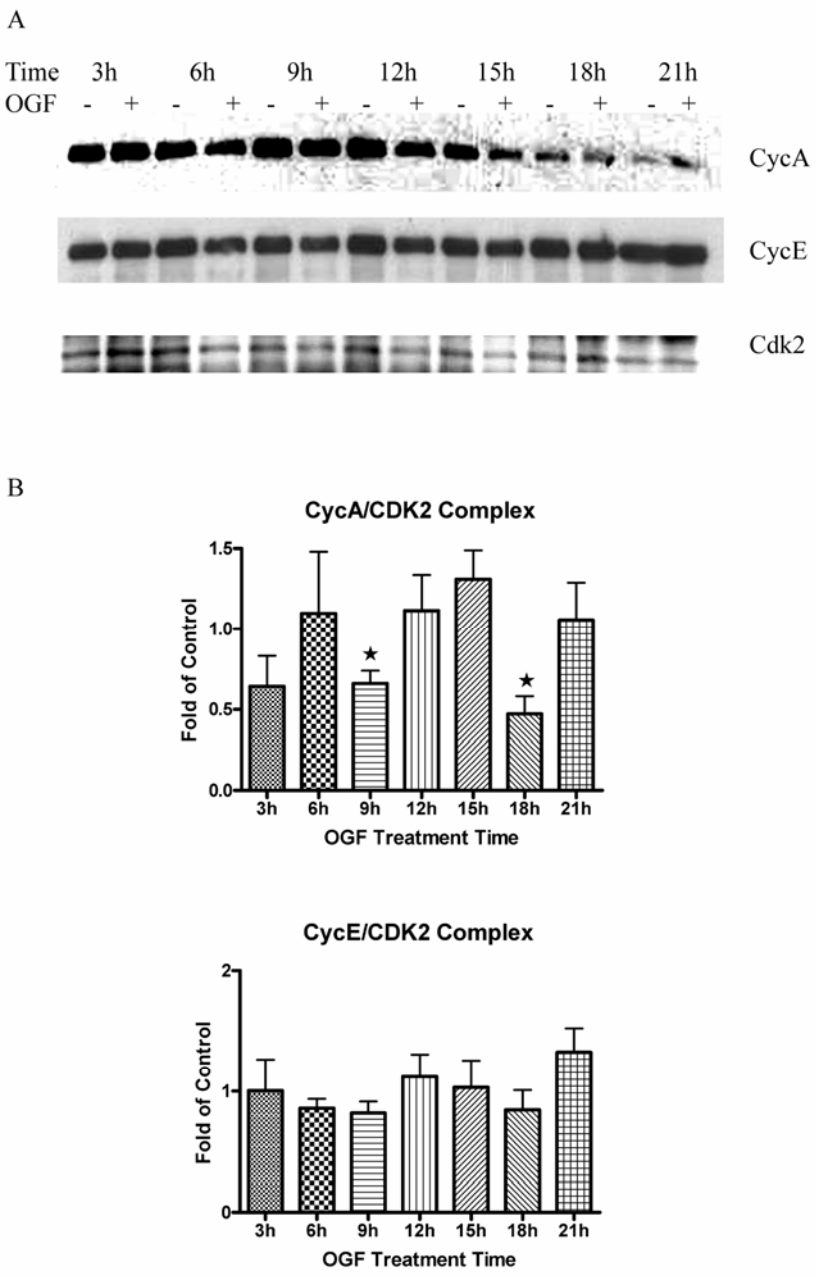

Figure 3.6 OGF affected Cyclin A/CDK2 complex formation, but OGF did not affect Cyclin E/CDK2 complex formation. (A)BxPC3 cells were synchronized by nocodazole (67 ng/ml) for 24 hours. Nocodazole were washed out and the cells were treated with or without OGF (10^{-6} M) for indicated times. Cell lysates were incubated with cdk2-protein A beads to immunoprecipitate total CDK2 and then immunoblotted with cyclin A antibody or cyclin E antibody. (B) Densitometric analysis was performed, and the ratio of Cyclin A/CDK2 complex or Cyclin E/CDK2 complex was expressed relative to controls. Values represent means ± S.E.M of 3 independent experiments.

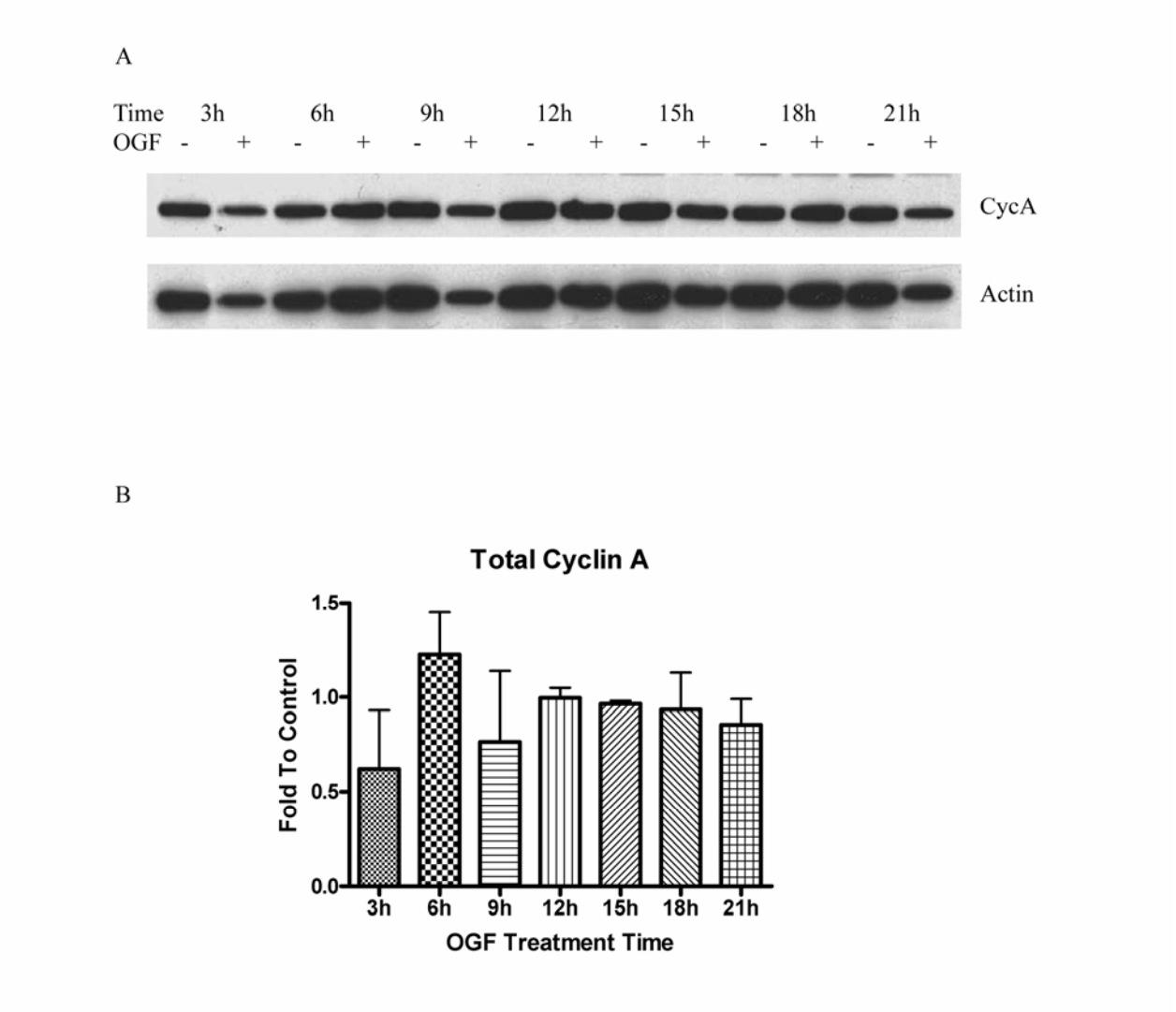

Figure 3.7 OGF did not affect total cyclin A expression. (A) BxPC3 cells were synchronized by nocodazole (67 ng/ml) for 24 hours. Nocodazole were washed out and the cells were treated with or without OGF (10^{-6} M) for indicated times. Total proteins were resolved by SDS-PAGE and subjected to western blotting of cyclin A. (B) Densitometric analysis of the Western blots was performed, and the OGF induced cyclin A was expressed relative to controls. Values represent means ± S.E.M for 3 independent experiments.

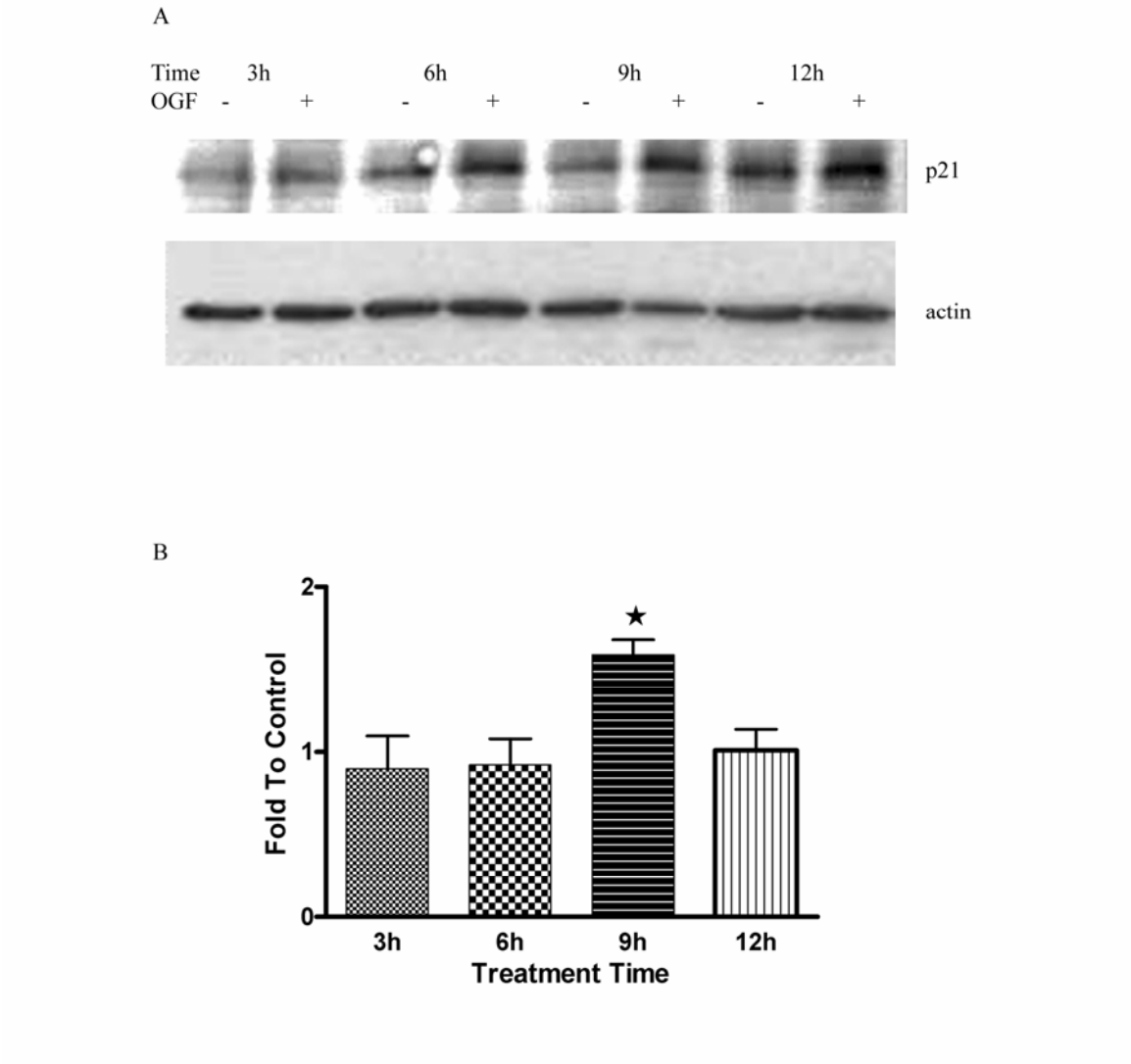

Figure 3.8 OGF increased p21 expression. (A) BxPC3 cells were synchronized by nocodazole (67 ng/ml) for 24 hours. Nocodazole was washed out and the cells were treated with or without OGF (10^{-6} M) for indicated times. Total proteins were resolved by SDS-PAGE and subjected to western blotting of p21. (B) Densitometric analysis of the Western blots was performed, and the OGF induced p21 was expressed relative to controls. Values represent means ± S.E.M for 3 independent experiments.

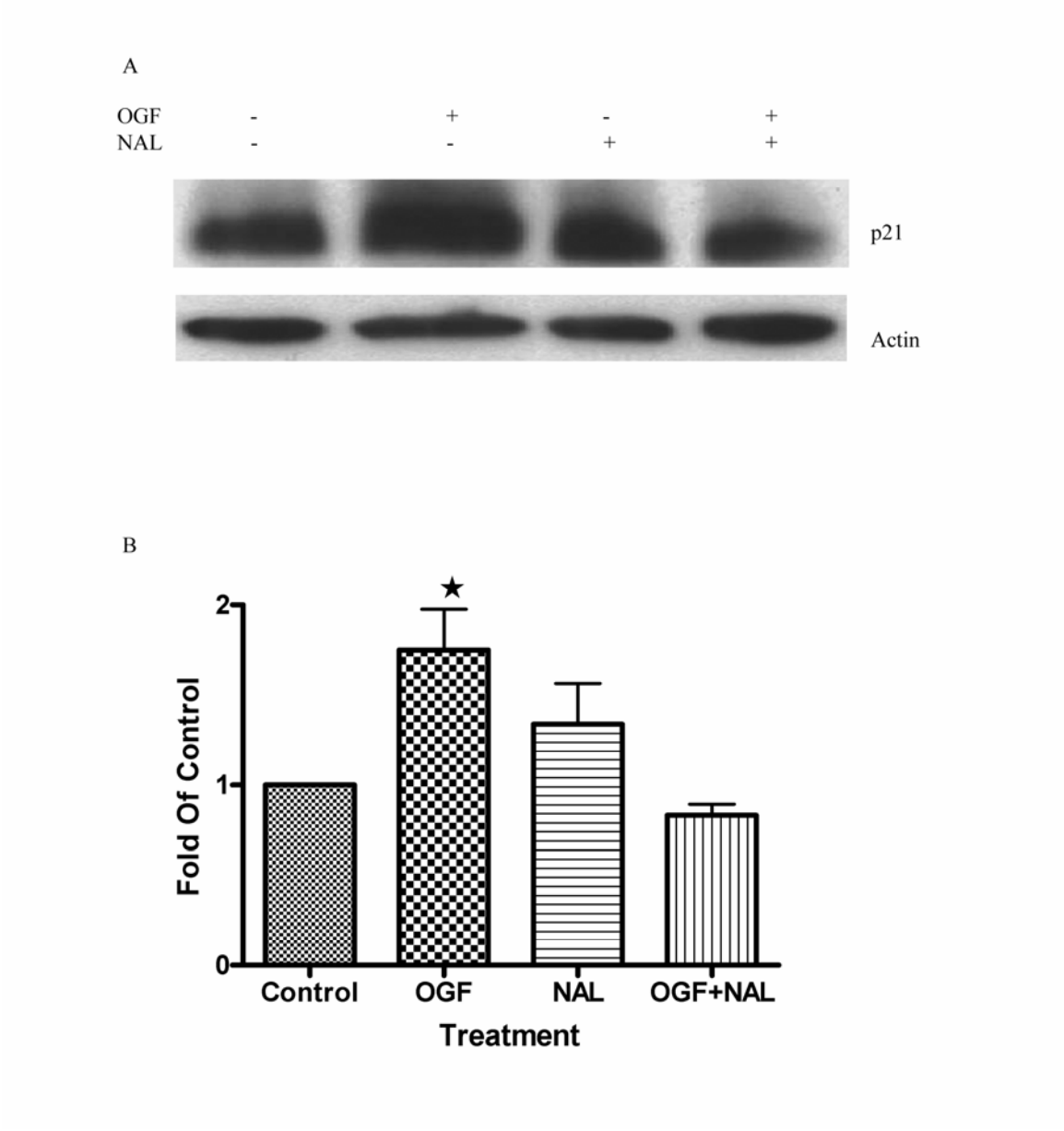

Figure 3.9. OGF induced p21 expression through OGFr. (A) BxPC3 cells were synchronized by nocodazole (67ng/ml) for 24 hours. Nocodazole was washed out and the cells were treated with OGF (10^{-6} M) alone, NAL (10^{-5} M) alone or both OGF (10^{-6} M) and NAL (10^{-5} M) for 9 hours. Total lysates were resolved by SDS-PAGE and subjected to Western blotting for P21 expression. (B) Densitometric analysis was performed, and p21 expression was expressed relative to control. Values represent means ± S.E.M of 3 independent experiments. Significantly different from the control group at $p<0.05$ (*).

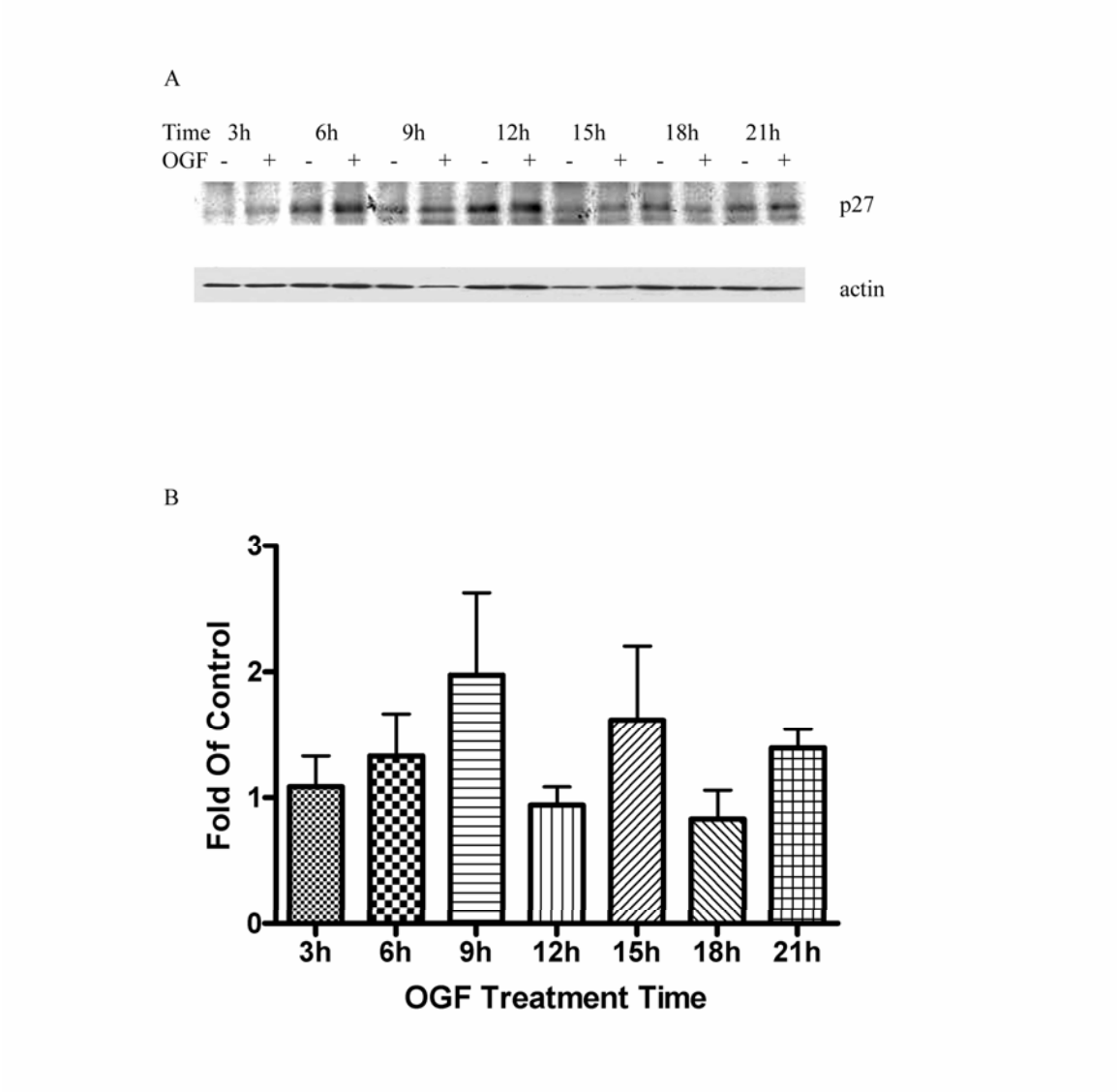

Figure 3.10 OGF did not affect p27 expression. (A) BxPC3 cells were synchronized by nocodazole (67 ng/ml) for 24 hours. Nocodazole was washed out and the cells were treated with or without OGF (10^{-6} M) for indicated times. Total proteins were resolved by SDS-PAGE and subjected to western blotting of p27. (B) Densitometric analysis of the Western blots was performed, and the OGF induced p27 was expressed relative to controls. Values represent means ± S.E.M for 3 independent experiments.

Capan2 and Panc1 cells, which were known to express p21, Western blot analysis revealed that OGF treatment resulted in an induction of p21 expression at 3 hours in Capan 2 cells at 1.6 fold (comparing to control) (Fig 3.12 A and B) and 6 hours in Panc1 cells at 1.45 fold (comparing to control) (Fig. 3.13 A and B). p21 is known as a cell cycle inhibitor by forming heterotrimeric complexes with CDKs and cyclins. Therefore, the data suggested that under the effect of OGF, p21 protein level was upregulated, inhibited cyclin A/CDK2 activity, and inhibited Rb phosphorylation that, in turn, mediated the cell cycle block.

SiRNA directed against p21 blocked OGF inhibiting action. To test the role of p21 in OGF-induced inhibitory action on BxPC3 cell growth, siRNA knockdown experiments were used. BxPC3 cells were treated with p21 siRNA or, as controls, with negative control siRNA. As revealed by Western blot analysis, the p21 siRNA efficiently reduced the level of p21 protein compared to control cells at 48 hours, 72 hours, 96 hours and 120 hours (Fig. 3.11A). Strikingly, in cells that lack sufficient p21, OGF exposure no longer leads to inhibit cell growth (Fig. 3.11B). p21 siRNA effect in Capan2 and Panc1 pancreatic cancer cell lines were also tested. Capan2 or Panc1 cells were treated with p21 siRNA or, as controls, with negative control siRNA. As revealed by Western blot analysis, the p21 siRNA efficiently reduced the level of p21 protein compared to control cells at 72 hours in Capan2 cells (see Appendix Fig 3). Strikingly, in cells that lack sufficient p21, OGF no longer leads to inhibit Capan2 cell growth (Fig. 3.12C). As

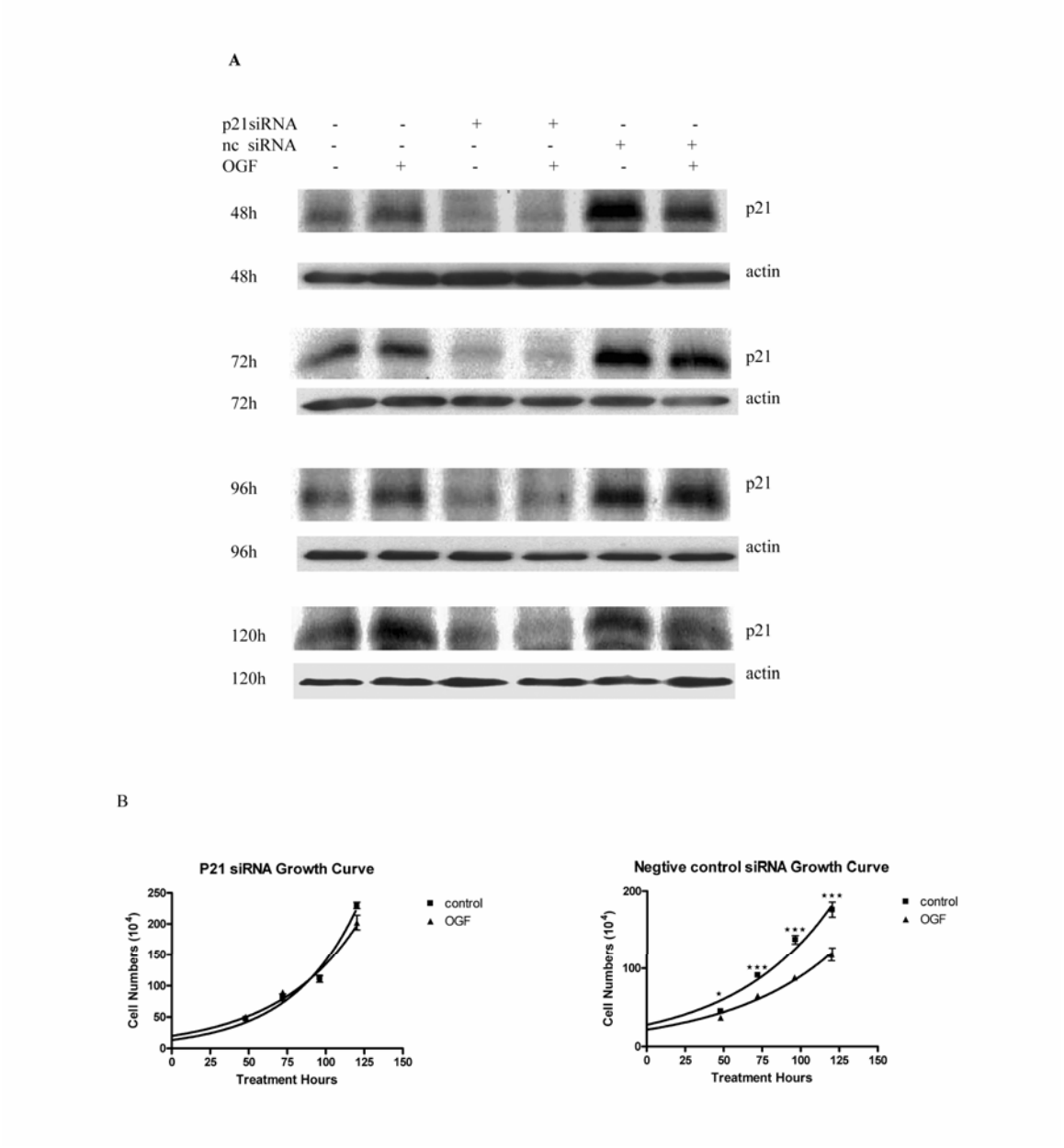

Figure 3.11 p21 is required for OGF induced growth inhibition in BxPC3. (A) siRNAs were transfected in BxPC3 cells 24h after cells were seeded at 200,000 cells/well; OGF were added 4h later after transfection. Media and OGF were replaced daily. Total proteins from BxPC3 cells transfected with either p21 siRNA or negative control siRNA for 48h, 72h, 96h or 120h were separated by SDS-PAGE and immunoblotted with monoclonal antibody to p21. (B) Growth curves for BxPC3 cells transfected with either p21 siRNA or negative control siRNA and grown in the presence or absence (control) of OGF. Data represent means ± S.E.M for 3 samples per treatment group for each time point. Significantly different from the control group at $p<0.05$ (*) or $p<0.001$ (***).

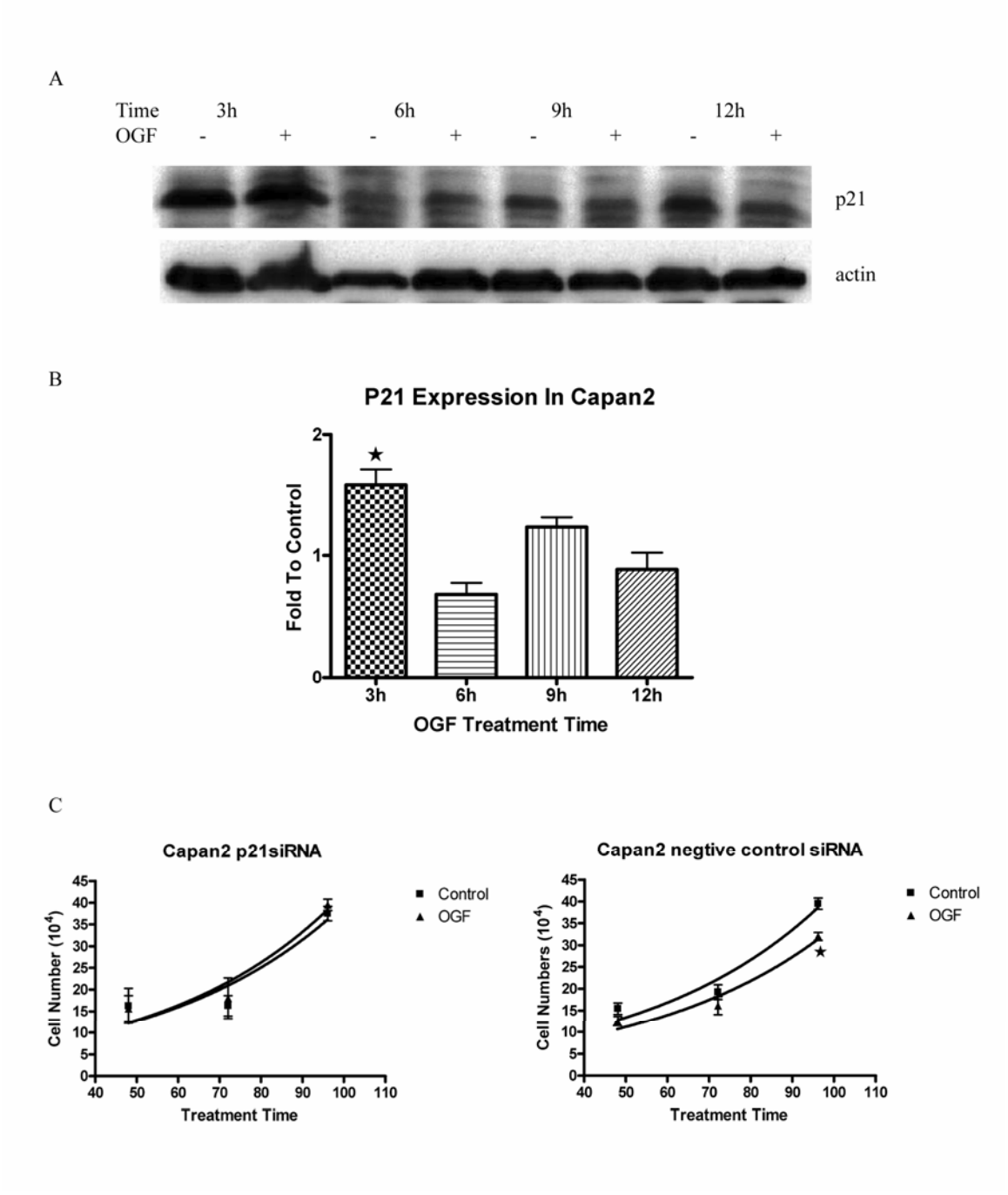

Figure 3.12 OGF increased p21 expression in Capan2 cells. (A) Total proteins were resolved by SDS-PAGE and subjected to western blotting of p21. (B) Densitometric analysis of the Western blots was performed, and the OGF induced p21 was expressed relative to controls. Values represent means ± S.E.M for 3 independent experiments. (C) Growth curves for Capan2 cells transfected with either p21 siRNA or negative control siRNA and grown in the presence or absence (control) of OGF. Data represent means ± S.E.M for 3 samples per treatment group for each time point. Significantly different from the control group at $p<0.05$ (*).

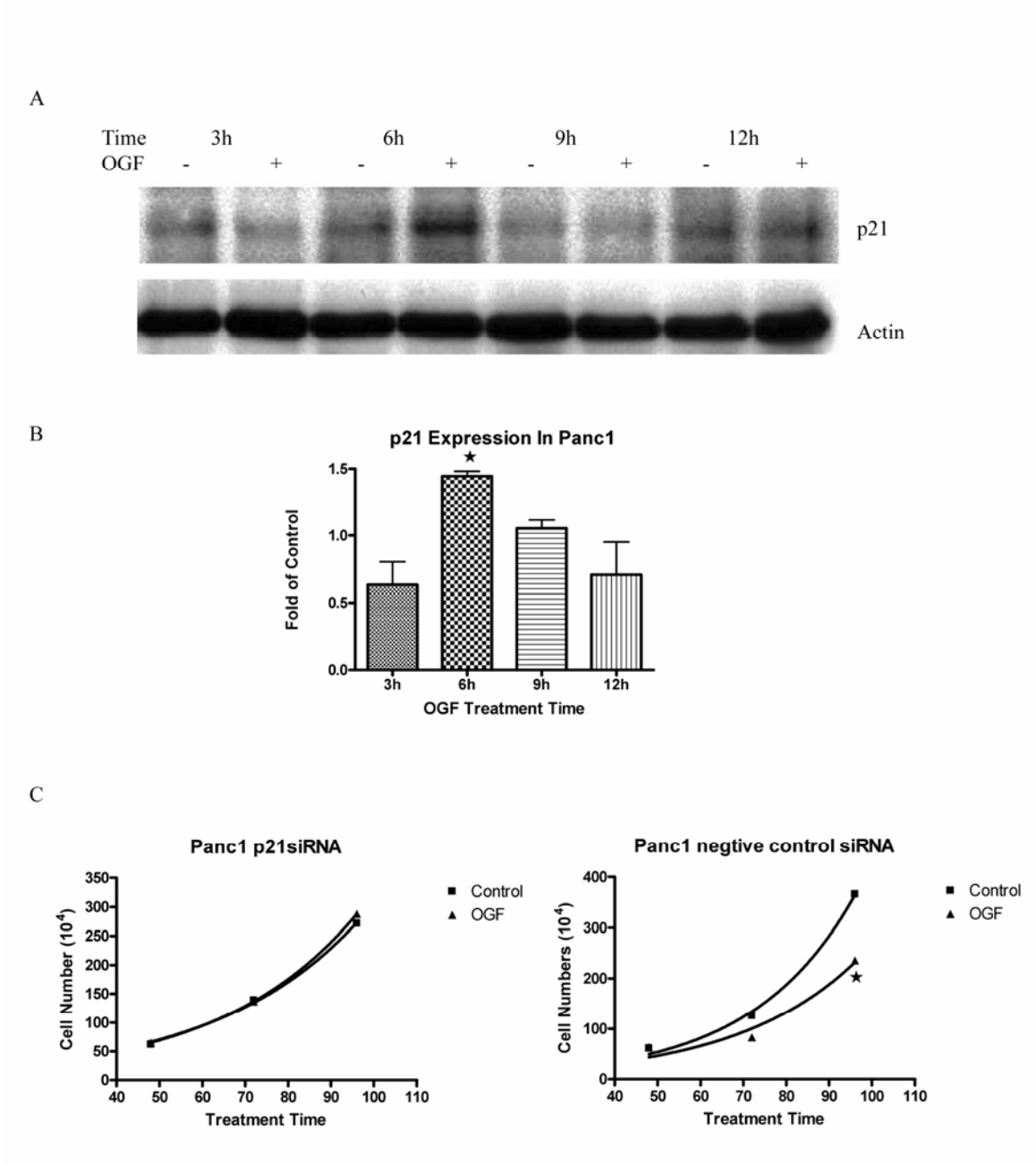

Figure 3.13 OGF increased p21 expression in Panc1 cells. (A)Total proteins were resolved by SDS-PAGE and subjected to Western blotting of p21. (B) Densitometric analysis of the western blots was performed, and the OGF induced p21 was expressed relative to controls. Values represent means ± S.E.M for 3 independent experiments. (C) Growth curves for Panc1 cells transfected with either p21 siRNA or negative control siRNA and grown in the presence or absence (control) of OGF. Data represent means ± S.E.M for 3 samples per treatment group for each time point. Significantly different from the control group at $p<0.05$ (*).

revealed by Western blot analysis, the p21 siRNA efficiently reduced the level of p21 protein compared to control cells at 96h in Panc1 cells (see Appendix Fig 4). Strikingly, in cells that lack sufficient p21, OGF no longer leads to an inhibition of Panc1 cell growth (Fig. 3.13C). These p21 siRNA knockdown assays suggest that p21 induction is sufficient for the OGF-induced inhibitory actions on pancreatic cancer cell growth.

Discussion

A Model for the OGF-OGFr Inhibitory Pathway

OGF, an endogenous autocrine peptide, was proposed to be a valuable anti-cancer agent because of its inhibitory effect on the growth of cancer cells. However, the mechanism of OGF-OGFr axis inhibitory action was poorly understood. Using pancreatic cancer cell line BxPC3, the present study suggests, for the first time, that OGF inhibits BxPC3 growth by up-regulation of the CDK inhibitor p21. Our results showed that BxPC3 treated with OGF decreased Rb phosphorylation, CDK2 kinase activity and increased CKI p21 expression. In addition, OGF antagonist, NAL, blocked OGF induced p21 upregualtion. Targeted decrease of p21 using siRNA blocked OGF inhibiting action. Our results suggest that the receptor-mediated, growth inhibitory effects of the OGF-OGFr axis in BxPC3 cells are associated with induction of p21/cdk2 inhibitor resulting in decreased Rb phosphorylation. The decreased level of Rb in its hyperphosphorylated state is antiproliferative, resulting in fewer cells exiting G0/G1 phase, thus, inhibiting cell growth.

Potential OGF-OGFr Targets

Initial studies in our lab demonstrated that OGF did not induce necrosis, apoptosis [43] or differentiation in *in vitro* models [44]. Previous studies in our lab also demonstrated that OGF induced less cells exiting G0/G1 phase [47]. These findings demonstrated that the inhibitory effect of OGF on cell replication is not related to a broad-based action on the cell cycle, but rather is directed to a singular phase of the cell cycle: G0/G1. These helped us to narrow down OGF targets. A key regulator of the G1 to S phase transition in the cell cycle is retinoblastoma (Rb) protein, a tumor suppressor. During the cell cycle progression, Rb is sequentially phosphorylated by different cyclin/CDK complexes [63]. Different phosphorylation sites in Rb have been demonstrated, with the preferred site being S^{795} by CDK2 or CDK4[59]. This coincided with our observation that OGF down-regulated the phosphorylation of Rb on S^{795}. Since OGF had no effect on $S^{807/811}$, which was specifically phosphorylated by CDK4 [59], we assumed that OGF decreased Rb phosphorylation because of a decreased CDK2 kinase activity. The *in vitro* CDK2 kinase assay demonstrated that OGF decreased CDK2 kinase activity in BxPC3 pancreatic cancer cells.

p21 has been shown to inhibit the growth of malignant cells *in vitro* and *in vivo* [75, 76]. Using recombinant adenoviral system (rAd-p21), Joshi et al. [75] found the growth of two pancreatic tumor cell lines can be inhibited by p21 in vitro, with significant numbers of tumor cells reverting from S to G0/G1. Studies also showed that TGF-beta induced $p21^{wafl}$ expression in Panc1 cells and subsequent growth inhibition [76]. Our studies in this report suggested that OGF inhibited cell growth by upregulating p21 expression. However, these changes are transient and not permanent. It suggests that OGF has cytostatic effect but not cytotoxic effect, which may explain why OGF has no

effect on apoptosis [43]. Since OGF has its effect on G1 phase, it can be synergic to gemcitabine, which acts by inhibiting DNA synthesis in S phase, to inhibit BxPC3 cell growth [42].

Clinical Correlations

p21 is a member of the Cip/Kip family and functions as an inhibitor of cyclin-dependent kinase. Loss of p21 activity has been observed in approximately 30% of pancreatic tumor specimens [91]. Biankin et al. [95] examined the protein expression of p21 in 125 patients and they found that 79% tumors are positively stained for p21. Song et al. [109] examined the p21 protein expression in 90 patients and they found p21 expression was present in 56% tumors and was significantly ($p=0.01$) associated with longer survival following chemotherapy. In pancreatic ductal adenocarcinoma cell lines, the K-ras, p53, and $p16^{Ink4}$ genes were found to be mutated in over 90% of the cell lines [110, 111]. In most pancreatic tumors, loss of p16 expression is also observed [91]. In this study, we suggested that OGF promoted the accumulation of p21. Since most of pancreatic cancer patients' tumors contain p21 and OGF targets p21 in pancreatic tumor cells, these data suggest that OGF may be a useful drug for pancreatic cancer patients.

Taken together, our findings indicate that the upregulation of p21 after OGF treatment occurs with decreasing Cdk2 kinase activity and Rb phosphorylation. We anticipate that a more complete understanding of OGF regulating p21 expression will explain crucial links underlying the regulation of genes that control tumor suppression.

CHAPTER IV

OVERVIEW AND DISCUSSION

4.1 Overview

The main goal of this thesis is to identify the mechanism of OGF-OGFr axis inhibitory functions on cell proliferation. I have used various *in vitro* molecular techniques to identify critical components of the event and determine their mechanism of action. The central hypothesis of this thesis is that OGF-OGFr axis inhibits cell proliferation through cell cycle regulatory proteins. The studies performed here support that OGF-OGFr inhibits cell proliferation through CKI-Rb pathway. A number of novel findings are presented in this thesis:

1. OGF inhibited Rb phosphorylation.
2. OGF inhibited CDK4 kinase activity in SCC1 cells. OGF inhibited CDK2 kinase activity in BxPC3 cells.
3. OGF increased p16 expression in HNSCC cells in a receptor mediated manner (i.e. blocked by NAL). OGF increased p21 expression in pancreatic cancer cells in a receptor mediated manner (i.e. blocked by NAL).
4. CKIs are important for OGF-OGFr inhibitory function.

In summary, the data from these studies have supported one of the molecular pathways that link the cell cycle arrest at G1 with OGF. In SCC1 cells, the binding of OGF to its specific receptor OGFr up-regulated p16 expression. p16 forms a complex with Cdk4, leading to repressed Cdk4 activity, resulting in less phosphorylation of Rb. The lower levels of phosphorylated Rb eventually caused fewer cells to exit the G1 phase of cell cycle. In BxPC3 cells, the binding of OGF to its specific receptor OGFr up-regulated p21 expression. p21 forms a complex with Cdk2, leading to repressed Cdk2

activity, resulting in less phosphorylation of Rb. This reduced phosphorylated Rb eventually caused fewer cells to exit the G1 phase of the cell cycle.

4.2 Discussion

4.2.1. Regulation of cell proliferation by the OGF-OGFr axis

OGF and its receptor OGFr are widely expressed in many tissues and regulate a diverse array of biological processes including cell proliferation, development, cellular renewal, cancer, wound healing and angiogenesis [6]. Among these effects, the anti-proliferative effect of the OGF-OGFr system is especially important in that it is observed not only in cultured tumor cells, but also in tumors *in vivo*. Previous studies in our lab showed that OGF treatment decreased the growth of a variety of human cancer cells both *in vivo* and *in vitro* including head and neck squamous cell carcinoma cell lines [37], pancreatic tumor cells [35, 36], colon adenocarcinoma cell lines [40], and renal cancer [38]. OGF has been identified as a negative growth regulator [7]. This thesis was designed to investigate the mechanism of the OGF-OGFr axis inhibitory activity on cell proliferation.

Initially, the growth of the HNSCC cells (SCC1) and pancreatic cancer cells (BxPC3) were measured daily over 72 hours or 96 hours. Cell doubling time for HNSCC SCC1 control cells was about 20 hours. Cell growth was also measured in cultures treated chronically with exogenous OGF. Significant growth inhibition was observed after 72 hours of OGF treatment (Fig 2.1). Total cell doubling time increased significantly in OGF treated cultures to approximately 30 h, a 49% increase relative to controls. Cell doubling time for pancreatic cancer BxPC3 control cells was about 29 h. Cell growth was

also measured in cultures treated chronically with exogenous OGF. Significant growth inhibition was observed after 48 hours of OGF treatment (Fig 3.1). Total cell doubling time increased significantly in OGF treated cultures to approximately 51 h, a 78% increase over controls. Similar inhibitory action of OGF was also observed in a variety of pancreatic and head and neck cancer cell lines, including CAL27, SCC4, Capan2 and Panc1 cells. These data supported the previous findings that OGF regulate human HNSCC growth [37] and human pancreatic cancer cell growth in tissue culture [36].

Zagon et al [47] reported previously that the OGF-OGFr axis action was directed at the G_0/G_1 phase. Furthermore, Zagon et al [43, 44] reported that the growth inhibitory function of the OGF-OGFr system was associated with inhibition of DNA synthesis, but did not lead to changes in differentiation, apoptosis, or necrosis. These findings that a mechanism of the OGF action is a specific alteration of the cell cycle lead us to investigate what aspect of the cell cycle is involved with OGF activity.

To begin to address mechanisms associated with the change in cell growth, cell cycle phase percentages were calculated using FACS analysis. In both HNSCC SCC1 and pancreatic cancer cells BxPC3, G_0/G_1 phase percentages were simultaneously increased and compensatory reduction in cells in S and G2/M phases in response to OGF (Fig 2.1 and Fig 3.1). These data are similar to Roesener's work [47] showing the effects of OGF on the cell cycle phases of BxPC3 cells.

In addition, the study presented in this thesis extends the previous work, in which we documented that OGF-OGFr axis has its effect in G1 phase [47], to examine the precise mechanism of G1 phase regulation. Other reports have shown negative growth regulation following growth factor addition in several neoplastic systems [112, 113].

Transforming growth factor-β (TGF-β) is characterized by G1 arrest and altered gene expression of p21 and p15 [112]. Hepatocyte growth factor (HGF) arrested cells in G1 phase by induction of p16 and repression of Cdk2 activity [113]. HNSCC cell lines studied herein, OGF induced p16 expression and p16 is important for OGF-OGFr inhibitory action. In pancreatic cancer cell lines studied, which are absent of p16, OGF induced p21 expression and p21 is important for OGF-OGFr inhibitory action. This different CKI induction by OGF in different cell lines may be because they are different tumor cell lines with different origins and/or gene expression patterns.

Different cell lines have different response to OGF treatment. For example, in SCC1 cells, OGF inhibited growth optimally at 96 h, with percentage in cell number of controls as about 59% (Fig. 2.1A). In BxPC3 cells, OGF inhibited growth at 72 h, with percentage in cell number of controls as 55% (Fig 3.1A). In Capan2 cells, OGF inhibited growth most at 96 h, with percentage in cell number of controls as approximately 68%. This difference may be because each cell line contains different levels of OGFr, or the OGF-OGFr axis uses different CKI in different cell lines.

4.2.2 OGF signal transduction

4.2.2.1 CKI-Rb pathway

Retinoblastoma (Rb) is a key regulator of cell cycle progression. Rb phosphorylation status controls the cell cycle progression in G1 phase. Cyclin/CDK complexes control Rb phosphorylation through their ordered activation and inactivation. The CKI family regulates the activity of cyclin/CDK complex and subsequently cell cycle restriction point. In the present study, we observed that the OGF-OGFr axis

increased CKI levels (p16 or p21), decreased CDK4 or CDK2 activity and decreased Rb phosphorylation levels. The less hyperphosphorylated Rb eventually causes fewer cells to exit the cell cycle G1 phase following OGF treatment.

4.2.2.2 Up-stream Activity of CKI

OGF is an endogenous opioid peptide and synthesized from its precursor proenkephalin. OGFr has a nuclear localization signal. After OGF interacts with OGFr, the peptide and receptor form a complex that accumulates in a perinuclear location [6]. Our data also showed that the OGF-OGFr axis increased p16 or p21 level. However, the precise mechanisms of the OGF-mediated induction of p16 or p21 level are still not uncovered.

Recent studies have shown that hSNF5, a chromatin remolding complex, can directly regulate p16 and p21 transcription and cause growth arrest [114]. Chromatin immunoprecipitation data confirmed that hSNF5 regulated p16 and p21 transcription by binding to the appropriate promoter regions of each gene [114]. Interestingly, the authors also found that p21 remains up-regulated by hSNF5 in the absence of p16 [114]. In our study, we found that p16 can be regulated by OGF in the absence of elevated p21 in SCC1 cells. In BxPC3 cells, we found that loss of p16 expression seems to result in compensatory induction of p21. These imply that cross-talk may occur among CKI proteins, such as p16 and p21, which involve OGF-OGFr axis. It will be interesting to study whether the OGF-OGFr axis cooperates with gene regulatory machinery to control CKI transcription in a complex and precise manner.

We showed that the OGF-OGFr axis inhibited cell growth through p16 in SCC1 cells (figure 2.9). We also showed that in cells that lack sufficient p16 using siRNA, OGF

no longer leads to inhibition of cell growth (Fig. 2.10B) even it has p21 expression in SCC1 cells. However, in BxPC3 cells, which lack p16 expression, the OGF-OGFr axis still inhibits cell growth through p21 pathway. These differences could reflect the requirement of dissimilar factors in different cell types for OGF activity or a different spectrum of mutations in other genes in these cell lines.

4.2.2.3 Other signal pathways

It will also be interesting to identify other signaling pathways of OGF-OGFr besides cell cycle pathway. These are presumed to exist because OGF-OGFr induced transient increasing of CDK4 kinase activity in SCC1 cells and other studies showed that OGF is related to MAPK signaling pathway [115, 116]. Identification of other pathway components of OGF-OGFr axis in addition to the studies mentioned above will complete our understanding of this important growth regulatory system.

4.2.3 Role of OGF in cancer

The anti-proliferative effect of OGF seems to be concerned with the control of tumorigenesis, which is also an important aspect to understanding the biological process of carcinogenesis. Due to the anti-proliferative function of the OGF-OGFr axis, tumor cells may lose the tumor-suppressive responses to OGF during tumor progression.

In HNSCC cells, OGFr is reduced markedly compared with control epithelium [117]. Since the OGF-OGFr system is a tonically active growth inhibitory factor, diminishment in OGFr in HNSCC constitutes a loss of control of cell replicative activities [117].

Since our study suggests OGF-OGFr induced CKI-Rb pathway to inhibit cell growth, tumor cells may acquire somatic mutations in components of the CKI-Rb signal transduction pathway in order to evade the OGF antiproliferative function. It could be predicted that if a tumor cell loses p16 and p21 gene expression, OGF treatment won't inhibit proliferation.

4.3 Clinical Correlations

The endogenous CDK inhibitor p16 is a known tumor suppressor. In this report, we suggested that OGF promoted that accumulation of p16. In HNSCC, overexpression of cyclin D1, LOH (loss of heterozygosity) of 9p21 (p16) and MTS2 (p15) have been demonstrated [88, 105, 106]. However, studies also showed that in primary HNSCC tumors, p16 mutations and deletion were not as frequent as in HNSCC cell lines [68, 88, 107, 108]. Zhang et al. [68] have reported 10% of mutations and deletions of p16 in primary tumors and 44% in cell lines. Lydiatt et al. [88] have reported 19% of genetic alterations of p16 in HNSCC tumors and 75% in cell lines. Since most of HNSCC patients' tumors contain p16 and OGF targets p16 in HNSCC cells, this information suggests that OGF may be a useful drug for HNSCC patients.

p21 is a member of the Cip/Kip family and functions as an inhibitor of cyclin-dependent kinase. Loss of p21 activity has been observed in approximately 30% of pancreatic tumor specimens [91]. Biankin et al. [95] examined the protein expression of p21 in 125 patients and they found that 79% tumors are positively stained for p21. Song et al. [109] examined the p21 protein expression in 90 patients, and they found that p21

expression was present in 56% tumors and was significantly (p=0.01) associated with longer survival following chemotherapy. In pancreatic ductal adenocarcinoma cell lines, the K-ras, p53, and $p16^{Ink4}$ genes were found to be mutated in over 90% of the cell lines [110, 111]. In most pancreatic tumors, loss of p16 expression is also observed [91]. In this study, we suggested that OGF promoted the accumulation of p21. Since most of pancreatic cancer patients' tumors contain p21 and OGF targets p21 in pancreatic tumor cells, these information suggest that OGF may be a useful drug for pancreatic cancer patients.

Another clinical significance of this study is that using p16 or p21 as biomarkers for HNSCC or pancreatic cancer patients. If we can detect p16 expression in a HNSCC patient's tumor or p21 expression in a pancreatic cancer patient's tumor, this patient can be selected for OGF therapy. This selective method for OGF responder will be a more economic and effective way for clinical trials.

4.4 Future Experiments

Some questions remain to be answered for more complete understanding of OGF-OGFr axis and cell growth control.

We have demonstrated that the OGF-OGFr axis inhibited cell growth through CKI p16 or p21 levels. However, we do not know if it uses the same mechanism to inhibit normal cell growth. Next, we may use some normal cell lines, such as endothelial cell, fibroblast cell, or keratinocyte cell, to detect if OGF-OGFr also increases CKI levels in these normal cells.

Since the OGF-OGFr axis targets p16 or p21 in HNSCC or pancreatic cancer, we also would like to know if the OGF-OGFr axis targets other CKI when both p16 and p21 are deleted. We may use p16 and p21 knockdown cell lines and exam if the OGF-OGFr axis still has growth inhibitory functions. We may transfect a normal cell line with both p16 siRNA and p21 siRNA to make a p16 and p21 knockdown cell line.

Our results suggest that OGF upregulated p16 expression; however, the exact mechanism by which OGF-OGFr axis increases the expression of p16 is still unknown. Gene expression can be regulated at several different levels, including initiation of transcription, stability of mRNA, initiation of translation or post-translational regulation. We may use reverse transcription PCR or real time PCR to measure p16 mRNA level. If OGF increases p16 mRNA level, then we need to find if OGF promotes the accumulation of p16 mRNA or alter p16 mRNA stability. First, we may test if OGF transactivate the p16 mRNA. We may use p16 promoter luciferase constructs to transfect cells with full-length promoter or constructs lacking known recognition sites, comparing the activation of different constructs. On the basis of these results, we may know the minimal p16 promoter region that is required for OGF to transactivate p16. To explore whether OGF alters p16 mRNA stability, cells can be treated with OGF followed by actinomycin D to prevent transcription [118]. Northern blot analysis will show the p16 mRNA stability using actin mRNA as the control. If OGF has no effect on p16 mRNA accumulation or stability, we may examine the effects of OGF on the stability of p16 protein. Cell can be treated with OGF followed by cycloheximide to prevent translation [118]. Western blot analysis will show the p16 protein stability level using actin protein as the control.

Our results also suggest that OGF upregulated p21 expression. The exact mechanism by which OGF-OGFr axis increases the expression of p21 is unknown. As mentioned before, gene expression can be regulated at several different levels, including initiation of transcription, stability of mRNA, initiation of translation or post-translational regulation. We may use reverse transcription PCR or real time PCR to measure p21 mRNA level. If OGF increases p21 mRNA level, then it will be further studied if OGF promotes the accumulation of p21 mRNA or alters p21 mRNA stability. To explore whether OGF increases transactivation of the p21 promoter, transient transfections can be performed with human p21 promoter constructs [119]. The plasmid DNA containing wild-type p21 promoter luciferase construct, and internal control construct can be cotransfected into the cells. After transfection, cells will be treated with OGF and the measurement of luciferase activities can be performed. On the basis of these results, we may know whether OGF stimulates p21 promoter activity. To explore whether OGF alters p21 mRNA stability, cells can be treated with OGF followed by actinomycin D to prevent transcription [118]. Northern blot analysis will show the p21 mRNA stability using actin mRNA as the control. If OGF has no effect on p21 mRNA accumulation or stability, we may examine the effects of OGF on the stability of p21 protein. Cell can be treated with OGF followed by cycloheximide to prevent translation [118]. Western blot analysis will show the p21 protein stability level using actin protein as the control.

Since our results demonstrated that the OGF-OGFr axis inhibited cell growth through CKI p16 or p21 levels, we may use other compounds which increase p16 level, such as Indole-3-carbinol (I3C) [69], or compounds which increase p21 level, such as

TGF-beta [76], and combine them with OGF to exam the synergic effects on cell growth inhibition.

In summary, these experiments revealed the mechanism of action of the OGF-OGFr axis on cell proliferation and identified at least two CKI pathways that are used by OGF to execute its effects of retaining cells in the G_0/G_1 phase of the cell cycle. With the identification of p16 and p21 as molecular targets, we have begun to assimilate information that may serve in the design and implementation of therapeutic agents for two very devastating cancers.

APPENDIX

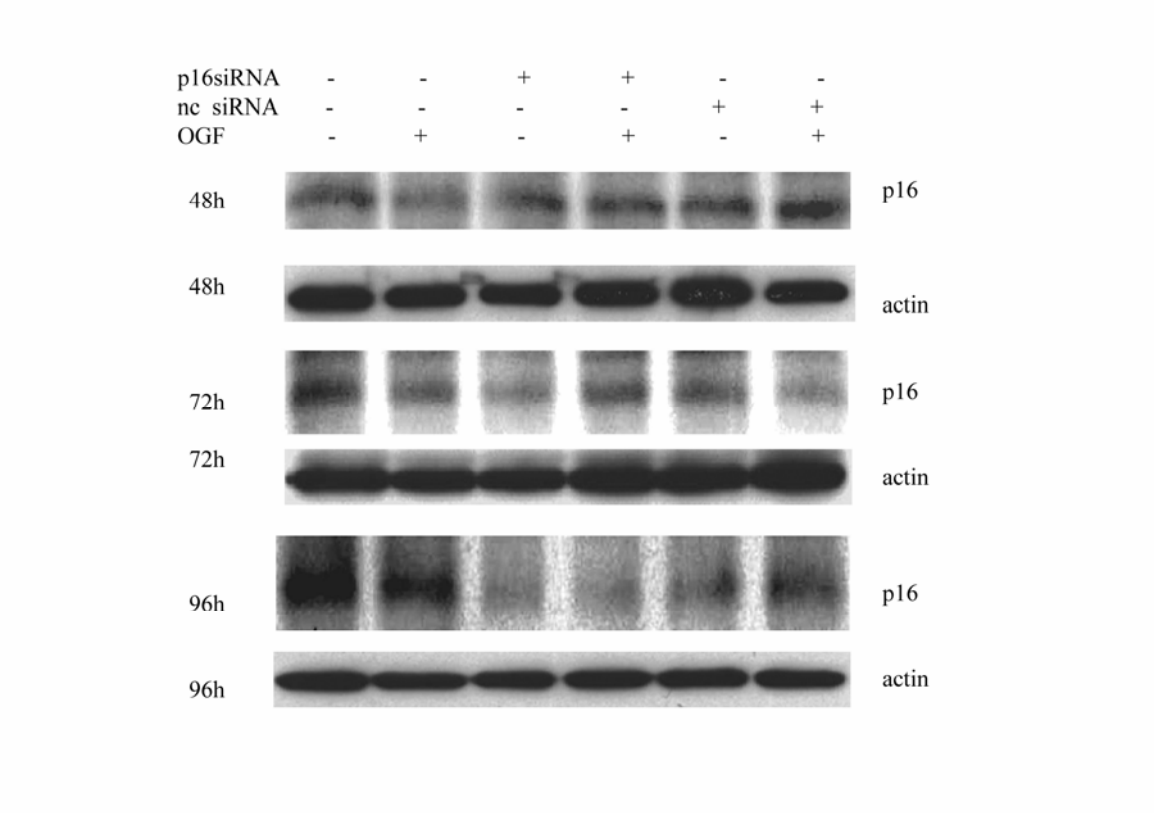

Appendix Figure 1. siRNAs were transfected in CAL27 cells 24h after cells were seeded at 200,000 cells/well; OGF was added 4h later after transfection. Media and OGF were replaced daily. Total proteins from CAL27 cells transfected with either p16 siRNA or negative control siRNA for 48h, 72h, or 96h were separated by SDS-PAGE and immunoblotted with antibody to p16.

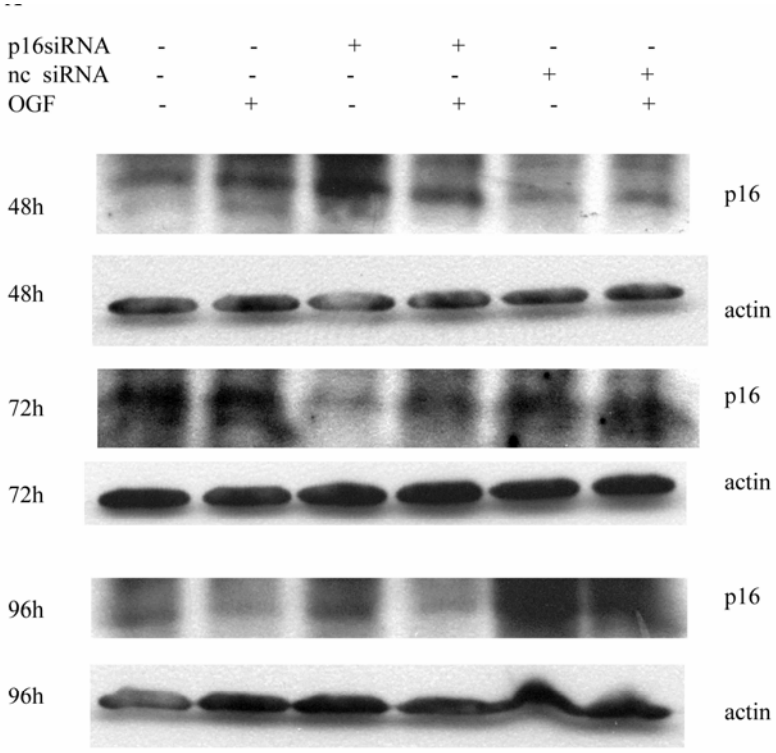

Appendix figure 2. siRNAs were transfected in SCC4 cells 24h after cells were seeded at 200,000 cells/well; OGF were added 4h later after transfection. Media and OGF were replaced daily. Total proteins from SCC4 cells transfected with either p16 siRNA or negative control siRNA for 48h, 72h, or 96h were separated by SDS-PAGE and immunoblotted with antibody to p16.

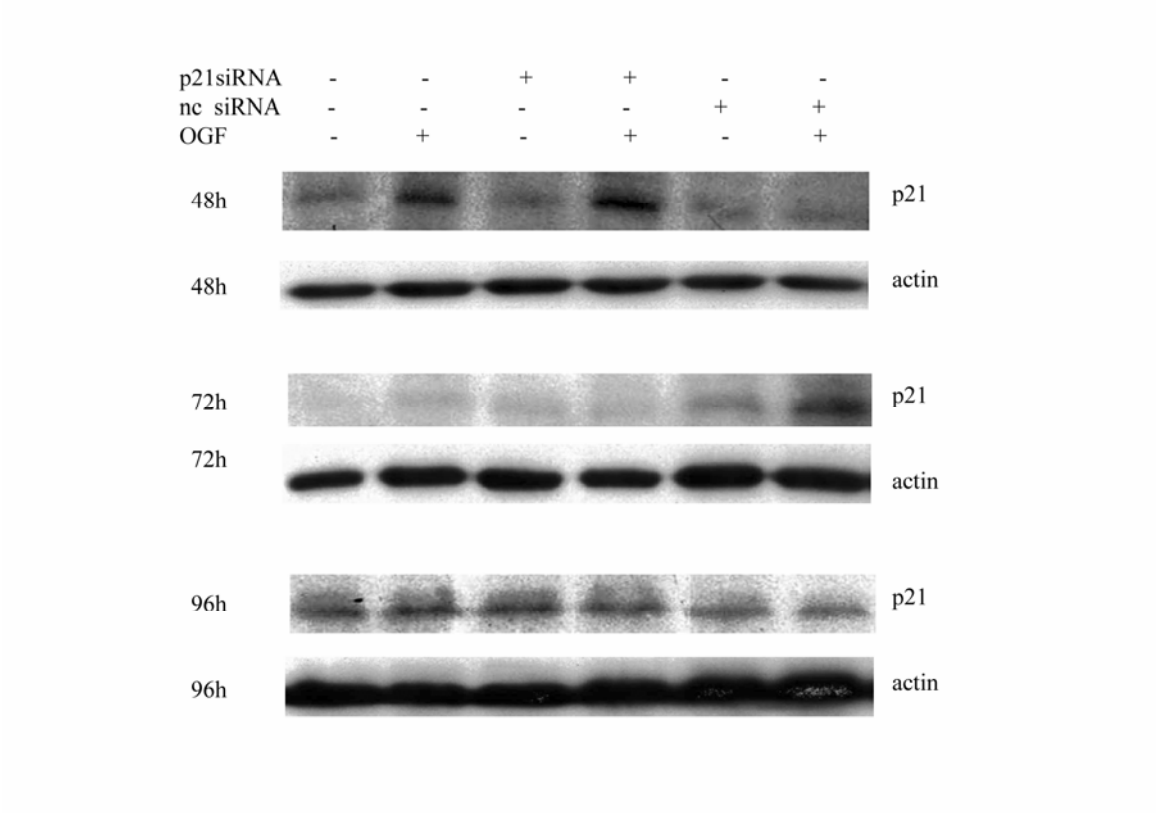

Appendix Figure 3. siRNAs were transfected in Capan2 cells 24h after cells were seeded at 200,000 cells/well; OGF were added 4h later after transfection. Media and OGF were replaced daily. Total proteins from Capan2 cells transfected with either p21 siRNA or negative control siRNA for 48h, 72h, or 96h were separated by SDS-PAGE and immunoblotted with monoclonal antibody to p21.

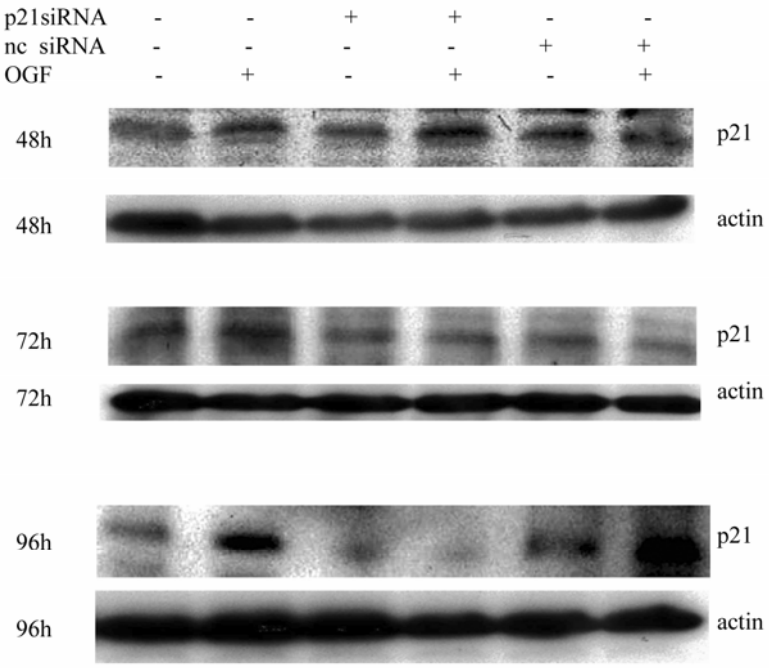

Appendix Figure 4. siRNAs were transfected in Panc1 cells 24h after cells were seeded at 200,000 cells/well; OGF were added 4h later after transfection. Media and OGF were replaced daily. Total proteins from Panc1 cells transfected with either p21 siRNA or negative control siRNA for 48h, 72h, 96h or 120h were separated by SDS-PAGE and immunoblotted with monoclonal antibody to p21.

BIBLIOGRAPHY

1. Dhawan, B.N., et al., *International Union of Pharmacology. XII. Classification of opioid receptors.* Pharmacol Rev, 1996. **48**(4): p. 567-92.
2. Akil, H., et al., *Endogenous opioids: biology and function.* Annu Rev Neurosci, 1984. **7**: p. 223-55.
3. Zagon, I.S. and P.J. McLaughlin, *Naltrexone modulates growth in infant rats.* Life Sci, 1983. **33**(24): p. 2449-54.
4. Zagon, I.S. and P.J. McLaughlin, *Naltrexone modulates tumor response in mice with neuroblastoma.* Science, 1983. **221**(4611): p. 671-3.
5. Zagon, I.S. and P.J. McLaughlin, *Increased brain size and cellular content in infant rats treated with an opiate antagonist.* Science, 1983. **221**(4616): p. 1179-80.
6. Zagon, I.S., M.F. Verderame, and P.J. McLaughlin, *The biology of the opioid growth factor receptor (OGFr).* Brain Res Brain Res Rev, 2002. **38**(3): p. 351-76.
7. Zagon, I.S. and P.J. McLaughlin, *Endogenous opioid systems regulate growth of neural tumor cells in culture.* Brain Res, 1989. **490**(1): p. 14-25.
8. Zagon, I.S., et al., *Cloning, sequencing, chromosomal location, and function of cDNAs encoding an opioid growth factor receptor (OGFr) in humans.* Brain Res, 2000. **856**(1-2): p. 75-83.
9. Hartvig, P., et al., *Kinetics of four 11C-labelled enkephalin peptides in the brain, pituitary and plasma of rhesus monkeys.* Regul Pept, 1986. **16**(1): p. 1-13.
10. Katzung, B.G., *Basic & clinical pharmacology*. A Concise medical library for practitioner and student. Vol. [1st ed.]-. 1982, Los Altos, Calif.: Lange Medical Publications. v.
11. Henderson, G. and A.T. McKnight, *The orphan opioid receptor and its endogenous ligand--nociceptin/orphanin FQ.* Trends Pharmacol Sci, 1997. **18**(8): p. 293-300.
12. Corbett, A.D., et al., *75 years of opioid research: the exciting but vain quest for the Holy Grail.* Br J Pharmacol, 2006. **147 Suppl 1**: p. S153-62.
13. Zagon, I.S., et al., *Cloning, sequencing, expression and function of a cDNA encoding a receptor for the opioid growth factor, [Met(5)]enkephalin.* Brain Res, 1999. **849**(1-2): p. 147-54.
14. Zagon, I.S., S.R. Goodman, and P.J. McLaughlin, *Demonstration and characterization of zeta (zeta), a growth-related opioid receptor, in a neuroblastoma cell line.* Brain Res, 1990. **511**(2): p. 181-6.
15. Zagon, I.S., D.M. Gibo, and P.J. McLaughlin, *Zeta (zeta), a growth-related opioid receptor in developing rat cerebellum: identification and characterization.* Brain Res, 1991. **551**(1-2): p. 28-35.
16. Zagon, I.S., S.R. Goodman, and P.J. McLaughlin, *Zeta (zeta), the opioid growth factor receptor: identification and characterization of binding subunits.* Brain Res, 1993. **605**(1): p. 50-6.
17. Zagon, I.S., Y. Wu, and P.J. McLaughlin, *Opioid growth factor inhibits DNA synthesis in mouse tongue epithelium in a circadian rhythm-dependent manner.* Am J Physiol, 1994. **267**(3 Pt 2): p. R645-52.
18. McLaughlin, P.J., *Regulation of DNA synthesis of myocardial and epicardial cells in developing rat heart by [Met5]enkephalin.* Am J Physiol, 1996. **271**(1 Pt 2): p. R122-9.

19. Zagon, I.S., Y. Wu, and P.J. McLaughlin, *Opioid growth factor is present in human and mouse gastrointestinal tract and inhibits DNA synthesis.* Am J Physiol, 1997. **272**(4 Pt 2): p. R1094-104.
20. Zagon, I.S., Y. Wu, and P.J. McLaughlin, *The opioid growth factor, [Met5]-enkephalin, and the zeta opioid receptor are present in human and mouse skin and tonically act to inhibit DNA synthesis in the epidermis.* J Invest Dermatol, 1996. **106**(3): p. 490-7.
21. Zagon, I.S., D.M. Gibo, and P.J. McLaughlin, *Ontogeny of zeta (zeta), the opioid growth factor receptor, in the rat brain.* Brain Res, 1992. **596**(1-2): p. 149-56.
22. Zagon, I.S., T. Isayama, and P.J. McLaughlin, *Preproenkephalin mRNA expression in the developing and adult rat brain.* Brain Res Mol Brain Res, 1994. **21**(1-2): p. 85-98.
23. Wu, Y., P.J. McLaughlin, and I.S. Zagon, *Ontogeny of the opioid growth factor, [Met5]-enkephalin, preproenkephalin gene expression, and the zeta opioid receptor in the developing and adult aorta of rat.* Dev Dyn, 1998. **211**(4): p. 327-37.
24. Zagon, I.S., Y. Wu, and P.J. McLaughlin, *Opioid growth factor and organ development in rat and human embryos.* Brain Res, 1999. **839**(2): p. 313-22.
25. Kornyei, J.L., et al., *Developmental changes in the inhibition of cultured rat uterine cell proliferation by opioid peptides.* Cell Prolif, 2003. **36**(3): p. 151-63.
26. Zagon, I.S., J.W. Sassani, and P.J. McLaughlin, *Opioid growth factor modulates corneal epithelial outgrowth in tissue culture.* Am J Physiol, 1995. **268**(4 Pt 2): p. R942-50.
27. Zagon, I.S., et al., *Homeostasis of ocular surface epithelium in the rat is regulated by opioid growth factor.* Brain Res, 1997. **759**(1): p. 92-102.
28. Zagon, I.S., et al., *Particle-mediated gene transfer of opioid growth factor receptor cDNA regulates cell proliferation of the corneal epithelium.* Cornea, 2005. **24**(5): p. 614-9.
29. Zagon, I.S., J.W. Sassani, and P.J. McLaughlin, *Re-epithelialization of the rat cornea is accelerated by blockade of opioid receptors.* Brain Res, 1998. **798**(1-2): p. 254-60.
30. Zagon, I.S., J.W. Sassani, and P.J. McLaughlin, *Re-epithelialization of the rabbit cornea is regulated by opioid growth factor.* Brain Res, 1998. **803**(1-2): p. 61-8.
31. Zagon, I.S., J.W. Sassani, and P.J. McLaughlin, *Reepithelialization of the human cornea is regulated by endogenous opioids.* Invest Ophthalmol Vis Sci, 2000. **41**(1): p. 73-81.
32. Sassani, J.W., I.S. Zagon, and P.J. McLaughlin, *Opioid growth factor modulation of corneal epithelium: uppers and downers.* Curr Eye Res, 2003. **26**(5): p. 249-62.
33. Blebea, J., et al., *Differential effects of vascular growth factors on arterial and venous angiogenesis.* J Vasc Surg, 2002. **35**(3): p. 532-8.
34. Hytrek, S.D., et al., *Identification and characterization of zeta-opioid receptor in human colon cancer.* Am J Physiol, 1996. **271**(1 Pt 2): p. R115-21.
35. Zagon, I.S., et al., *Opioid growth factor (OGF) inhibits human pancreatic cancer transplanted into nude mice.* Cancer Lett, 1997. **112**(2): p. 167-75.
36. Zagon, I.S., J.P. Smith, and P.J. McLaughlin, *Human pancreatic cancer cell proliferation in tissue culture is tonically inhibited by opioid growth factor.* Int J Oncol, 1999. **14**(3): p. 577-84.
37. McLaughlin, P.J., R.J. Levin, and I.S. Zagon, *Regulation of human head and neck squamous cell carcinoma growth in tissue culture by opioid growth factor.* Int J Oncol, 1999. **14**(5): p. 991-8.
38. Bisignani, G.J., et al., *Human renal cell cancer proliferation in tissue culture is tonically inhibited by opioid growth factor.* J Urol, 1999. **162**(6): p. 2186-91.

39. Zagon, I.S. and P. McLaughlin, *Endogenous opioids and the growth regulation of a neural tumor.* Life Sci, 1988. **43**(16): p. 1313-8.
40. Zagon, I.S., S.D. Hytrek, and P.J. McLaughlin, *Opioid growth factor tonically inhibits human colon cancer cell proliferation in tissue culture.* Am J Physiol, 1996. **271**(3 Pt 2): p. R511-8.
41. Zagon, I.S. and P.J. McLaughlin, *Opioid growth factor (OGF) inhibits anchorage-independent growth in human cancer cells.* Int J Oncol, 2004. **24**(6): p. 1443-8.
42. Zagon, I.S., et al., *Combination chemotherapy with gemcitabine and biotherapy with opioid growth factor (OGF) enhances the growth inhibition of pancreatic adenocarcinoma.* Cancer Chemother Pharmacol, 2005. **56**(5): p. 510-20.
43. Zagon, I.S. and P.J. McLaughlin, *Opioids and the apoptotic pathway in human cancer cells.* Neuropeptides, 2003. **37**(2): p. 79-88.
44. Zagon, I.S. and P.J. McLaughlin, *Opioids and differentiation in human cancer cells.* Neuropeptides, 2005. **39**(5): p. 495-505.
45. Weinberg, R.A., *The retinoblastoma protein and cell cycle control.* Cell, 1995. **81**(3): p. 323-30.
46. Sherr, C.J., *Cancer cell cycles.* Science, 1996. **274**(5293): p. 1672-7.
47. Zagon, I.S., et al., *Opioid growth factor regulates the cell cycle of human neoplasias.* Int J Oncol, 2000. **17**(5): p. 1053-61.
48. Sherr, C.J. and J.M. Roberts, *CDK inhibitors: positive and negative regulators of G1-phase progression.* Genes Dev, 1999. **13**(12): p. 1501-12.
49. Zieske, J.D., C.M. Francesconi, and X. Guo, *Cell cycle regulators at the ocular surface.* Exp Eye Res, 2004. **78**(3): p. 447-56.
50. Sherr, C.J., *The Pezcoller lecture: cancer cell cycles revisited.* Cancer Res, 2000. **60**(14): p. 3689-95.
51. Kamb, A., et al., *A cell cycle regulator potentially involved in genesis of many tumor types.* Science, 1994. **264**(5157): p. 436-40.
52. Zhu, L., *Tumour suppressor retinoblastoma protein Rb: a transcriptional regulator.* Eur J Cancer, 2005. **41**(16): p. 2415-27.
53. Classon, M. and N. Dyson, *p107 and p130: versatile proteins with interesting pockets.* Exp Cell Res, 2001. **264**(1): p. 135-47.
54. Ohlson, L.C., L. Koroxenidou, and I. Porsch-Hallstrom, *Mitoinhibitory effects of the tumor promoter 2-acetylaminofluorene in rat liver: loss of E2F-1 and E2F-3 expression and cdk 2 kinase activity in late G1.* J Hepatol, 2004. **40**(6): p. 957-62.
55. Akiyama, T., et al., *Phosphorylation of the retinoblastoma protein by cdk2.* Proc Natl Acad Sci U S A, 1992. **89**(17): p. 7900-4.
56. Pan, W., et al., *A cyclin D1/cyclin-dependent kinase 4 binding site within the C domain of the retinoblastoma protein.* Cancer Res, 2001. **61**(7): p. 2885-91.
57. Connell-Crowley, L., J.W. Harper, and D.W. Goodrich, *Cyclin D1/Cdk4 regulates retinoblastoma protein-mediated cell cycle arrest by site-specific phosphorylation.* Mol Biol Cell, 1997. **8**(2): p. 287-301.
58. Hinds, P.W., et al., *Regulation of retinoblastoma protein functions by ectopic expression of human cyclins.* Cell, 1992. **70**(6): p. 993-1006.
59. Zarkowska, T. and S. Mittnacht, *Differential phosphorylation of the retinoblastoma protein by G1/S cyclin-dependent kinases.* J Biol Chem, 1997. **272**(19): p. 12738-46.

60. Boylan, J.F., et al., *Analysis of site-specific phosphorylation of the retinoblastoma protein during cell cycle progression.* Exp Cell Res, 1999. **248**(1): p. 110-4.
61. Adams, P.D., et al., *Retinoblastoma protein contains a C-terminal motif that targets it for phosphorylation by cyclin-cdk complexes.* Mol Cell Biol, 1999. **19**(2): p. 1068-80.
62. Lundberg, A.S. and R.A. Weinberg, *Functional inactivation of the retinoblastoma protein requires sequential modification by at least two distinct cyclin-cdk complexes.* Mol Cell Biol, 1998. **18**(2): p. 753-61.
63. Harbour, J.W., et al., *Cdk phosphorylation triggers sequential intramolecular interactions that progressively block Rb functions as cells move through G1.* Cell, 1999. **98**(6): p. 859-69.
64. Serrano, M., G.J. Hannon, and D. Beach, *A new regulatory motif in cell-cycle control causing specific inhibition of cyclin D/CDK4.* Nature, 1993. **366**(6456): p. 704-7.
65. Kamb, A., et al., *Analysis of the p16 gene (CDKN2) as a candidate for the chromosome 9p melanoma susceptibility locus.* Nat Genet, 1994. **8**(1): p. 23-6.
66. Ortega, S., M. Malumbres, and M. Barbacid, *Cyclin D-dependent kinases, INK4 inhibitors and cancer.* Biochim Biophys Acta, 2002. **1602**(1): p. 73-87.
67. Lee, M.H. and H.Y. Yang, *Negative regulators of cyclin-dependent kinases and their roles in cancers.* Cell Mol Life Sci, 2001. **58**(12-13): p. 1907-22.
68. Zhang, S.Y., et al., *Higher frequency of alterations in the p16/CDKN2 gene in squamous cell carcinoma cell lines than in primary tumors of the head and neck.* Cancer Res, 1994. **54**(19): p. 5050-3.
69. Zhang, J., et al., *Indole-3-carbinol induces a G1 cell cycle arrest and inhibits prostate-specific antigen production in human LNCaP prostate carcinoma cells.* Cancer, 2003. **98**(11): p. 2511-20.
70. Li, L., T. Yang, and X. Lian, *Effects of exogenous wild-type P16 gene transfection on the expression of cell cycle-related proteins in bladder cancer cell line.* Cancer Invest, 2005. **23**(4): p. 309-15.
71. Gartel, A.L. and S.K. Radhakrishnan, *Lost in transcription: p21 repression, mechanisms, and consequences.* Cancer Res, 2005. **65**(10): p. 3980-5.
72. Xiong, Y., et al., *p21 is a universal inhibitor of cyclin kinases.* Nature, 1993. **366**(6456): p. 701-4.
73. Harper, J.W., et al., *The p21 Cdk-interacting protein Cip1 is a potent inhibitor of G1 cyclin-dependent kinases.* Cell, 1993. **75**(4): p. 805-16.
74. LaBaer, J., et al., *New functional activities for the p21 family of CDK inhibitors.* Genes Dev, 1997. **11**(7): p. 847-62.
75. Joshi, U.S., et al., *Inhibition of pancreatic tumor cell growth in culture by p21WAF1 recombinant adenovirus.* Pancreas, 1998. **16**(2): p. 107-13.
76. Grau, A.M., et al., *Induction of p21waf1 expression and growth inhibition by transforming growth factor beta involve the tumor suppressor gene DPC4 in human pancreatic adenocarcinoma cells.* Cancer Res, 1997. **57**(18): p. 3929-34.
77. el-Deiry, W.S., et al., *WAF1, a potential mediator of p53 tumor suppression.* Cell, 1993. **75**(4): p. 817-25.
78. el-Deiry, W.S., et al., *WAF1/CIP1 is induced in p53-mediated G1 arrest and apoptosis.* Cancer Res, 1994. **54**(5): p. 1169-74.
79. Waldman, T., K.W. Kinzler, and B. Vogelstein, *p21 is necessary for the p53-mediated G1 arrest in human cancer cells.* Cancer Res, 1995. **55**(22): p. 5187-90.

80. Michieli, P., et al., *Induction of WAF1/CIP1 by a p53-independent pathway.* Cancer Res, 1994. **54**(13): p. 3391-5.
81. Dulic, V., et al., *Nuclear accumulation of p21Cip1 at the onset of mitosis: a role at the G2/M-phase transition.* Mol Cell Biol, 1998. **18**(1): p. 546-57.
82. Niculescu, A.B., 3rd, et al., *Effects of p21(Cip1/Waf1) at both the G1/S and the G2/M cell cycle transitions: pRb is a critical determinant in blocking DNA replication and in preventing endoreduplication.* Mol Cell Biol, 1998. **18**(1): p. 629-43.
83. Shiohara, M., et al., *p21WAF1 mutations and human malignancies.* Leuk Lymphoma, 1997. **26**(1-2): p. 35-41.
84. Dunn, G., et al., *Dendritic cells and HNSCC: a potential treatment option? (Review).* Oncol Rep, 2005. **13**(1): p. 3-10.
85. Hardisson, D., *Molecular pathogenesis of head and neck squamous cell carcinoma.* Eur Arch Otorhinolaryngol, 2003. **260**(9): p. 502-8.
86. Thomas, G.R., H. Nadiminti, and J. Regalado, *Molecular predictors of clinical outcome in patients with head and neck squamous cell carcinoma.* Int J Exp Pathol, 2005. **86**(6): p. 347-63.
87. Raschke, S., et al., *Homozygous deletions of CDKN2A caused by alternative mechanisms in various human cancer cell lines.* Genes Chromosomes Cancer, 2005. **42**(1): p. 58-67.
88. Lydiatt, W.M., et al., *Homozygous deletions and loss of expression of the CDKN2 gene occur frequently in head and neck squamous cell carcinoma cell lines but infrequently in primary tumors.* Genes Chromosomes Cancer, 1995. **13**(2): p. 94-8.
89. Gonzalez, M.V., et al., *Deletion and methylation of the tumour suppressor gene p16/CDKN2 in primary head and neck squamous cell carcinoma.* J Clin Pathol, 1997. **50**(6): p. 509-12.
90. Liggett, W.H., Jr., et al., *p16 and p16 beta are potent growth suppressors of head and neck squamous carcinoma cells in vitro.* Cancer Res, 1996. **56**(18): p. 4119-23.
91. Garcea, G., et al., *Molecular prognostic markers in pancreatic cancer: a systematic review.* Eur J Cancer, 2005. **41**(15): p. 2213-36.
92. Ghaneh, P., et al., *Molecular prognostic markers in pancreatic cancer.* J Hepatobiliary Pancreat Surg, 2002. **9**(1): p. 1-11.
93. Sasaki, S., et al., *Differential roles of alterations of p53, p16, and SMAD4 expression in the progression of intraductal papillary-mucinous tumors of the pancreas.* Oncol Rep, 2003. **10**(1): p. 21-5.
94. Dergham, S.T., et al., *Prevalence and clinical significance of combined K-ras mutation and p53 aberration in pancreatic adenocarcinoma.* Int J Pancreatol, 1997. **21**(2): p. 127-43.
95. Biankin, A.V., et al., *DPC4/Smad4 expression and outcome in pancreatic ductal adenocarcinoma.* J Clin Oncol, 2002. **20**(23): p. 4531-42.
96. Song, M.M., et al., *Comparison of K-ras point mutations at codon 12 and p21 expression in pancreatic cancer between Japanese and Chinese patients.* J Surg Oncol, 2000. **75**(3): p. 176-85.
97. Kawa, S., et al., *Inhibitory effect of 22-oxa-1,25-dihydroxyvitamin D3, maxacalcitol, on the proliferation of pancreatic cancer cell lines.* J Steroid Biochem Mol Biol, 2005. **97**(1-2): p. 173-7.

98. Hong, J., et al., *Peroxisome proliferator-activated receptor gamma-dependent activation of p21 in Panc-28 pancreatic cancer cells involves Sp1 and Sp4 proteins.* Endocrinology, 2004. **145**(12): p. 5774-85.
99. Nagai, M.A., *Genetic alterations in head and neck squamous cell carcinomas.* Braz J Med Biol Res, 1999. **32**(7): p. 897-904.
100. Zagon, I.S., et al., *Opioid growth factor ([Met5]enkephalin) prevents the incidence and retards the growth of human colon cancer.* Am J Physiol, 1996. **271**(3 Pt 2): p. R780-6.
101. McLaughlin, P.J., et al., *Opioid growth factor inhibition of a human squamous cell carcinoma of the head and neck in nude mice: dependency on the route of administration.* Int J Oncol, 2004. **24**(1): p. 227-32.
102. Zhou, H.W., S.Q. Lou, and K. Zhang, *Recovery of function in osteoarthritic chondrocytes induced by p16INK4a-specific siRNA in vitro.* Rheumatology (Oxford), 2004. **43**(5): p. 555-68.
103. Jaglowski, J.R., et al., *Opioid growth factor enhances tumor growth inhibition and increases the survival of paclitaxel-treated mice with squamous cell carcinoma of the head and neck.* Cancer Chemother Pharmacol, 2005. **56**(1): p. 97-104.
104. McLaughlin, P.J., et al., *Enhanced growth inhibition of squamous cell carcinoma of the head and neck by combination therapy of paclitaxel and opioid growth factor.* Int J Oncol, 2005. **26**(3): p. 809-16.
105. Roesler, J.M., et al., *Deletion of P15 (MTS2) in head and neck squamous cell carcinomas.* J Surg Res, 1998. **77**(1): p. 50-4.
106. Michalides, R., et al., *Overexpression of cyclin D1 correlates with recurrence in a group of forty-seven operable squamous cell carcinomas of the head and neck.* Cancer Res, 1995. **55**(5): p. 975-8.
107. Cairns, P., et al., *Rates of p16 (MTS1) mutations in primary tumors with 9p loss.* Science, 1994. **265**(5170): p. 415-7.
108. Spruck, C.H., 3rd, et al., *p16 gene in uncultured tumours.* Nature, 1994. **370**(6486): p. 183-4.
109. Ahrendt, S.A., et al., *p21WAF1 expression is associated with improved survival after adjuvant chemoradiation for pancreatic cancer.* Surgery, 2000. **128**(4): p. 520-30.
110. Moore, P.S., et al., *Genetic profile of 22 pancreatic carcinoma cell lines. Analysis of K-ras, p53, p16 and DPC4/Smad4.* Virchows Arch, 2001. **439**(6): p. 798-802.
111. Sipos, B., et al., *A comprehensive characterization of pancreatic ductal carcinoma cell lines: towards the establishment of an in vitro research platform.* Virchows Arch, 2003. **442**(5): p. 444-52.
112. Seoane, J., *Escaping from the TGF{beta} anti-proliferative control.* Carcinogenesis, 2006.
113. Han, J., et al., *Hepatocyte growth factor induces redistribution of p21(CIP1) and p27(KIP1) through ERK-dependent p16(INK4a) up-regulation, leading to cell cycle arrest at G1 in HepG2 hepatoma cells.* J Biol Chem, 2005. **280**(36): p. 31548-56.
114. Chai, J., et al., *Loss of the hSNF5 gene concomitantly inactivates p21CIP/WAF1 and p16INK4a activity associated with replicative senescence in A204 rhabdoid tumor cells.* Cancer Res, 2005. **65**(22): p. 10192-8.
115. Cao, Z., L. Liu, and D.M. Van Winkle, *Met5-enkephalin-induced cardioprotection occurs via transactivation of EGFR and activation of PI3K.* Am J Physiol Heart Circ Physiol, 2005. **288**(4): p. H1955-64.

116. Li, P.F., et al., *Signaling pathway involved in methionine enkephalin-promoted survival of lymphocytes infected by simian immunodeficiency virus in the early stage in vitro.* Int Immunopharmacol, 2004. **4**(1): p. 79-90.
117. McLaughlin, P.J., et al., *Defects in the opioid growth factor receptor in human squamous cell carcinoma of the head and neck.* Cancer, 2003. **97**(7): p. 1701-10.
118. Kim, H.S., et al., *p21WAF/CIP1/SDI1 is upregulated due to increased mRNA stability during hydroxyurea-induced senescence of human fibroblasts.* Mech Ageing Dev, 2005. **126**(12): p. 1255-61.
119. Han, S., et al., *Up-regulation of p21 gene expression by peroxisome proliferator-activated receptor gamma in human lung carcinoma cells.* Clin Cancer Res, 2004. **10**(6): p. 1911-9.

CURRICULUM VITAE
Fan Cheng

Education
08/02-present Ph.D. Candidate, Cell and Molecular Biology, Milton S. Hershey Medical Center, Pennsylvania State University
08/00-07/02 Masters of Science Program in Biomedical Technology Department, University of Vermont, Vermont
09/92-06/97 Bachelor of Medicine in Pediatrics, Tongji Medical University, China

Experience
09/01-07/02 Teaching assistant in Immunology, Microbiology and Undergraduate Research II, University of Vermont, Vermont
07/97-07/99 Resident in Department of Pediatric Surgery, Wuhan Children's Hospital, China

Manuscripts
1. Cheng, F., Zagon, I.S., Verderame, M.F., McLaughlin, P.J. "OGF-OGFr axis utilizes the p16 pathway to inhibit progression of human squamous cell carcinoma of the head and neck". In preparation.
2. Cheng, F., Verderame, M.F., McLaughlin, P.J., Zagon, I.S. "Inhibition of pancreatic cancer through the OGF-OGFr axis is mediated by the cyclin-dependent kinase inhibitor p21". In preparation.

Abstracts/Posters
1. "OGF-OGFr axis utilizes the p16 pathway to inhibit progression of human squamous cell carcinoma of the head and neck"-The Penn State Cancer Institute (PSCI) Retreat, 09/06.
2. "Inhibition of pancreatic cancer through the OGF-OGFr axis is mediated by the cyclin-dependent kinase inhibitor p21"-97th Annual Meeting of the American Association for Cancer Research, 04/06.
3. "OGF-OGFr axis utilizes the p16 pathway to inhibit progression of human squamous cell carcinoma of the head and neck"-97th Annual Meeting of the American Association for Cancer Research, 04/06.
4. "OGF-OGFr axis and its inhibitory actions on cell cycle progression of Head and Neck Cancer"- 18th Annual Graduate Student Research Forum, Penn State College of Medicine, 3/06.
5. " OGF-OGFr axis and its inhibitory actions on cell cycle progression of Head and Neck Cancer"- 45th Annual Meeting of the American Society for Cell Biology, 12/05.
6. "OGF-OGFr axis and its inhibitory actions on cell cycle progression of Head and Neck Cancer Cell Line SCC1"-17th Annual Graduate Student Research Forum, Penn State College of Medicine, 3/05.